2mΨ

CR-134126

AIRESEARCH MANUFACTURING COMPANY

A DIVISION OF THE GARRETT CORPORATION

2525 WEST 190TH STREET · TORRANCE, CALIFORNIA 90509

[213] 323-9500 · 321-5000

AIRESEARCH MANUFACTURING COMPANY

Los Angeles, California

FINAL REPORT

DESICCANT HUMIDITY CONTROL SYSTEM
NATIONAL AERONAUTICS AND SPACE ADMINISTRATION
JOHNSON SPACE CENTER (NASA JSC)
CONTRACT NAS9-12956

73-9313   17 September 1973

Number of pages __114__

Original date __15 August 1973__

Prepared by __Staff__

Edited by __J. Amazeen__

Approved by __T. C. Coull__

CONTENTS

CONTENTS (Cont)

CONTENTS (Cont)

ILLUSTRATIONS

TABLES

SECTION 1

INTRODUCTION

This report describes the results of the work performed by the AiResearch Manufacturing Company of Los Angeles, California on a program sponsored by the NASA Johnson Space Center under Contract NAS 9-12956, Desiccant Humidity Control System.

Experience gained from the use of condensing heat exchangers for humidity control in current manned space flight programs has indicated the desirability of an alternate method that will better support the Shuttle requirements. The purpose of the contract was to develop the technology for a regenerable sorbent system that will control the humidity and carbon dioxide concentration of the Space Shuttle cabin atmosphere.

The basic system concept, as defined in the statement of work, is that the humidity control system would consist of canisters containing a desiccant through which cabin atmosphere is circulated for moisture removal. In addition, the humidity control device should have the capability of adsorbing carbon dioxide from the cabin atmosphere. Bed regeneration is to be accomplished by exposure to vacuum; there is no requirement to save the water or carbon dioxide being desorbed.

The main sources of water vapor and carbon dioxide in a manned space vehicle cabin are the occupants in the cabin. For design purposes, the moisture generation rate is almost to be considered always greater than the carbon dioxide production rate. The steady-state, latent heat load and carbon dioxide production of the occupants are shown to be directly related under conditions of constant cabin temperature and respiratory quotient. Since the allowable concentration levels for carbon dioxide and water vapor on a weight percentage basis are approximately the same, the buildup of humidity occurs more rapidly than carbon dioxide; therefore, by modulating the cabin atmosphere flow to control humidity, the carbon dioxide level is also properly controlled.

The sorbents considered for water and carbon dioxide removal include silica gel and molecular sieves 3A, 13X, 4A and 5A. The last wo sorbents are currently produced in two forms; with and without binder. Both forms were considered.

Details of the investigations which resulted in the selection of silica gel as a desiccant and Davison binderless molecular sieve 4A as a CO_2 sorbent are presented in Section 2. Supporting data obtained from related NASA-funded contracts and company research and development programs, as well as the results of testing performed under this program, are included in Appendix A. This data is presented in the form of equilibrium isotherms and dynamic breakthrough curves.

An update of the AiResearch Computer Program S9960 and how it was used for preliminary bed sizing and for predicting system performance is described in Section 3.

Discussions on bed optimization and preliminary system design are presented in Section 4. The design point conditions based on the Shuttle requirements are defined, and an evaluation of the candidate approaches (including penalty trade-offs) that led to the selection of an adiabatic, center-desorption type composite adsorbent bed is discussed. Preliminary system design investigations that included comparison of three- and four-bed configurations and reliability assessment were conducted. The four-bed approach was selected as optimum for space shuttle application.

Laboratory tests were conducted on a full-scale unit to verify analytical and experimental data. A comparison of this test data with performance predictions made by the computer program is presented in Section 5.

System optimization studies and weight penalty evaluations for a four-bed system are contained in Section 6. These studies were conducted with a computer program updated by incorporation of data obtained on the full-scale test unit. Preliminary problem statements for the components of the four-bed system also are included in Section 6.

The requirement for the detection and measurement of certain toxicants that may be given off from the adsorbent bed has been rescinded by NASA.

AiResearch Report 72-8851, Test Plan, Desiccant Humidity Control System, Contract NAS 9-12956, dated November 20, 1972 is included as Appendix B. It contains material that is relevant to this report such as a sketch of the test canister and schematic diagrams of the system test plumbing and instrumentation setup.

SECTION 2

SORBENT EVALUATION AND SELECTION

GENERAL CONSIDERATIONS

The technical approach to the selection of suitable sorbents for a regenerable humidity and carbon dioxide control system was greatly simplified by establishing the proper selection criteria. The two principal selection criteria were: (1) the general sorbent characteristics should be well known and (2) these sorbents should not only be chemically stable with regards to undesirable reactions, but also physically rugged. These criteria led almost directly to the selection of inorganic solid adsorbents such as silica gel and zeolites (molecular sieves) because of their proven stability and durability. Moreover, their use results in relatively simple system concepts.

The advantages offered by inorganic solid adsorbents such as silica gel and molecular sieves are described below.

Chemical and Physical Properties

The chemical inertness of inorganic solid adsorbents virtually precludes corrosion or material compatibility problems. These sorbents are nontoxic and are not known to generate toxicants. They should be immune to the traces of solvents that may exist in the Shuttle cabin atmosphere. Although some dusting may be caused by vibration, experience with existing bed designs, where suitable filters are used, indicates no problems from dust particles impairing the crew or causing equipment damage or malfunction. No eye or lung irritation has been experienced from the regenerable CO_2 removal system developed for the Airlock module of the Skylab vehicle, nor have the valves, exposed to the effluent flows from molecular sieve beds for over 12,000 cycles, experienced mechanical problems due to dusting.

Long Life

Silica gel and molecular sieve sorbents are virtually unaffected in their basic character by high temperatures (up to 600°F), vacuum, or repeated adsorption-desorption cycles. AiResearch has tested beds that have been in place nearly one year, and found virtually no change in performance during

3<

that time. Since these adsorbents are highly porous, it should be expected that over a very long period of usage a loss in adsorptive capacity will occur through closure of some pores by impurities or contaminants in the cabin atmosphere.

Basic Characteristics

The general characteristics of silica gel and molecular sieves are well known for they have been used in industry for many years. Adsoprtion capacity increases as the temperature decreases toward the liquification point of the gas; it also increases as the pressure, at a given temperature, rises to the point necessary to condense the gas to a liquid. In general, gases of low volatility (heavier molecular weight) are absorbed more readily than those of high volatility.

Although these adsorbents show selective preference for different gases and vapors, there is no chemical specificity. Any gas or vapor will be adsorbed if the temperature is sufficiently low or the pressure is sufficiently high.

CANDIDATE ADSORBENTS

For the desiccant material, the candidate adsorbents investigated were:

Silica gel
Linde 3A molecular sieve (regular)
Linde 13X molecular sieve (regular)
Davison 4A molecular sieve (binderless)

For carbon dioxide removal, the candidate materials were:

Davison 4A molecular sieve (binderless)
Davison 5A molecular sieve (regular)
Davison 5A molecular sieve (binderless)
Linde 4A molecular sieve (regular)
Linde 5A molecular sieve (regular)

These candidate materials were selected primarily on the basis of their relatively high adsorption capacities in the operating temperature and pressure ranges of interest for the design of the Shuttle system. As described later, final selection of the most promising desiccant and the CO_2 sorbent was made by

evaluating their net capacities (available adsorption capacity between representative adsorption and regeneration pressure and temperature levels), their equilibrium capacities for oxygen and nitrogen, and their dynamic properties under flow conditions.

The new binderless molecular sieves were included as candidate sorbents because their physical stability appeared suitable for space applications, the elimination of the binder from the pellets should significantly improve adsorption capacity, even though the characteristics of these new materials were not well defined.

Silica Gel

Silica gel is a hard glassy material similar in appearance to clear quartz sand. It has a highly porous structure with uniformity in the arrangement of the pores and their size, and its surface area has been found to be in excess of 50,000 sq ft/cu in. Silica gel is a rugged, highly inert, nontoxic, heat-stable substance, with a specific heat of 0.2 $Btu/lb^{o}F$. The particles are physically stable (no change in size or shape) as they become saturated and do not give off corrosive or harmful compounds.

The equilibrium and dynamic adsorption properties of silica gel are well known. It has a much higher capacity than molecular sieves at the water vapor pressures (50° to $60^{o}F$ dewpoint) encountered in the Shuttle cabin atmosphere; it was the only desiccant considered other than the molecular sieves listed previously.

Molecular Sieves

Molecular sieves belong to the class of materials called zeolites which are generally crystalline, hydrated metal alumino silicates. Many types of zeolites are known. The molecular sieve type of zeolite has a special crystal-line structure which contains many interconnecting cavities, all of uniform size. The cavities, or cages, are interconnected by narrow openings, sometimes called windows. When formed, the cages are filled with water. Upon heating, the water can be driven out leaving a very large internal surface area capable of adsorbing many different gases and liquids, especially polar molecules like CO_2 and water.

The unique property of molecular sieves--the property for which they are named--is that the openings between cavities are very uniform in size and small enough (3 to 10 A, depending on the crystal type) to prohibit the entry and subsequent adsorption of large molecules. Thus, in many instances separation of gases or vapor can be made strictly on the basis of the size of the molecules.

Because of their inorganic crystalline nature, molecular sieves are extremely inert and stable. For example, with normal commercial regeneration temperatures of about 600° to $700^{\circ}F$, an indefinite number of regenerations of the basic crystal are possible without affecting adsorption performance. Excellent repeatability of performance has been experienced with molecular sieves.

Most molecular sieves are first manufactured in the form of fine crystallites. The crystallites (4A and 5A molecular sieves manufactured by Linde) are cubic with crystal sides measuring from 1 to 5 μ, with the average being about 3μ. This material (usually referred to as a powder) is not practical for packed-bed operation because bed pressure drop would be too large. Therefore, the base powder is usually combined with an inert clay binder and formed into pellets or spheres of practical dimensions (e.g., 1/16 to 1/8 in.). A properly produced molecular-sieve pellet or bead has relatively large-diameter pores (1000 to 10,000 A) in the clay binder. These macropores allow rapid sorbate diffusion to the myriad crystals suspended in the clay. Diffusion of the sorbate then takes place in the micropores of the crystals; between cages where sorption takes place.

There have been several previous attempts by the manufacturers to produce pellets or beads from molecular sieve powders without introducing the binder. These attempts generally resulted in poor sorbents; either there was little structural integrity of the sorbent pellet, leading to breakage and severe powdering, or the structure between crystals was so restrictive that diffusion throughout the pellet was extremely difficult. Recently, Davison has produced strong, open-pore-structure beads in both 4A and 5A without binders. Linde also markets 4A and 5A binderless pellets. Since these sorbents should have at least 20 percent higher capacity than their respective binder-containing counterparts, they were included as promising candidate materials.

SORBENT EQUILIBRIUM DATA

The equilibrium capacity is a measure of the ultimate capacity of a sorbent to adsorb another material (sorbate) under given conditions of temperature and sorbate partial pressure. The increase in weight of the sorbent at saturation is measured and is usually expressed as weight percent of the sorbent charge. Although rate processes as well as equilibrium capacity are important considerations in practical design, equilibrium data is useful in preliminary comparisons of sorbents for a given application.

The sources of the equilibrium data used in the evaluation of candidate adsorbents are presented in Table 2-1. The data source identified as NAS 1-8859 in Table 2-1 refers to AiResearch Report 72-8417, Development of Design Information for Molecular-Sieve Type Regenerative CO_2-Removal Systems, dated December 1972, which was prepared under Contract NAS 1-8559 for the NASA-Langley Research Center. The source identified as NAS 9-12956 refers to test data obtained by laboratory testing conducted under this program.

Binderless molecular sieves were not investigated under NAS 1-8559, since they were not commercially available at the time. As shown in Table 2-1, all equilibrium data for the binderless molecular sieves were obtained through testing conducted under this program.

Equilibrium Test Rig

The equilibrium test setup is shown schematically in Figure 2-1, and a photograph of the apparatus is shown in Figure 2-2. The test setup schematic is shown divided into six functional subsystems identified by numbers enclosed in circles. These subsystems are:

> Pressure Control Section--Provides the vacuum source to maintain the system pressure and to allow drying of the system and sorbent sample.

> Gas Supply System--Provides gas supply for controlled gas distribution to the sorbent under test.

> Water Supply System--Provides water vapor for controlled vapor distribution to the sorbent under test.

TABLE 2-1

ABSORBENT EQUILIBRIUM DATA SOURCES

Absorbent	Manufacturer	H_2O	CO_2	N_2	O_2
Silica gel	Davison	NAS 1-8559	---	NAS 9-12956	NAS 9-12956
MS 4A binderless	Davison	NAS 9-12956	NAS 9-12956	NAS 9-12956	NAS 9-12956
MS 5A binderless	Davison	---	NAS 9-12956	NAS 9-12956	NAS 9-12956
MS 5A regular	Davison	---	NAS 1-8559	---	---
MS 3A regular	Linde	NAS 9-12956	---	NAS 9-12956	NAS 9-12956
MS 4A regular	Linde	---	NAS 9-12956	NAS 9-12956	NAS 1-8559
MS 5A regular	Linde	---	NAS 1-8559	NAS 1-8559	NAS 1-8559
MS 13X regular	Linde	NAS 1-8559	---	NAS 1-8559	NAS 1-8559

NOTE: NAS 1-8559, Development of Design Information for Molecular-Sieve Type Regenerative CO_2 -
Removal Systems, AiResearch Report 72-8417, December 1972.

Reference Number	General Description and Model Identification	Remarks
1	Pressure control section	Controls test system from 0.02 to 760 mm Hg
1.1	Weight vacuum pump, model 1402	Controls test system from 3 to 760 mm Hg
1.2	Mercury diffusion pump	Controls test system from 0.02 to 3 mm Hg
1.3	Fabco dewar	Thermal sink
1.4	Fabco dewar	Thermal sink
1.5	Pyrex valve, V-type	Selects system route
2	Gas supply system	Provides gas to sorbent
2.1	Fabco dewar	Thermal sink
2.2	Wallace and Tiernan pressure gauge RN 44S015	Monitors gas supply pressure
2.3	Hoke gas plenum	Stores gas for test use
2.4	Valves	Fill and system supply valves
3	Water supply system	Provides water vapor for the test
3.1	Walch vacuum pump, model 1405	Provides low pressure source for vaporizing water
3.2	Fabco dewar	Thermal sink
3.3	Water reservoir	Water supply for system test
3.4	Pyrex valves, V-type	Activates water distribution
4	Pressure measurement section	Provides accurate system pressure measurement capability
4.1	MKS Baratron pressuremeter, type 77 RN 44S946	System pressure readout
4.2	MKS Baratron pressure heads, type 77	Transducers for item 4.1
4.3	McLeod gauge type GM100-A	Reference system pressure readout
4.4	Ion tube IG 100/C	
4.5	Fabco dewar	Thermal sink
4.6	Valves	Used for calibration of MKS heads and system monitoring
4.7	Pyrex valves, V-type	System valves
5	Temperature control section	Maintains and monitors sorbent temperature
5.1	Leeds Northrop temperature bridge SN 8690, RN 43B179	Readout for temperature
5.2	Reference thermocouple	Reference for temperature measurement
5.3	Constant temperature bath	Temperature control for sorbent
6	Electrobalance system	Provides weight monitoring
6.1	Cahn electrobalance SN 10307	Electrobalance device
6.2	Cahn electrobalance control RN 46B009	Controls for weight output
6.3	Leeds Northrop speedomax RN 430296	Chart recorder for weight change
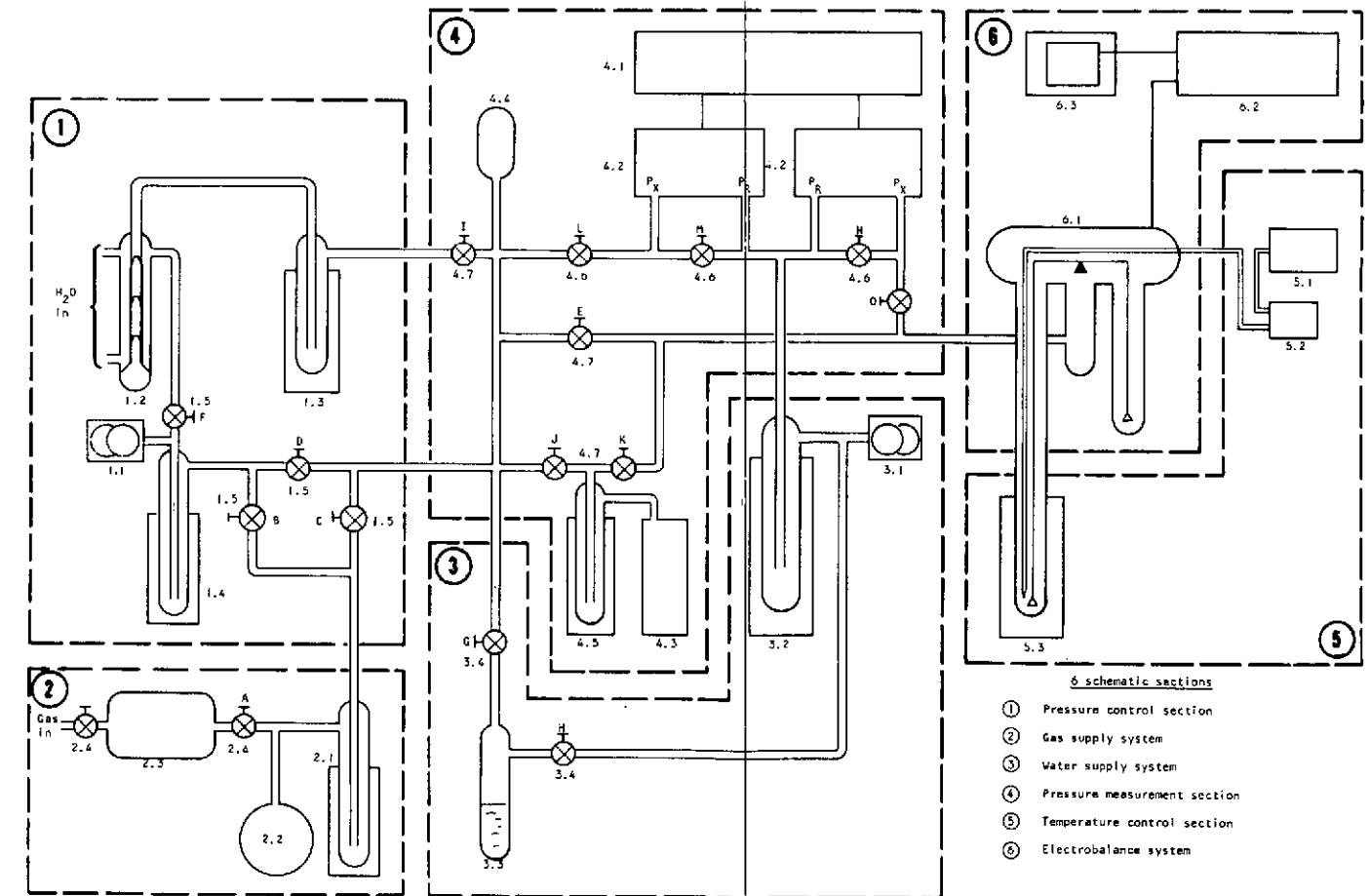
S-81007

Figure 2-1. Equilibrium Test Equipment and Setup

CAHN ELECTROBALANCE BEAM

CONSTANT TEMPERATURE BATH

ELECTROBALANCE CONTROL

CAHN ELECTROTEMPERATURE READOUT

ELECTROBALANCE CHART RECORDER

BARATRON PRESSURE METER
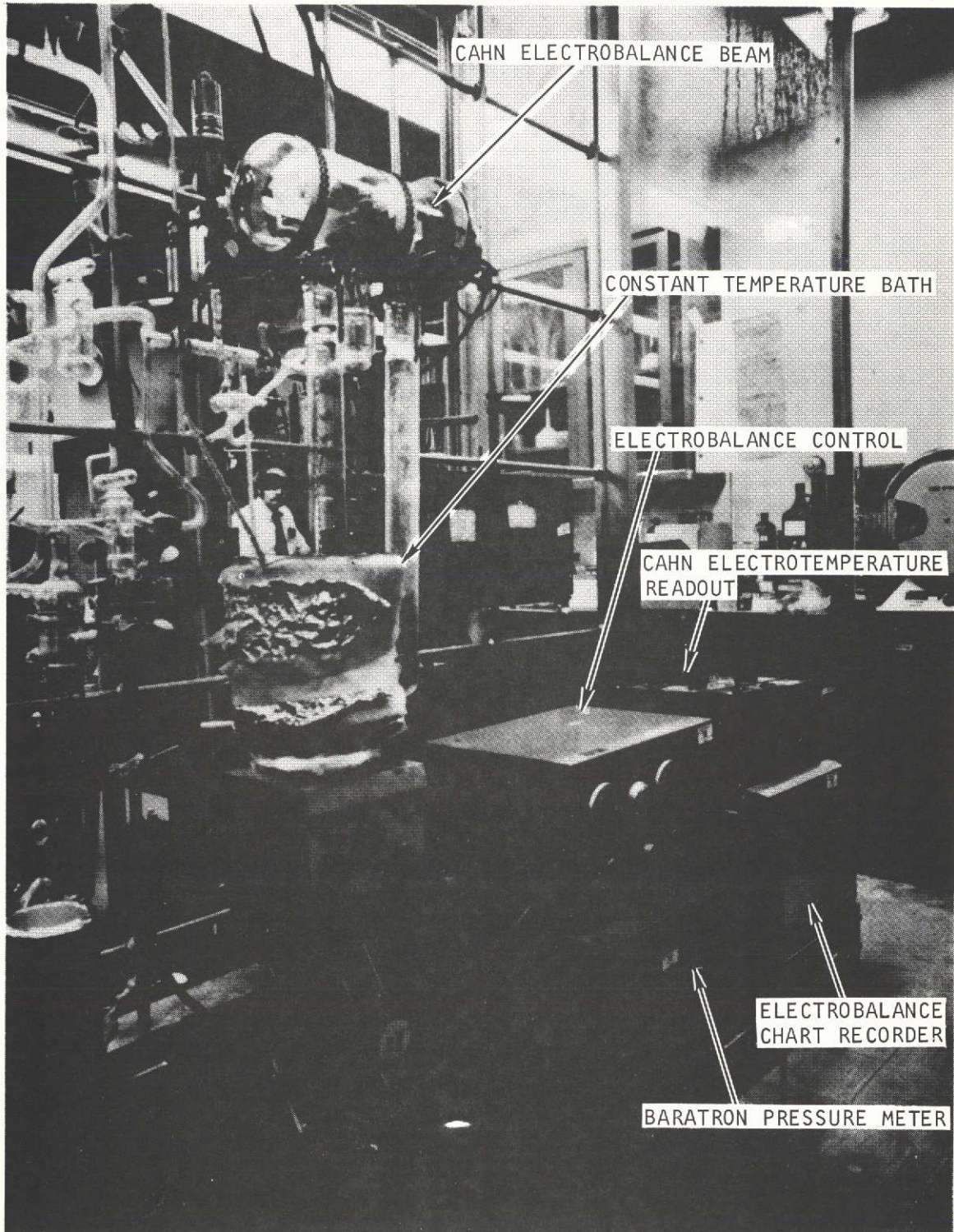
F-17876-A

Figure 2-2. Photo of Equilibrium Test Setup

Pressure Measurement Section--Provides accurate system pressure measurement.

Temperature Control Section--Provides accurate temperature control and monitoring of the sorbent temperature.

Electrobalance System--Provides accurate real-time weight measurement of the sorbent sample.

A list of the test equipment used (referenced by item numbers) and a brief description of their function is given in Figure 2-1. All active lines and valves of the setup were made of Pyrex glass; materials which exhibit off-gassing characteristics at low pressures or high temperatures were not used.

The heart of the system is the electrobalance module, consisting of a Cahn RG electrobalance and its auxiliary equipment. This device is a beam balance with a feedback servo system designed to keep the beam level. Sensing of the rotation of the balance beam is done optically. The optical sensor produces a signal which, after amplification, is directed to an electromagnet located at the beam fulcrum. The electromagnet produces a torque which restores the balance to a level position. The electromagnet current is accurately measured and translated into a weight reading.

Equilibrium Test Procedures

To obtain accurate data, the electrobalance system is maintained in a thoroughly dry, leak-tight condition throughout the test runs. First, the Cahn electrobalance is calibrated and then loaded with the sample and sealed. Next, the sorbent sample of approximately 70 mg is baked out under vacuum at $600^{\circ}F$ until the system pressure is stable and the electrobalance shows no weight change taking place. Upon completion of the bakeout, the sorbent sample is allowed to cool to $70^{\circ}F$ (still under vacuum), after which the weight indicated by the electrobalance is read and recorded. This initial weight reading is the dry weight of the sorbent. Then the test gas is introduced from the gas supply subsystem at the pressure required for the first datum point. Constant system conditions are maintained until the pressure is stable and the electrobalance indicates no weight change taking place. The sorbent gas loading is determined by the change in weight from the initial dry weight.

Other data points are obtained by repeating the above procedure at higher sorbate gas pressures at a constant temperature of 70°F.

Upon completion of each equilibrium test run, the system was pumped down to a pressure of approximately 5 mm Hg and allowed to stabilize. The system was then exposed to a vacuum until the sample weight decreased to its initial dry value. In some cases, following water adsorption runs, bakeout at high temperature was necessary to completely drive off the adsorbed gases.

After completion of desorption, dry nitrogen was introduced into the system to determine the adsorption capacity for this gas at approximately 286 mm Hg and room temperature. Also nitrogen adsorption tests for silica gel at 286 mm Hg and room temperature (approximately 70°F) were conducted; these data were not available from either AiResearch or other sources.

Equilibrium tests also were conducted to determine oxygen adsorption at 65 mm Hg and room temperature (approximately 70°F) for silica gel, Linde 3A regular, Davison 4A regular and binderless, and Davison 5A regular.

Equilibrium Test Results

The following equilibrium adsorption isotherms have been plotted from the test data and are presented in Appendix A:

(a) H_2O adsorption - Linde 3A regular (Figure A-1)

(b) H_2O adsorption - Davison 4A binderless (Figure A-2)

(c) CO_2 adsorption - Linde 4A regular (Figure A-3)

(d) CO_2 adsorption - Davison 4A binderless (Figure A-4)

(e) CO_2 adsorption - Davison 5A binderless (Figure A-5)

Equilibrium test data obtained under this program for water adsorption on Linde 3A regular molecular sieve and for carbon dioxide adsorption on Davison 5A binderless molecular sieve agree closely with the data published by the sorbent manufacturers shown in Figures A-1 and A-5.

The carbon dioxide adsorption isotherm plotted from test data for Linde 4A regular molecular sieve presented in Figure A-3 exhibits as much as 25 percent

lower capacity in contrast to data published by the manufacturer. As noted in Figure A-3, the Linde curve is for a 77°F isotherm and would be expected to fall slightly below the 70°F isotherm of the test curve. Because of the serious discrepancy between the two curves, the test curve was compared with unpublished AiResearch test data from a research program conducted in 1970. As the test curve shown in Figure A-3 was found to be nearly identical to the earlier test data, it is concluded that the test curve in Figure A-3 is accurate.

Test results for nitrogen and oxygen adsorption capacity are presented in Table 2-2.

TABLE 2-2

NITROGEN AND OXYGEN EQUILIBRIUM ADSORPTION CAPACITY

Sorbent	Manufacturer	Adsorption Capacity*, Percent by Weight	
		Nitrogen	Oxygen
Silica gel	Davison	0.023	0.0047
MS 3A regular	Linde	0.078	0.0098
MS 4A regular	Linde	0.39	0.065
MS 4A binderless	Davison	0.48	0.07
MS 5A binderless	Davison	0.67	0.084

*Except for molecular sieve 3A regular, the adsorption capacity given in Table 2-2 is for nitrogen at 286 mm Hg and room temperature (approximately 70°F); the test for 3A regular was made at 600 mm Hg. Oxygen capacities are given for 65 mm Hg except for 3A regular which was tested under an oxygen pressure of 160 mm Hg.

Sorbent Comparison

Equilibrium isotherms of the candidate sorbents considered for moisture adsorption and for carbon dioxide adsorption are presented in Figures 2-3 and 2-4, respectively.
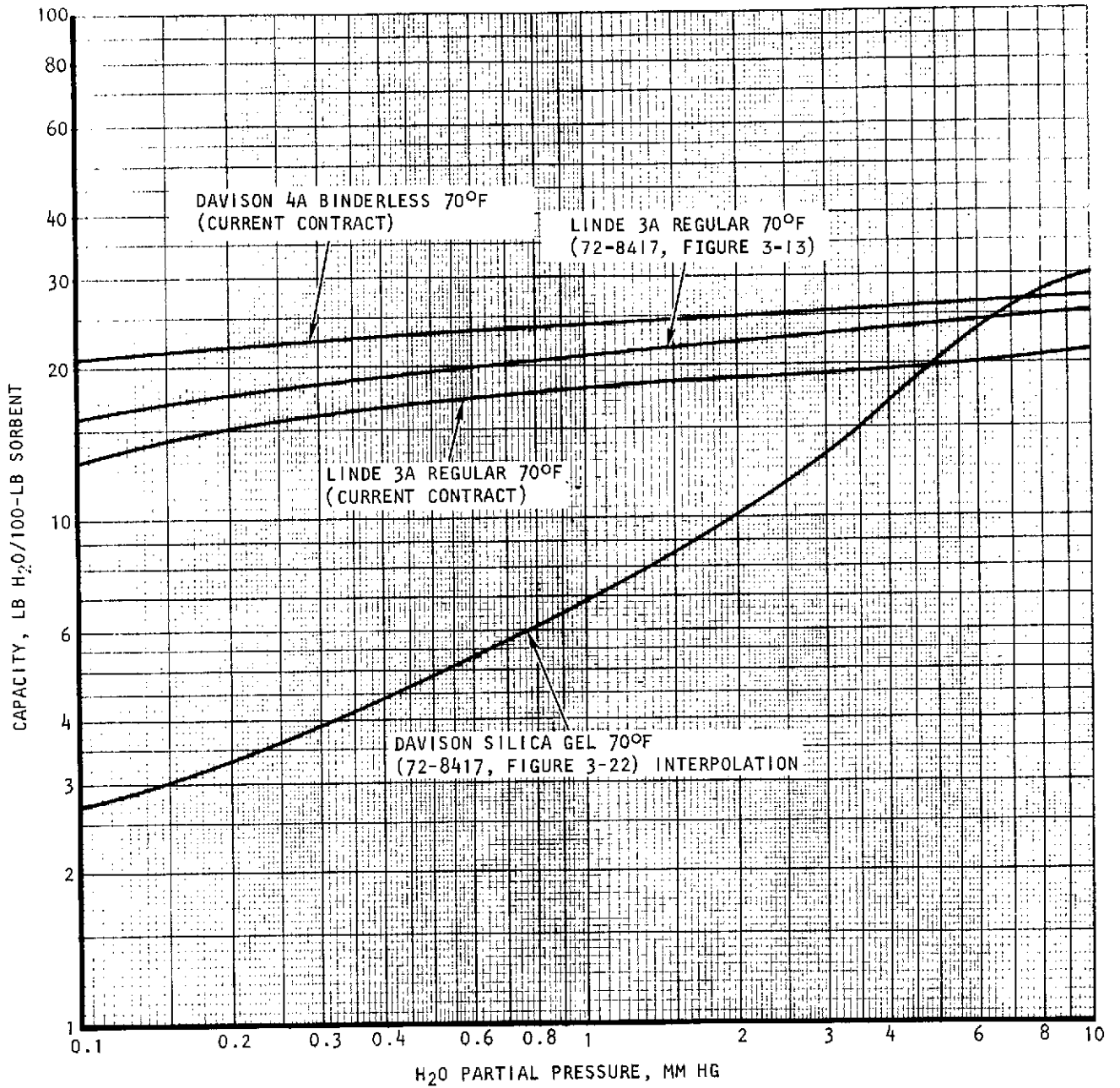
Figure 2-3. Water Equilibrium Data

① DAVISON 4A BINDERLESS, 70°F (CURRENT CONTRACT)

② LINDE 4A REGULAR, 70°F (CURRENT CONTRACT)

③ DAVISON 5A REGULAR (72-8417, FIGURE 3-3), 70°F

④ LINDE 5A REGULAR (72-8417, FIGURE 3-4), 70°F

⑤ DAVISON 5A BINDERLESS, 70°F (CURRENT CONTRACT)
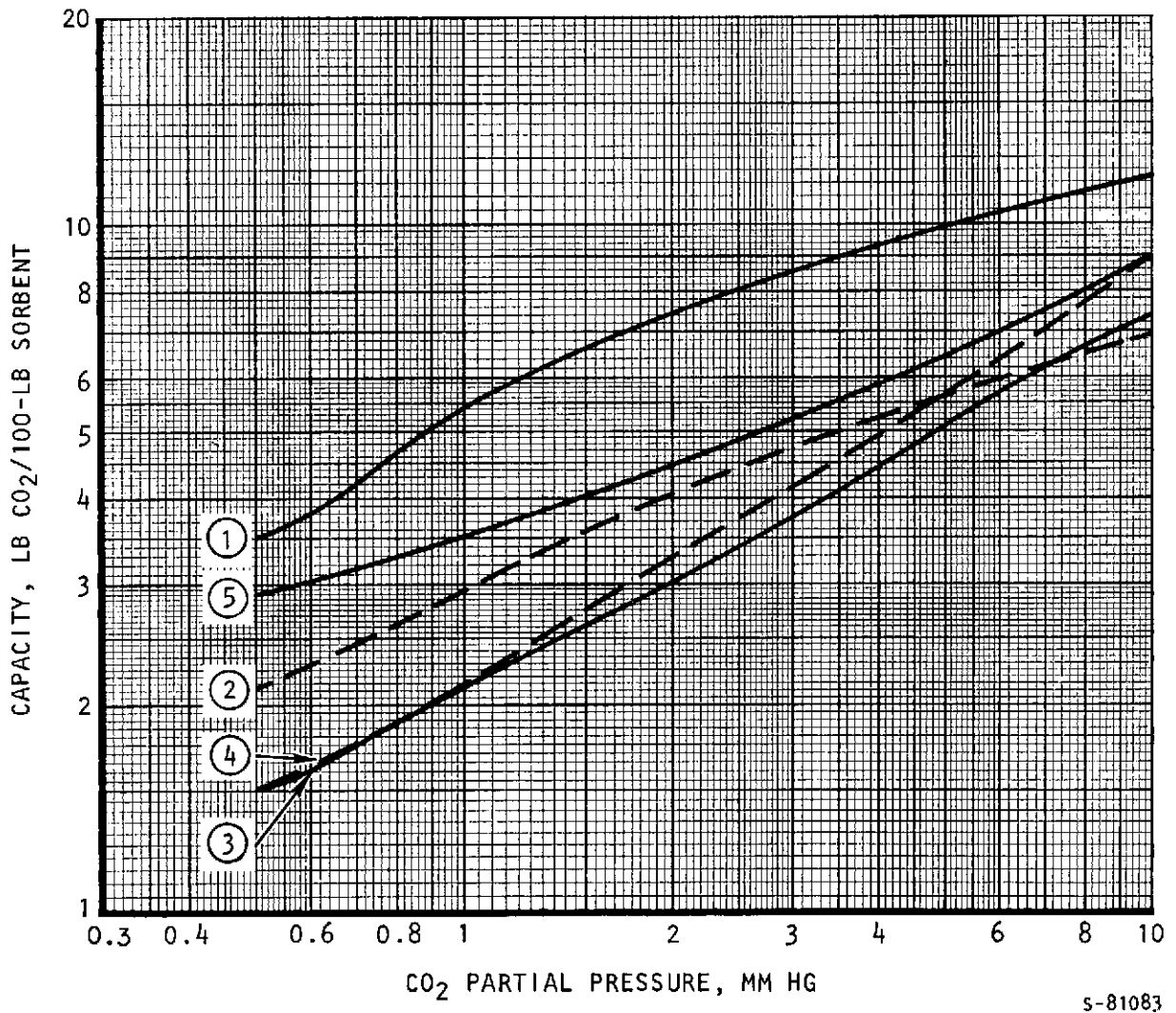
Figure 2-4. Carbon Dioxide Equilibrium Data

In Figure 2-3, the isotherms shown for Linde 3A regular and Davison 4A binderless were replotted from the test curves of Figures A-1 and A-2; the isotherms for Linde 13X regular and silica gel were taken from AiResearch Report 72-8417.

In Figure 2-4, isotherms for Linde 4A regular, Davison 4A binderless, and Davison 5A binderless were replotted from Figures A-3, A-4, and A-5, respectively; the curves for Davison 5A regular and Linde 5A regular were taken from AiResearch Report 72-8417.

Table 2-3 presents a comparison of the net working adsorption capacities for water vapor and carbon dioxide as well as the equilibrium capacities for nitrogen and oxygen exhibited by the candidate sorbents. Values for the net working capacity were determined from the equilibrium isotherms of Figures 2-3 and 2-4 by taking the difference in adsorption capacity between representative adsorption and desorption partial pressures as indicated in Table 2-3. Two partial pressure ranges are included for the water adsorption capacity because the actual bed design would consist of a primary and a secondary desiccant section. That is, in operation the cabin atmosphere will be introduced first into the primary desiccant section, which serves to remove the bulk of the humidity load, followed by the secondary section, which functions to remove practically all the remaining moisture to prevent poisoning of the carbon dioxide adsorbent.

This nitrogen equilibrium data for Linde 5A regulat and Linde 13X regular shown in Table 2-3 is taken from AiResearch Report 72-8417; other nitrogen data is from Table 2-2. The oxygen equilibrium data for Linde 4A regular, Linde 5A regular, and Linde 13X regular is also taken from AiResearch Report 72-8417; the other oxygen data is included from Table 2-2. No tests were conducted to determine the nitrogen and oxygen capacity for Davison 5A regular, and there is no published data available, but its characteristics are probably similar to Linde 5A regular.

An inspection of Table 2-3 reveals that silica gel is clearly the best choice for use as a desiccant; since it has higher capacity in the range from 6.0 to 1.5 mm Hg, comparable capacity in the range from 1.5 to 0.1 mm Hg, and lower oxygen and nitrogen capacity. Silica gel was, therefore, tentatively selected as the optimum desiccant.

TABLE 2-3

COMPARISON OF CANDIDATE ADSORBENTS

Adsorbent	Net Working Capacity, Percent by Weight			Equilibrium Capacity, Percent by Weight	
	P_{H_2O}, 6.0 to 1.5 mm Hg	P_{H_2O}, 1.5 to 0.1 mm Hg	P_{CO_2}, 3.5 to 1.5 mm Hg	P_{N_2}, 268 mm Hg	O_2, 65 mm Hg
Davison silica gel	14.7	5.8	-	0.023	0.0047
Linde 3A regular	1.4	5.6	-	0.040*	0.005*
Linde 13X regular	2.7	5.8	-	0.39	0.062
Davison 4A binderless	1.9	3.5	2.35	0.48	0.07
Linde 5A regular	-	-	1.70	0.58	0.073
Davison 5A regular	-	-	1.5	-	-
Davison 5A binderless	-	-	1.6	0.67	0.084
Linde 4A regular	-	-	1.43	0.39	0.065

*Estimated from 600 and 160 mm Hg pressures given in Table 2-2.

For carbon dioxide adsorption, the Davison 4A binderless molecular sieve was selected as the optimum adsorbent because of its higher CO_2 capacity in the range of interest, combined with lower or comparable oxygen and nitrogen capacity.

Following this preliminary selection of optimum adsorbents, testing was conducted to determine their dynamic characteristics.

DYNAMIC ADSORPTION DATA

Although the equilibrium data are useful is useful in initial evaluations of promising sorbents, dynamic characteristics must be considered before the optimum material can be selected. In multiple bed regenerative systems of the type under consideration (overboard vacuum desorption), a knowledge of sorbent performance characteristics under dynamic conditions is a prerequisite for optimum bed design. Dynamic adsorption data provides the necessary information so that the proper cycle period for bed switchover can be determined to achieve minimum penalty in terms of weight, power, and overboard gas loss.

Dynamic tests were conducted on adsorption of water vapor by Linde 3A regular molecular sieve and on adsorption of carbon dioxide by Davison 4A binderless molecular sieve. Molecular sieve 3A was considered to be used with silica gel as a predryer or primary sorbent, since it offered potential as a secondary dryer. Since dynamic water adsorption characterisitics of silica gel were well known from previous programs conducted by AiResearch, the Davison silica gel was not included for dynamic testing.

Dynamic Testing

The test setup for dynamic mass-transfer testing is shown schematically in Figure 2-5. Dry nitrogen from a high-pressure bottle was used as the carrier gas for the water adsorption tests. Nitrogen flow as indicated by the Vol-o-Flo flowmeter (regulated to approximately 20 psia) was adjusted to the desired rate. A portion of this nitrogen flow was diverted through a water bubbler to introduce water vapor into the dry nitrogen stream. The humidified gas stream was then directed via the test bed bypass circuit through the dewpoint instrument (AiResearch optical type) from which it was

1 PERCENT CO₂

CALIBRATION FLOW

FLOW METER

WATER BUBBLER

METER

CHART RECORDER

PSIA

FLOW METER

CO₂ ANALYZER

LABORATORY AMBIENT

TEST BED

WATER BATH, TEMPERATURE CONTROLLED

N₂

CO₂

DEW POINT

LABORATORY AMBIENT

ANALYZER

CHART RECORDER
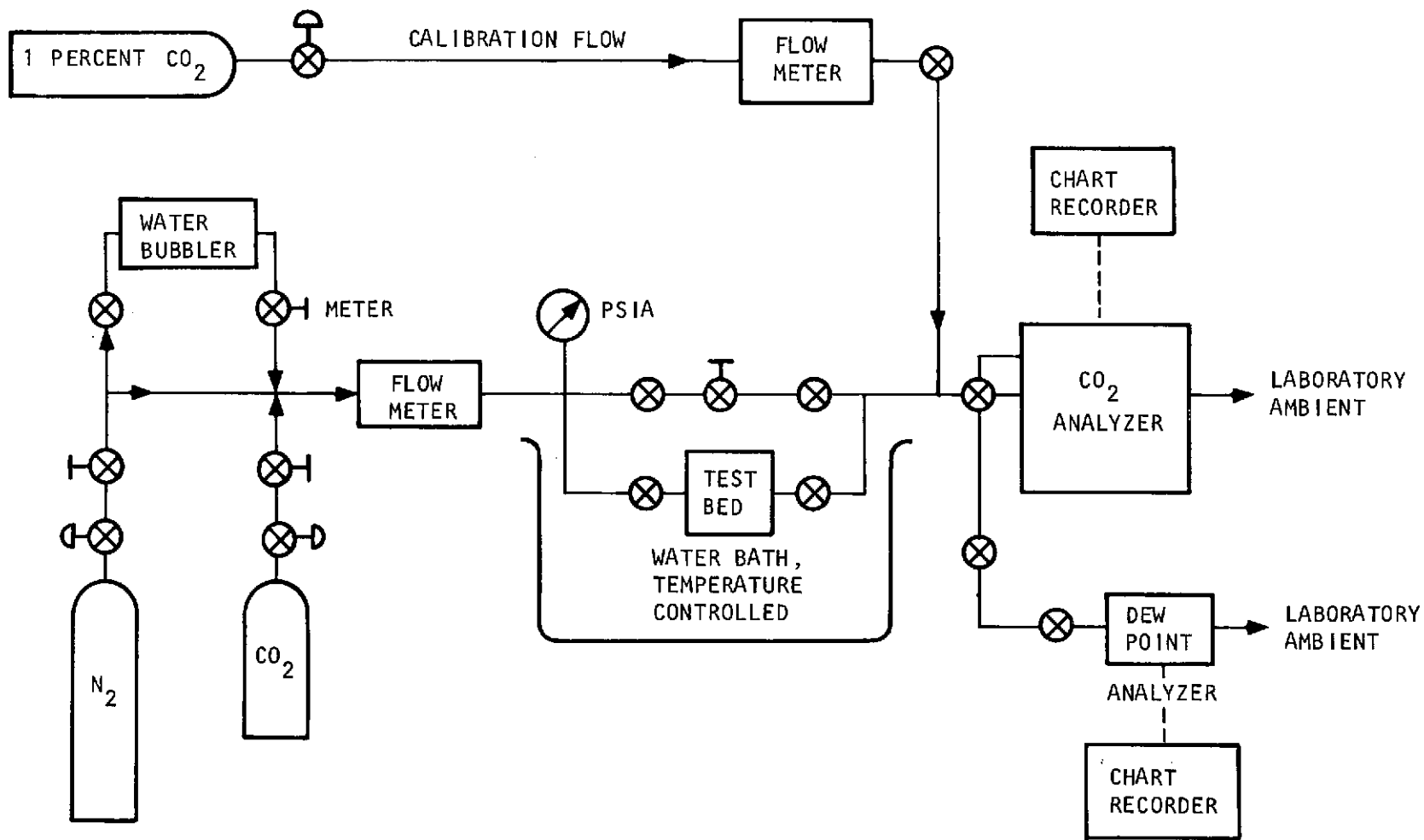
S-81013

Figure 2-5. Schematic of Dynamic Mass-Transfer Test Setup

exhausted to laboratory ambient. The pressure loss across this bypass circuit was adjusted, prior to the actual test run, to simulate the test bed pressure drop. After the proper conditions were imposed on the test bed, the bypass was closed off, the gas stream was routed through the test bed, and the dewpoint chart recorder was turned on. At the beginning of the chart recorded run, final adjustments were made to compensate for the slightly different conditions between the bypass and the test bed circuits. The test run was continued until inlet and outlet dewpoints were the same, indicating breakthrough.

For the carbon dioxide tests, the CO_2 analyzer (Beckman IR15A) was initially calibrated using a known mixture of 1 percent CO_2 in nitrogen. The calibration flow was then shut off and dry nitrogen carrier gas flow was adjusted to nearly the required rate. Following this preliminary flow and pressure adjustment, dry carbon dioxide from a high-pressure bottle was introduced and mixed with the nitrogen upstream of the flowmeter. The required inlet condition to the test bed was first established by passing the mixed gas stream through the CO_2 analyzer via the bypass circuit. Upon stabilization of the required bed inlet conditions, the bypass was closed off, the gas stream was directed through the test bed circuit, and the CO_2 chart recorder was turned on; the testing was continued until breakthrough. Upon completion of each run, the CO_2 analyzer was recalibrated to check for possible calibration drift.

The test bed used in these tests consisted of a 0.83-in. ID by 1.0-in. long stainless steel tubing packed with the adsorbent being investigated. Fine mesh stainless steel screens were used to hold the adsorbent pellets in place. Half-inch line shutoff valves with quick disconnect fittings were provided at the inlet and outlet as an integral part of the test bed assembly.

Preceding each test, the test bed was subjected to a prolonged vacuum bakeout at $400^{\circ}F$ and allowed to cool to laboratory ambient temperature. After the test bed assembly was installed in the test setup, it was immersed in a water bath to maintain the bed at a constant temperature. Throughout each test run all inlet conditions (flow rate, pressure levels, and concentration) were held constant.

Table 2-4 presents the conditions imposed on the test bed for dynamic testing.

TABLE 2-4

TEST CONDITIONS FOR DYNAMIC MASS-TRANSFER TESTING

Sorbate	Inlet Partial Pressure, mm Hg	Carrier Gas	Total Pressure, psia	Bed Temperature, °F	Flow Rate, Std. Liter per min
H_2O	14 to 17	N_2	20 to 22	70 120	10
	2 to 3	N_2	20 to 22	70 120	10
CO_2	7 to 9	N_2	20 to 22	70 120	10

In Table 2-4, the water partial-pressure range of 14 to 17 mm Hg represents the upper limit of humidity in the Shuttle cabin. The lower partial-pressure range of 2 to 3 mm Hg relates to a humidity level more representative of the secondary desiccant. The total pressure level of 20 to 22 psia is higher than the Shuttle cabin pressure of 14.7 psia, but was required to overcome the pressure losses encountered in the test setup.

The 70°F temperature corresponded to the nominal design Shuttle cabin atmosphere temperature, whereas the 120°F bed temperature was intended to bracket the probable maximum bed operating temperature. The flow rate of 10 standard liters per min was established so that breakthrough would be achieved in a reasonable time, not exceeding approximately half an hour.

Dynamic Mass-Transfer Test Results

Results of the dynamic adsorption tests have been plotted and are included in Appendix A as Figures A-6 through A-13. The figures are identified as follows:

Figure A-6, Water adsorption, Linde 3A regular, 16.6 mm Hg partial pressure, 70°F

AIRESEARCH MANUFACTURING COMPANY
Los Angeles, California

21<

Figure A-7, Water adsorption, Linde 3A regular, 14.9 mm Hg partial
pressure, 120°F

Figure A-8, Water adsorption, Linde 3A regular, 2.34 mm Hg partial
pressure, 70°F

Figure A-9, Water adsorption, Linde 3A regular, 2.35 mm Hg partial
pressure, 120°F

Figure A-10, CO_2 adsorption, Davison 4A binderless, 7.44 mm Hg
partial pressure, 70°F

Figure A-11, CO_2 adsorption, Davison 4A binderless, 8.27 mm Hg
partial pressure, 120°F

Figure A-12, CO_2 adsorption, Davison 5A binderless, 7.27 mm Hg
partial pressure, 70°F

Figure A-13, CO_2 adsorption, Davison 5A binderless, 7.64 mm Hg
partial pressure, 120°F

Test conditions are noted in each figure. From the dynamic character-
istics shown in Figures A-6 through A-13, mass-transfer coefficients and
intra-particle diffusivities were determined with the aid of the performance-
prediction computer program.

Table 2-5 summarizes the dynamic properties of the candidate sorbents in
the form of intraparticle diffusivity, Dk, and gas-phase, mass-transfer
coefficient, Kg. Molecular sieves 13X and 5A regular are included in the
table to provide a basis for comparison of the water and CO_2 sorbents,
respectively. The relationship governing adsorption rate ($\dot{w}$, lb/hr) of a
gas as vapor over a sorbent is expressed as

$$\dot{w} = K_g (P_s - P^*) AM$$

where K_g: mass-transfer coefficient, lb/mole/ hr-sq ft-mm Hg

P_s: the partial pressure of the sorbate in the process gas
stream, mm Hg

P^*: the pressure of the sorbate on the surface of the sorbent
exposed to the gas stream, mm Hg

A: external sorbent area exposed to the process gas stream, sq ft

M: molecular weight of the sorbent, lb/mole

TABLE 2-5

MASS-TRANSFER DATA FOR CANDIDATE SORBENTS

Sorbent/Sorbate	Intraparticle Diffusivity, D_k, sq ft/hr	Gas-Phase, Mass-Transfer Coefficient, K_g, lb/mole/hr-sq ft-mm Hg
Silica gel/H_2O*	0.001 to 0.0001	0.0004
3A regular/H_2O	0.000001	0.0005
13X regular/H_2O	0.000002	0.0005
5A regular/CO_2*	0.001	0.0002 to 0.0004
4A binderless/CO_2	0.00005	0.001

*Data from NAS 1-8559. (Ref. AiResearch Report 72-8417)

While the adsorption rate is directly proportional to the mass-transfer coefficient, it is only indirectly related to the diffusivity, D_k, which determines the rate at which the sorbate is transported from the sorbent surface to the interior of the sorbent pellets, so that $P^* = f(D_k)$. In the sorbent/sorbate systems under consideration, the coefficient, D_k, offers only a negligible resistance in the adsorption process until its value drops below approximately 0.0001. In practice for D_k values above 0.0001, the adsorption rate is controlled entirely by the mass-transfer coefficient, K_g.

Sorbent Selection

Examination of the data given in Table 2-5 reveals that silica gel has a comparable mass-transfer coefficient, K_g, and a higher diffusivity than either of the other two candidates considered as potential desiccant: 3A and 13X regular. Since silica gel also has a higher working capacity for water and a lower capacity for oxygen and nitrogen, it was selected as the optimum desiccant.

Comparison of the candidate CO_2 sorbents shows that the much higher mass-transfer coefficient of the 4A binderless molecular sieve far offsets the lower diffusivity in comparison with the 5A regular material. For this reason, the 4A binderless material was selected as the CO_2 sorbent in view of (1) the higher working capacity of 4A binderless for CO_2, and (2) its lower capacity for oxygen and nitrogen.

The correlation of the data presented enabled the use of the computer program for optimizing bed design under various operating conditions with a high level of confidence. Furthermore, the dynamic and equilibrium information was utilized to properly size the beds for an optimum regnerative cycle time. The results of these optimization studies are presented in subsequent sections of this report.

SECTION 3

COMPUTER PROGRAM UPDATE

GENERAL

Computer techniques were employed to (a) optimize the regenerable sorbent system operating parameters, (b) compare candidate system arrangements, (c) design the development test program, and (d) optimize bed size, geometry and operation of the humidity/CO_2 control system recommended for Space Shuttle.

The basic computer program (MAIN4B) used was developed under Contract NAS 1-8559 and is described in AiResearch Report 72-8786.

This program deals with systems where both water and CO_2 are vented to vacuum. The program also allows for internal coolant passages or adiabatic beds to be simulated. Any sorbents can be employed in the desiccant and CO_2-removal sections of the bed. Vacuum desorption is the main desorption mode, but gas stripping simulations can be made by proper input data assignments. The following features are included in the program: (1) the poisoning effect of gradual water buildup on the CO_2 sorbent, (2) estimation of overboard gas losses, (oxygen and nitrogen), and (3) the capability to analyze desorption when vacuum pumping is included in the system.

By considering the poisoning of the CO_2-removal bed by water and the adsorption and subsequent loss of atmospheric gases O_2 and N_2, this program treats some of the very important second-order effects due to coadsorption. Even though the program does not handle the coadsorption in a thoroughly rigorous manner, it provides results that are quite valuable in system design and optimization work.

. Computer program, MAIN4B, was modified as necessary to (1) model particular bed geometries considered in subsystem comparison, and (2) incorporate equilibrium and dynamic data obtained for the selected sorbents: silica gel for water removal and molecular sieve type 4A binderless for CO_2 removal.

As discussed in more detail later, the selected bed configuration for Shuttle application features center point desorption. Figure 3-1 shows the geomtry of the recommended bed. The entire bed is divided into three major sections:

1. Primary predrier (silica gel)

2. Secondary predrier (silica gel)

3. CO_2 removal (molecular sieve Type 4A binderless)

The desorption port is located between the primary and secondary predriers. For the purpose of analysis, each major section is further subdivided along its axis into a number of thin beds or nodes in the direction of the process gas flow. A total of 18 nodes constitutes the entire bed. The nodes are identified in Figure 3-1 with the process gas flow circulated from node 18 to node 1 during the adsorption half cycle. Desorption is effected from node 9.5 (center of node 10).

Also identified in the schematic are the development test bed dimensions and the temperature and pressure instrumentation used to monitor performance during development testing. These are discussed in Section 5 of this report.

As mentioned above, program MAIN4B was modified as necessary to model the various bed/system arrangements considered as candidates under this contract. The following discussions describe the modifications to MAIN4B relevant to the selected configuration only. A listing of the modified program has been supplied to NASA separately in the form of a tape. The input data furnished reflects the updating found necessary to model accurately the performance of the full-scale development test bed.

COMPUTER PROGRAM MODIFICATIONS

Only minor modifications were necessary to apply the AiResearch sorbent bed program MAIN4B to the Space Shuttle bed shown in Figure 3-1. These modifications are described below.

Implementation of Centerpoint Desorption

The desorption scheme used in the present system cannot be directly simulated by MAIN4B. The calculation scheme incorporated in the program consists of finding the desorption pressure history at the bed outlet using an end-desorption scheme, and then using the same pressure history at the centerpoint node to predict the behavior of the bed during desorption. The vacuum duct was assumed to be 7.5 cm ID by 400 cm long.
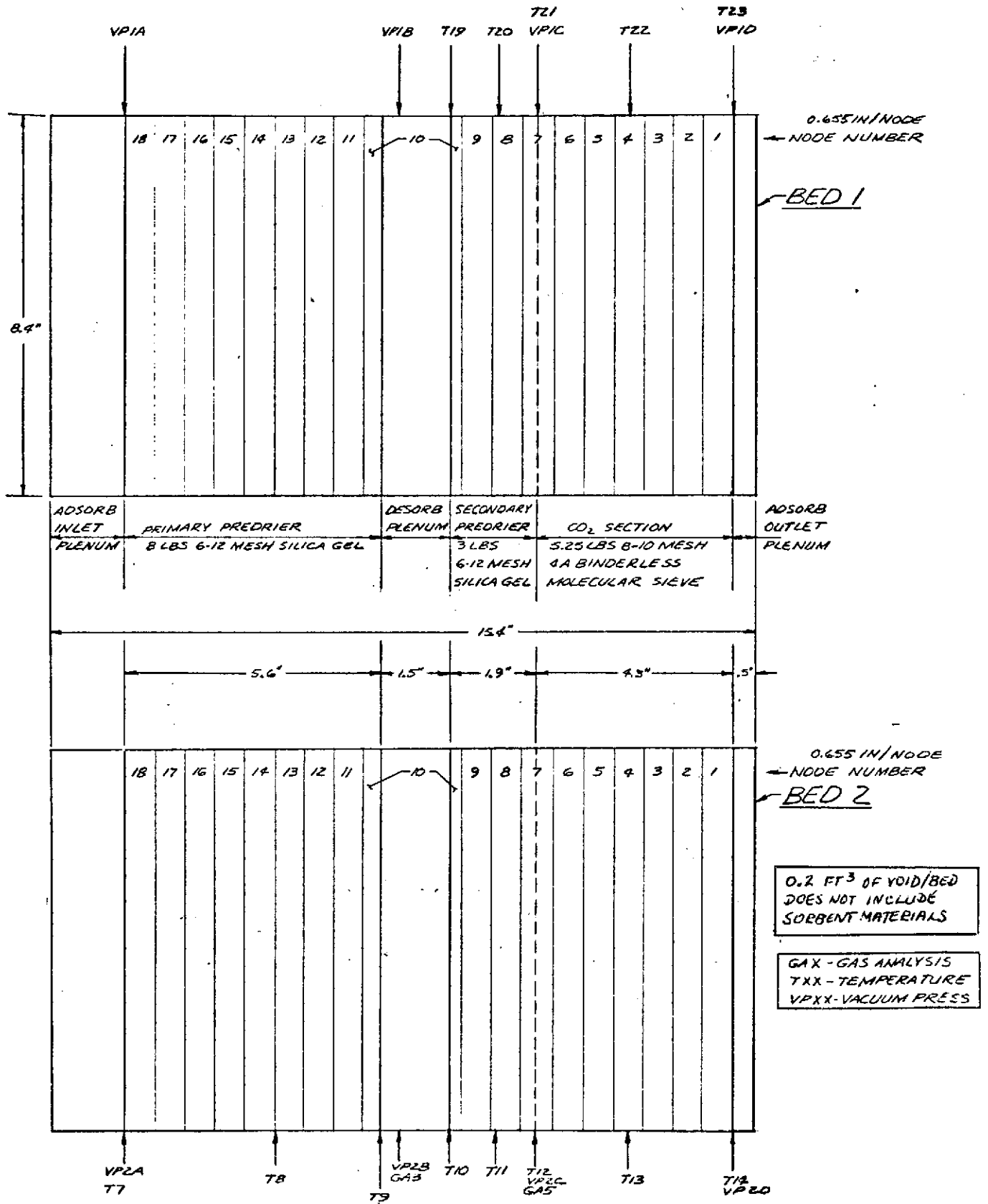
Figure 3-1. Desiccant Humidity System Beds Schematic

Equilibrium Data for New Sorbents

The data obtained under the present study for the systems 4A-binderless-CO_2, 4A-binderless-O_2 and N_2 was incorporated into subroutine EQPWT, which calculates the equilibrium pressure or capacity of various sorbents being used. The isotherms of various sorbent-sorbate systems are identified as shown in Table 3-1, which is an expanded version of the one shown in AiResearch Report 72-8786.

Mass-Transfer Characteristics

For the new CO_2 sorbent 4A binderless, the mass-transfer coefficient and diffusivity were established from the dynamic breakthrough curves as discussed in Section 2. The best fit was obtained by the set: $DIF = 0.5 \times 10^{-4}$, $GK = 10^{-3}$. These rate coefficients were incorporated in the program.

TABLE 3-1

TABULATION OF IS FOR EACH
COMBINATION OF IDSORB AND ID

IDSORB ID	1 (CO_2)	2 (H_2O)	3 (N_2)	4 (O_2)
1 (5A)	1	2	6	7
2 (S.G.)	10	3	11	12
3 (13X)	4	5	8	9
4 (4A)-binderless	13	14	15	16
5 (3A)	17	18	19	20

ID: Index identifying various sorbates.

IDSORB: Index identifying various sorbents.

IS: Index assigned to various isotherms.

28

SECTION 4

PRELIMINARY SYSTEM DESIGN

GENERAL

The optimization of a regenerable sorbent system for humidity and CO_2 control involves consideration of a number of interacting parameters related to bed design and thermal management, as well as system arrangement and control. The procedure followed was conducted in three major steps.

The first step involved the establishment of a baseline system configuration that satisfied the performance and reliability requirements of Space Shuttle. This system and its operating parameters were optimized in terms of equivalent weight including sorbent weight, hardware weight, and overboard gas-loss penalties.

The second step was to characterize candidate bed designs differing with respect to sorbent thermal management during adsorption-desorption. These competing designs were compared with the baseline and an optimum approach was selected.

Following the selection of a bed configuration, system analyses were conducted to optimize bed size and system arrangement so that all Space Shuttle reliability requirements were met.

In the performance of these studies, computer program MAIN4B was used extensively to assist in bed sizing and to determine system performance in terms of cabin humidity level, CO_2 partial pressure, and overboard gas losses. The following data formed the basis for the study.

DESIGN DATA AND ASSUMPTIONS

The requirements shown in Table 4-1 were used in the performance of the system optimization.

TABLE 4-1

PERFORMANCE REQUIREMENTS

Crew size:	4 men at maximum metabolic loads 10 men at nominal metabolic loads
Latent load:	maximum: 238 Btu/man-hr nominal: 193 Btu/man-hr
CO_2 production rate:	maximum: 0.104 lb/man-hr nominal: 0.095 lb/man-hr
Cabin pCO_2:	normal: 5 mm Hg normal maximum: 7.6 mm Hg emergency maximum (fail-safe): 10 mm Hg
Cabin dewpoint:	nominal: $53^{\circ}F$ maximum: $61^{\circ}F$
Cabin volume:	2000 cu ft
Cabin total pressure:	14.7 ±0.2 psia
Cabin oxygen partial pressure:	3.1 ±0.1 psia
Diluent:	Nitrogen
Cabin temperature:	$70^{\circ}F$
Oxygen storage penalty:	1.13 lb tot/lb O_2 (cryogenic)
Nitrogen storage penalty:	1.8 lb tot/lb N_2 (high-pressure gas)
Mission duration:	7-day nominal
Emergency contingency:	4 days
Reliability criterion	The system must maintain design performance after any one failure. Degraded operation at the maximum pCO_2 and dewpoint must be maintained after a second failure.
Power penalty:	66 lb/kw + 1.57 lb/kw-hr

BASELINE SYSTEM DEFINITION

A schematic of the baseline system is shown in Figure 4-1. Major features are as follows:

(a) System comprises 4 modules incorporating sorbent bed, selector valve, pressure equalization valve, and actuator control valve. The timer-controller has provisions for operation of any two modules as a pair.

(b) Two beds are on-stream with a 4-man crew. All four beds are operational with a 10-man crew. Any two beds can be operated as a pair.

(c) Desiccant: Silica gel

(d) CO_2 sorbent: 4A binderless

(e) Adiabatic bed operation

(f) Center point desorption (See Figure 3-1).

(g) Sorbent bed pressure equalization prior to vacuum desorption

(h) Design point performance can be achieved after second failure with a 4-man crew

(i) With a 10-man crew, cabin dewpoint and CO_2 removal performance will degrade but remain within normal range after first failure.

After second failure, pCO_2 will be maintained below 10 mm Hg.

Baseline System Optimization

1. Effect of Process Flow Rate

The design process flow rate through the regenerable systems will be the same for all candidate approaches considered and is determined by the water vapor removal requirements. The CO_2 removal capacity of the system will be adjusted by sizing the CO_2 sorbent bed so that the cabin CO_2 partial pressure will be maintained below 5 mm Hg at the design production rate with the process flow determined on the basis of humidity control.

Since the process air through the system is essentially dry at the outlet of the sorbent beds, the airflow requirements are dependent on cabin water partial pressure and on the latent load in the cabin. Figure 4-2 defines the process gas flow required for crew sizes of 4 and 10 men at the design metabolic rates and also at metabolic rates corresponding to sleep, discussed later under system control.
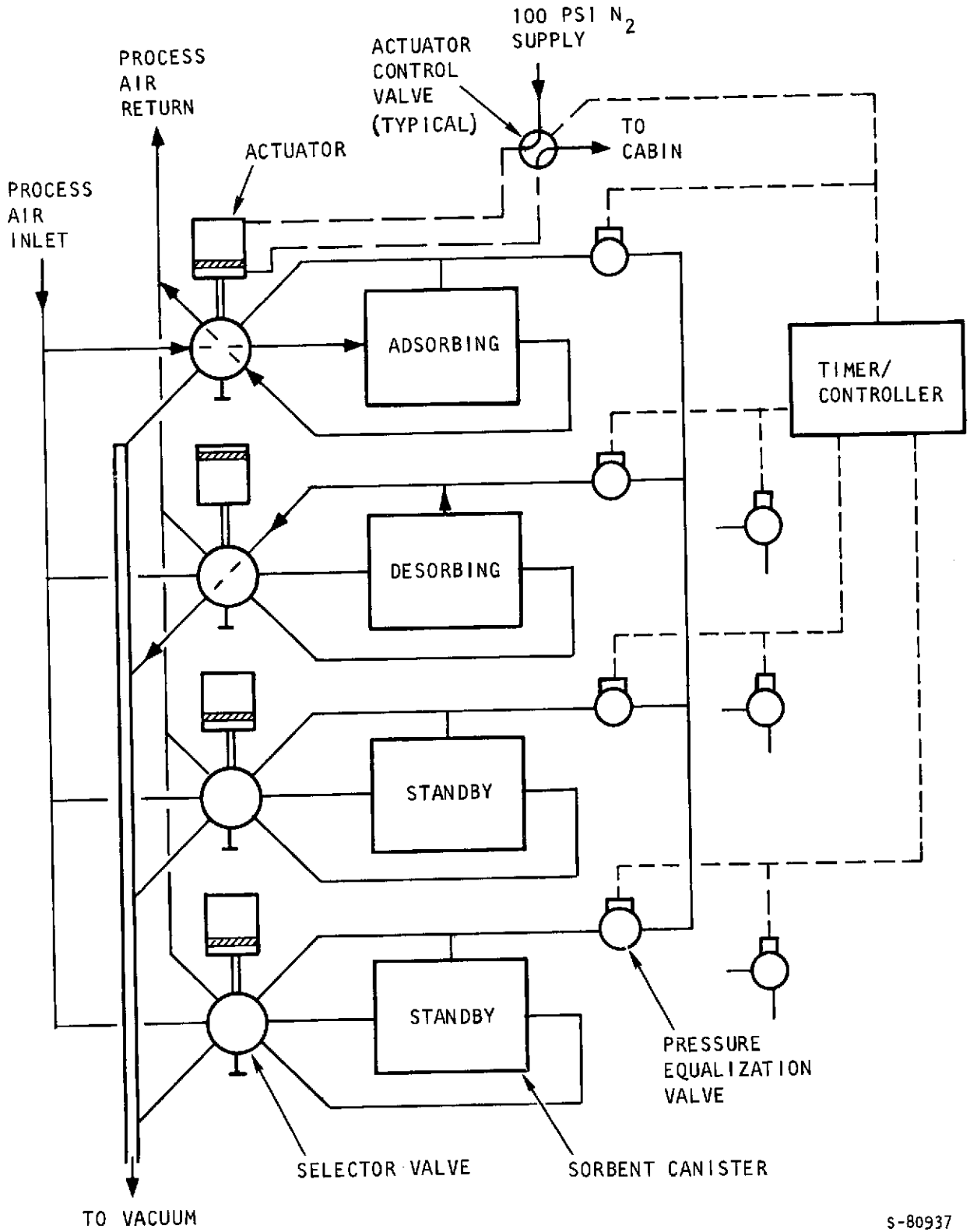
Figure 4-1. Baseline System

S-80937
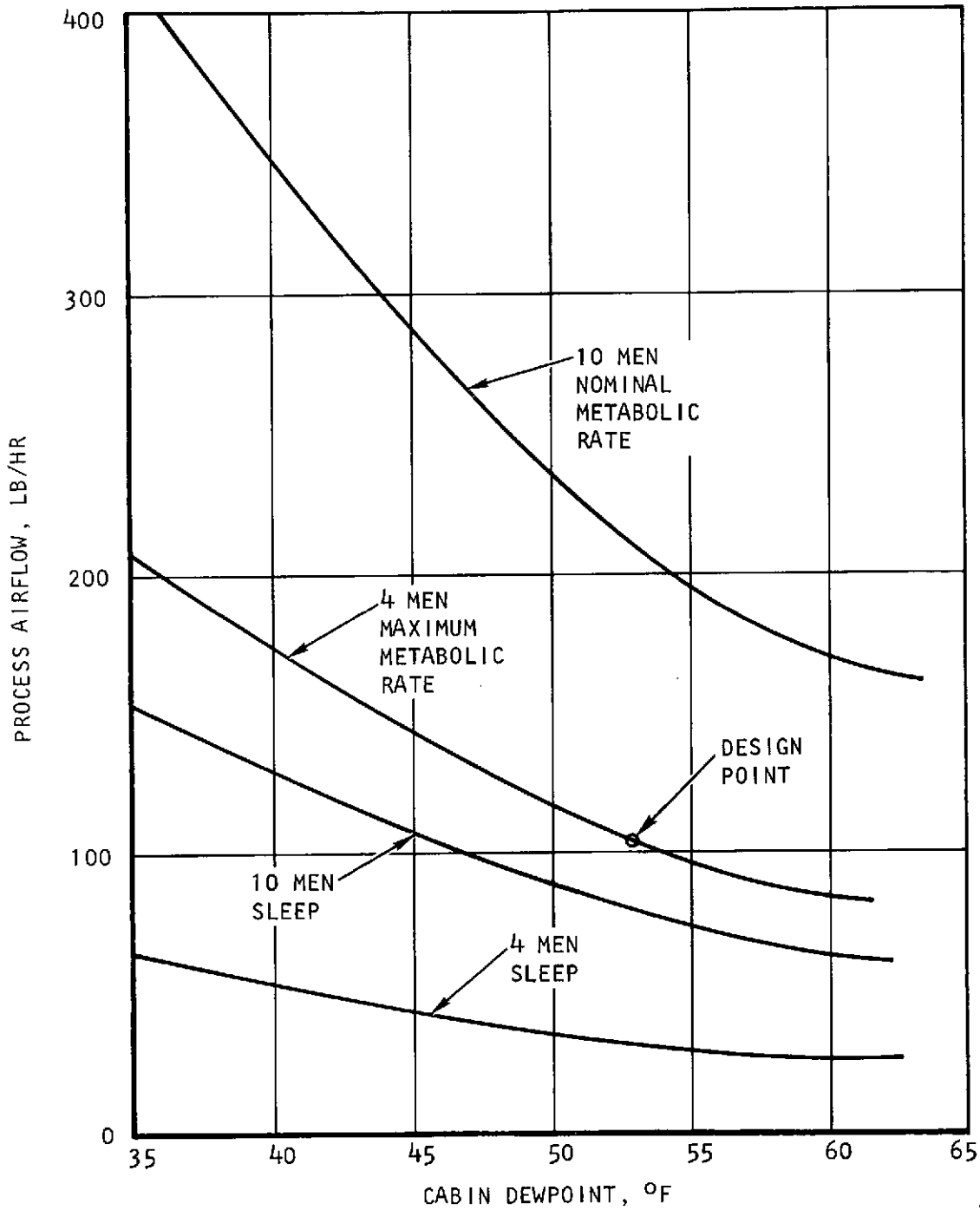
Figure 4-2. Process Flow Requirements

At the design cabin dewpoint ($53^{\circ}F$), the flow required to remove 0.417 lb/hr of water vapor (4-man load) from the cabin is 106 lb/hr. With two sorbent beds, the process air flow will be 212 lb/hr and cabin dewpoint will be maintained at $52.6^{\circ}F$ with 10 men in the cabin.

Cycle Time Optimization

The size of the sorbent bed will be nearly proportional to cycle time; thus, long cycle time will increase the fixed weight of the system. Long cycle time also will reduce losses of oxygen and nitrogen that are dumped overboard with the carbon dioxide and water on each cycle. A study was conducted to optimize cycle time for the system shown in Figure 4-1; parametric data is presented in Figure 4-3. The plot in Figure 4-3 shows the weight of a single loaded canister and the gas loss penalty, including tankage, for the 4-man, 7-day, baseline system. Data for a canister designed to handle a 10-man water and CO_2 load also is presented; this data will be used later in discussions of system arrangements.

The gas loss penalty is computed on the basis of a 7-day mission since the 4-day contingency constitutes an emergency situation not chargeable to this subsystem. Note that the sorbent bed was sized to provide design performance for a period of 11 days.

Figure 4-4 is a plot of equivalent weight including the fixed weight of the system depicted in Figure 4-1 and the gas loss penalty. In computing system fixed weight, all four modules were taken into account and a 15 percent allowance was made for structures, brackets, and electrical harnesses. The gas tankage weight was calculated using the penalties listed previously, which assumes that oxygen is supplied to the cabin from cryogenic storage while nitrogen is stored as a high pressure gas in composite gas tanks.

A 6-min half-cycle time was selected as optimum and used in further optimization and comparison studies.

DESORPTION TECHNIQUE

Two methods for sorbent desorption were evaluated: centerpoint and counterflow desorption. Figure 4-5 illustrates the two approaches. In the counterflow method, the CO_2 serves as a purge gas which assists in desorption
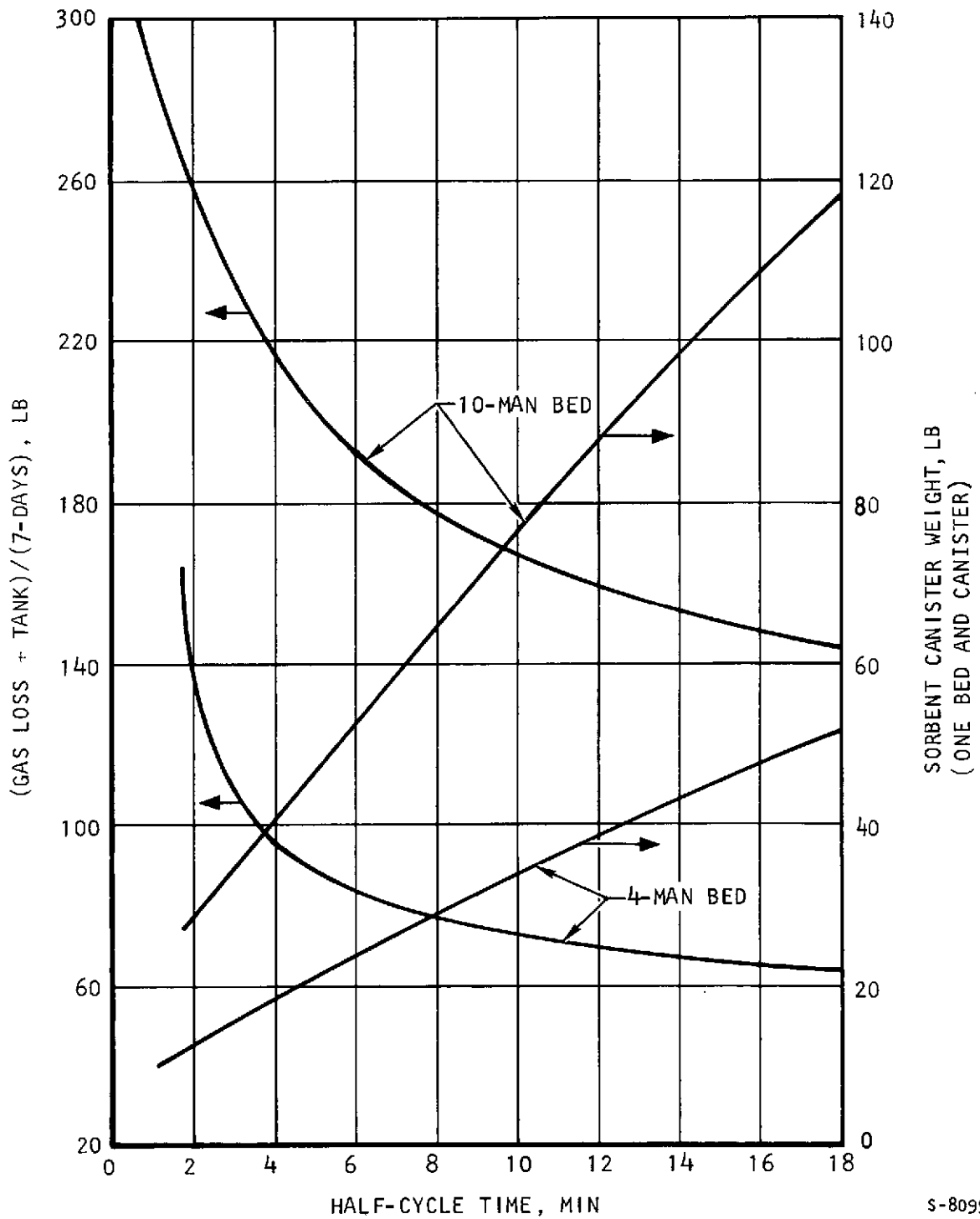
Figure 4-3. Parametric Sorbent Bed Data
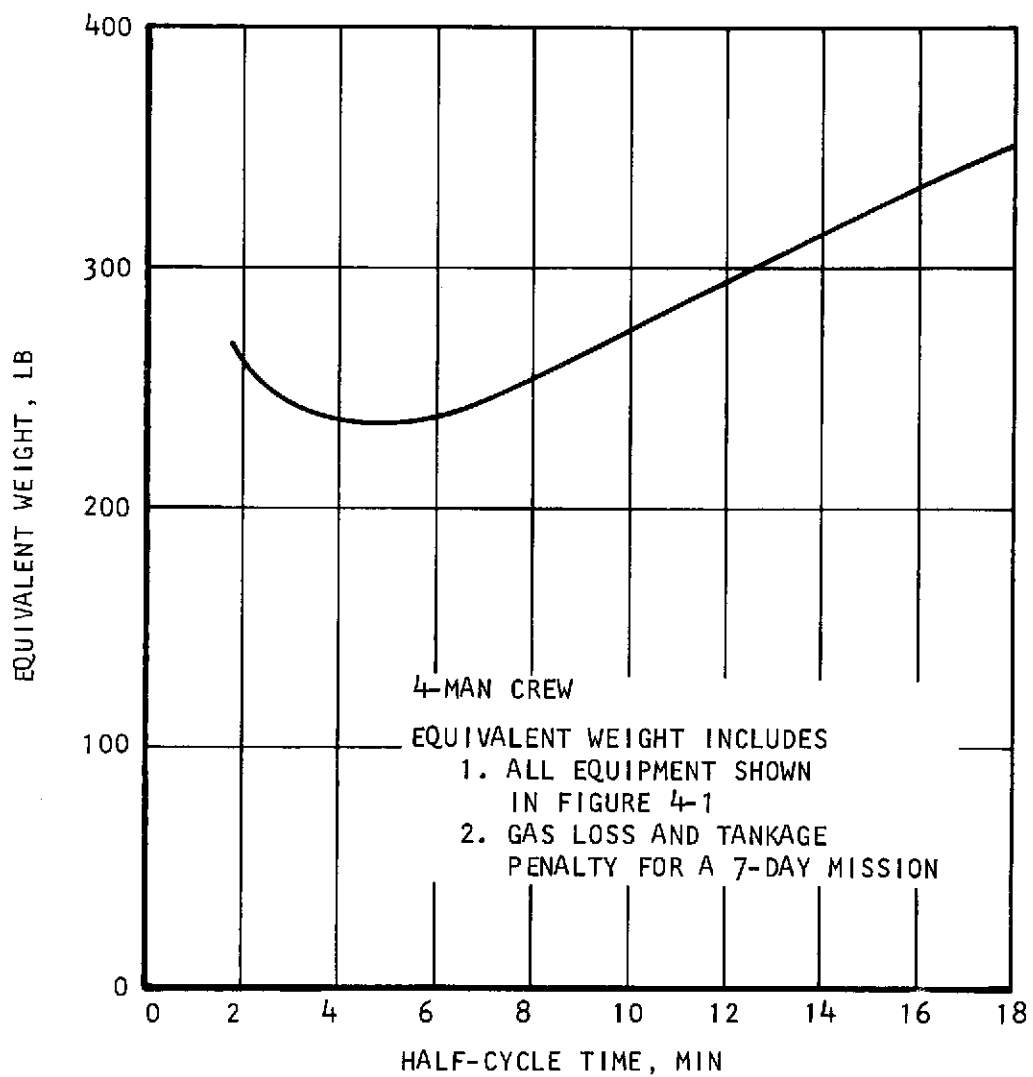
S-80993

Figure 4-4. Cycle Time Optimization

s-80997
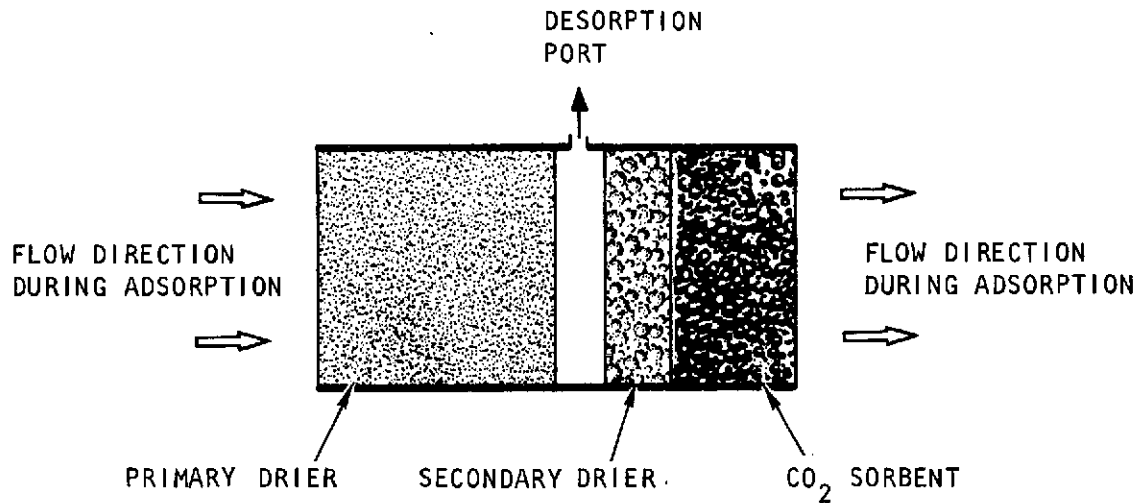
a. CENTERPOINT DESORPTION
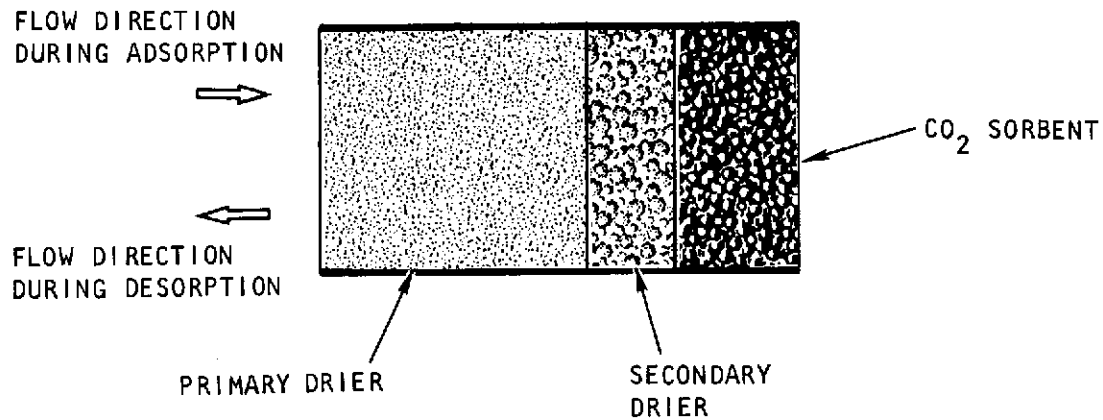
b. COUNTERFLOW DESORPTION

S-80938

Figure 4-5. Sorbent Desorption Approaches

of the desiccant. However, the desorption pressure over the CO_2 sorbent and also over the secondary predrier is relatively high because of the pressure drop through the bed during desorption.

Centerpoint desorption offers the advantages of lower pressure over the CO_2 sorbent and secondary predrier while preserving the advantages of the CO_2 purge over the secondary drier.

An analysis was made to determine sorbent weight and gas loss penalty for both approaches. Table 4-2 gives sorbent weight and gas loss for both bed configurations. In calculating cabin gas loss, it was assumed that the O_2 and N_2 pressures were equilibrated between the adsorbing and desorbing beds immediately prior to bed switchover. This is done by isolating both canisters and exposing the loaded bed to the desorbed bed for a few seconds prior to a cycle switchover.

TABLE 4-2

COMPARISON OF DESORPTION APPROACHES

Desorption Technique	Centerpoint Desorption	Counterflow Desorption
CO_2 sorbent (4A binderless) weight, lb/bed	4.2	5.95
Desiccant (silica gel) weight, lb/bed	9.0	8.55
Total sorbent weight, lb/bed	13.2	14.5
O_2-N_2 gas loss, lb/day	7.05	9.82

In this manner the bed saturated with cabin gases at the end of the adsorption period will be desorbed of roughly half of the adsorbed cabin gases.

The lower pressure achieved over the CO_2 sorbent with centerpoint desorption results in a higher sorbent working capacity and therefore a considerably smaller 4A binderless bed (4.2 lb versus 5.95 lb). On the other hand, the total desiccant necessary is increased because of the absence of gas

stripping in the primary drier. The net effect is a smaller sorbent bed with centerpoint desorption; more important is the lower gas loss because of the smaller quantity of 4A required.

On this basis, centerpoint desorption is recommended.

BED PUMPDOWN

Overboard gas losses could be reduced to a minimum by pumping down the sorbent beds prior to exposure to vacuum. Figure 4-6 shows this approach. The weight penalty of such a scheme will depend on the final bed pressure, since lower pressures will result in lower gas losses but higher pumping power and fixed equipment weight. Data generated under Contract NAS 9-11592 and presented in AiResearch Report 71-7553 shows that a final pressure of 1.0 psia is about optimum for this scheme.

In this case, the adsorption period will be longer than the desorption period to account for pumpdown time so that bed size will increase. To minimize power, a pumpdown time of 3 min. was assumed for a total half-cycle time of 9 min. Significant data for this system is listed in Figure 4-6. As shown, this system weighs about 30 lb more than the baseline (see Figure 4-4). Although a 70-lb reduction is gained through cabin gas conservation, the higher weight is due mainly to the pump (fixed weight and power consumption) and also to the larger bed size.

Lowering half-cycle time would reduce the equivalent weight of the pump-down system. This will result in shorter valve life. In view of the added complexity introduced by the pump, this approach is not recommended for Shuttle application.

SORBENT THERMAL MANAGEMENT

A regenerable sorbent system works on the principle that the sorbent capacity for the sorbate can be changed by pressure and temperature swings. Desorption can be accomplished by pressure swing alone, as in the baseline adiabatic system described previously. In such a bed, the sorbent temperature will increase during adsorption and drop during desorption due to the thermal energy exchange during the adsorption/desorption process. These temperature changes result in reduced sorbent working capacity.

AIRESEARCH MANUFACTURING COMPANY
Los Angeles, California

CANISTER WEIGHT: 33 LB
PUMP WEIGHT: 7 LB
GAS LOSS: 0.89 LB/DAY
PUMPING POWER: 120 WATTS
POWER PENALTY: 0.37 LB/7-DAY
EQUIVALENT WEIGHT (4-BED SYSTEM, TANKAGE AND POWER): 268 LB

PRIMARY DRIER

DESORPTION PLENUM

FLOW DIRECTION DURING ADSORPTION

CO_2 SORBENT

SECONDARY DRIER

PUMP

TO TIMER

TO CABIN

TO VACUUM

s-80939
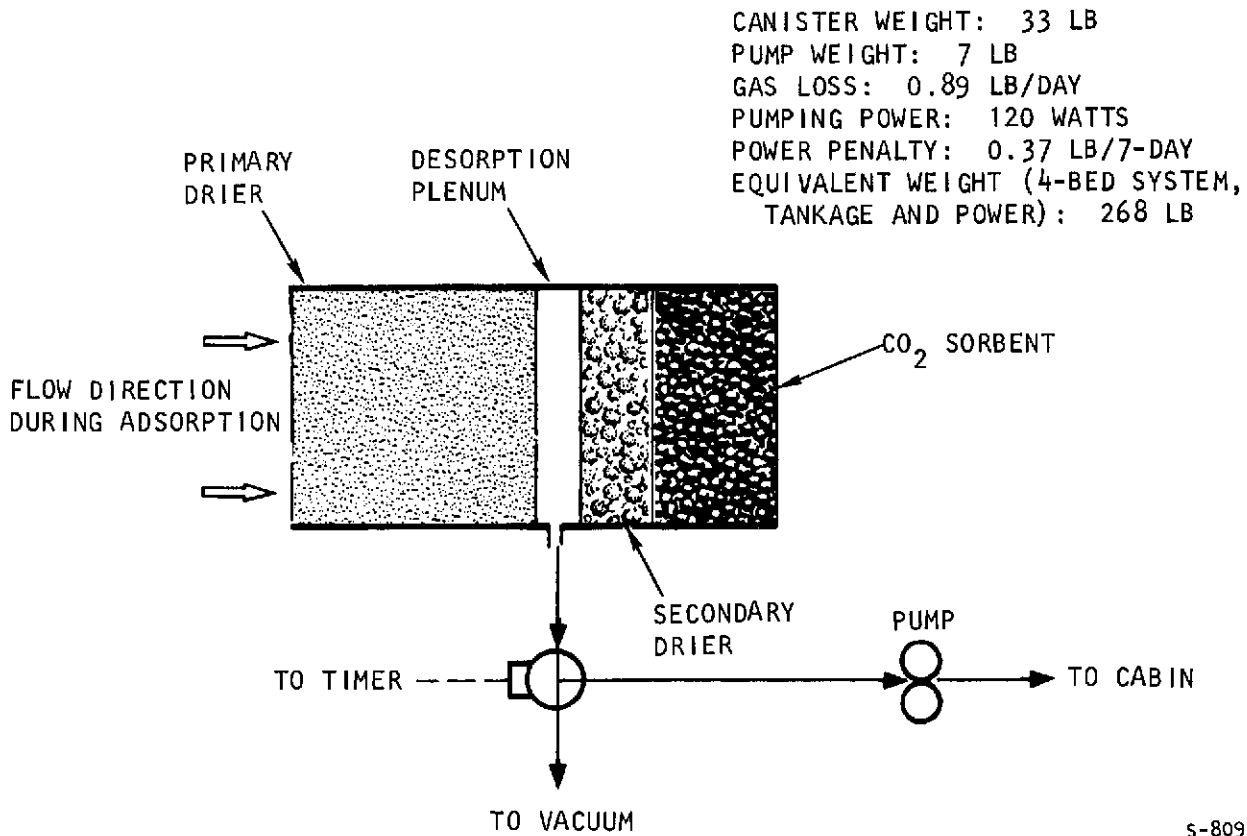
Figure 4-6. Adiabatic Bed with Pumpdown Prior to Desorption

40<

Two approaches were considered using sorbent bed thermal management in an effort to increase effective capacity by temperature control:

(a) Thermal swing beds where the sorbents are cooled during adsorption and heated during desorption. Here the sorbent is packed within the finned passages of heat exchanger. Heating and cooling are effected by circulating hot or cold coolant in heat exchanger passages adjacent to those where the sorbent is located. Figure 4-7 is a schematic of such a bed pair. Figure 4-7 shows a 4-man bed pair of a thermal swing system. The redundant water coolant loop passages and valving are not shown. For 10-man operation, two such systems will be required for a total of 4 beds.

(b) Thermally coupled beds where the adsorbing and desorbing beds are packed on either side of a heat exchanger so that the heat released in the adsorbing bed is transferred directly into the adjacent desorbing bed. This method of operation provides quasi-isothermal conditions while eliminating the requirements for separate coolant passages. Figure 4-8 is a schematic of this arrangement.

Thermal Swing System

The coolant temperatures used during adsorption and desorption were taken as 50° and 110^OF, respectively, corresponding to effective bed temperatures of 60° and 100^OF. Coolant at these temperature levels should be available from the cabin water coolant loop.

The characteristics of the thermal swing systems are summarized in Figure 4-7. The effective capacity of the 4A molecular sieve is increased by a factor of three by comparison with the adiabatic system. This results in a considerable reduction in sorbent requirement and also in a significant reduction in overboard gas loss. The relative weight of the canisters, however, is considerably higher because of the presence of heat transfer surfaces and manifolds, and fluid hold up. Canister weight is estimated at 25 lb (wet).

In the adiabatic system, the cabin humidity is removed in the sorbent bed so that the latent load does not appear in the cabin heat exchanger nor in the water coolant loop. In the thermal swing system the latent load is dumped in the coolant loop. In addition, cold coolant at 50^OF is necessary to reduce the

PROCESS
AIR
RETURN

PROCESS
AIR
INLET

TO VACUUM

GAS SELECTOR
VALVE

N$_2$
SWITCHOVER
VALVE

DESORBING BED

COOLANT
SELECTOR
VALVES

VALVE
ACTUATOR

TO CABIN

ADSORBING BED

HOT
COOLANT

TO CABIN

COLD
COOLANT

CONTROLLER
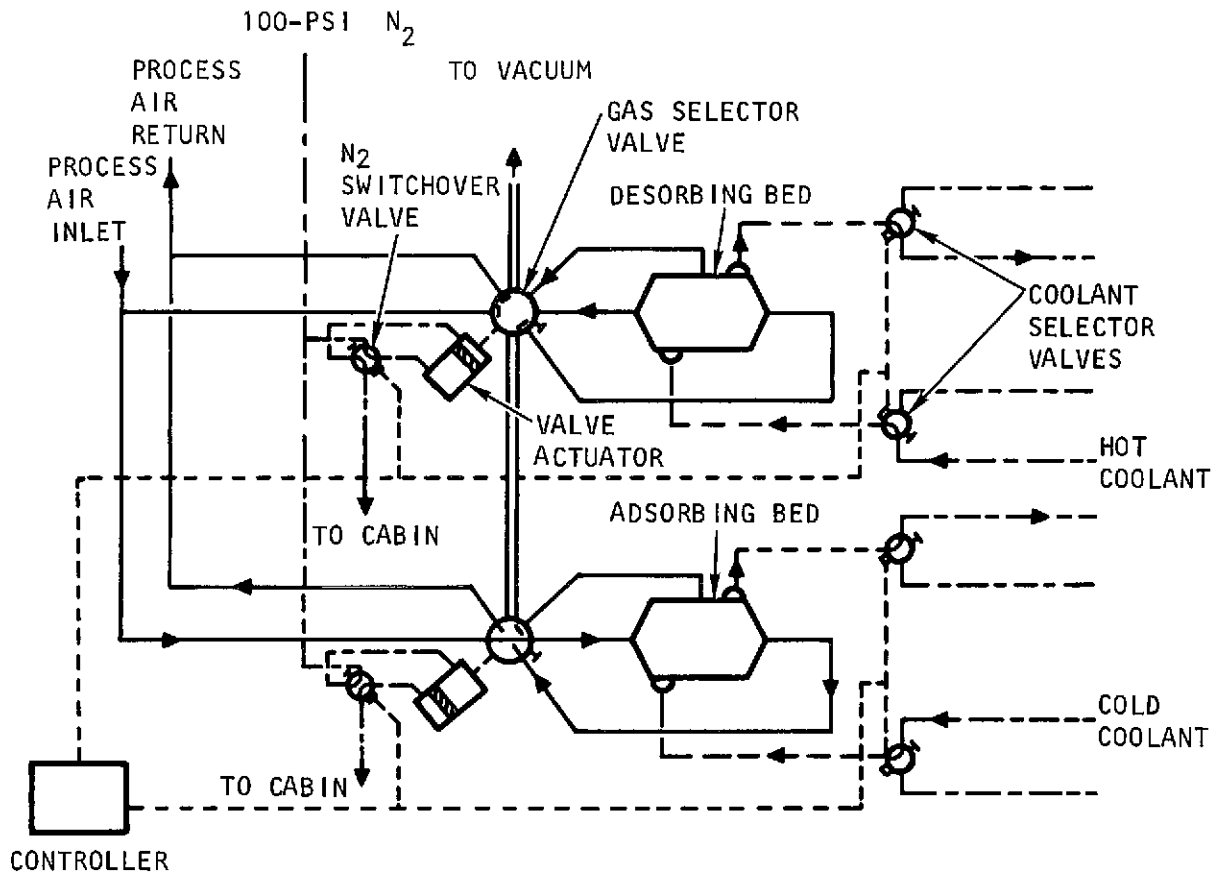
BED CHARACTERISTICS (4-MAN DESIGN)

CENTER POINT DESORPTION
COLD COOLANT TEMPERATURE: 50°F
HOT COOLANT TEMPERATURE: 110°F
SILICA GEL DESICCANT: 5.0 LB/BED
4A BINDERLESS: 1.5 LB/BED
GAS LOSS: 2.33 LB/DAY

SYSTEM CHARACTERISTICS

NUMBER OF BED PAIRS: 2
7 DAY GAS LOSS INCLUDING TANKAGE: 28.3 LB/7-DAY
EQUIPMENT FIXED WET WEIGHT: 189 LB
COOLING PENALTY: 9.4 LB
SYSTEM EQUIVALENT WEIGHT: 227 LB

S-80940

Figure 4-7. Thermal Swing System Arrangement

TO VACUUM

VENT TO
CABIN

PROCESS
GAS
RETURN

ACTUATOR
CONTROL
VALVE

100 PSI N_2

PROCESS
GAS
INLET

VALVE
ACTUATOR

GAS SELECTOR
VALVE

THERMALLY COUPLED
ADSORBING AND
DESORBING BEDS

CONTROLLER
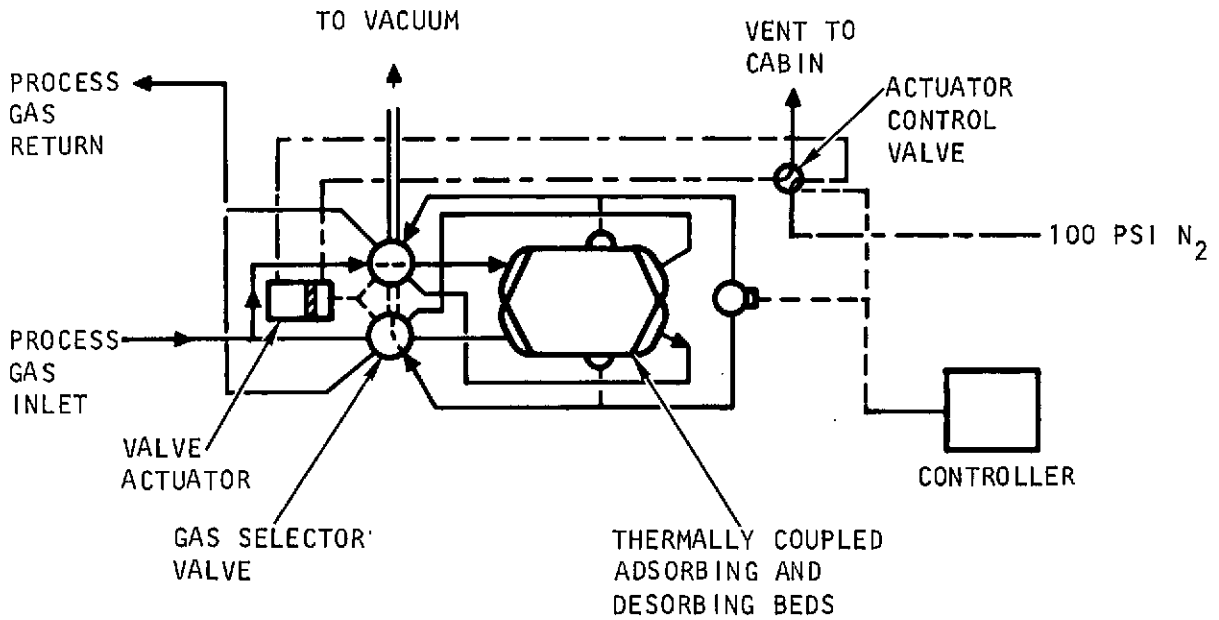
BED CHARACTERISTICS (4-MAN DESIGN)

CENTERPOINT DESORPTION
SILICA GEL DESICCANT: 5.4 LB
4A BINDERLESS: 3.2 LB
GAS LOSS: 5.4 LB/DAY

SYSTEM CHARACTERISTICS

THREE 4-MAN MODULES
7-DAY GAS LOSS INCLUDING TANKAGE: 60 LB
EQUIPMENT WEIGHT: 198 LB
SYSTEM EQUIVALENT WEIGHT: 258 LB

S-80941

Figure 4-8. Thermally Coupled Sorbents

bed temperature from $110^\circ F$ during desorption to $60^\circ F$ during adsorption. This deteriorates the performance of the water coolant loop and results in a drop in water temperature at the system interchanger as well as an increase in the coolant loop low temperature load. Since low temperature loads are a determining factor in sizing the interchanger, the weight penalty associated with cooling the adsorbing bed can be evaluated on that basis. The load from the adsorbing bed is estimated at 2750 Btu/hr.

The overall equivalent weight of the 4-bed thermal swing system arrangement is estimated at 227 lb, which is about 10-lb lighter than the weight of the baseline approach. However, this 10-lb advantage is more than offset by the higher reliability and flexibility of operation offered by the baseline system. For this reason, the thermal swing system arrangement is not recommended for Space Shuttle application. Note also that the cost of the thermal swing system will be more than double that of the adiabatic (Ref. AiResearch Report 71-7553, Contract NAS 9-11592).

Thermally Coupled Beds

Since the two beds are thermally coupled, both are required for normal operation; furthermore, valve failure considerations necessitate the use of three sets of beds. This constitutes a significant fixed weight penalty for this approach. Although the gas loss penalty is reduced significantly because of the lower 4A sorbent requirement, the overall weight of the system is higher than that of the adiabatic approach. The acquisition cost of the system will be higher because of the bed and gas selector valve construction. This approach is not recommended.

SYSTEM ARRANGEMENT CONSIDERATIONS

Previous discussions were based on a 4-bed system where two beds are operational with a 4-man crew and all four beds are necessary to handle the latent and CO_2 load of 10 men. This system arrangement, shown in Figure 4-1, was used as baseline for the purpose of comparison.

An alternate approach was considered and compared with the baseline in terms of varying crew size and system reliability. The alternate approach is based on the use of three adiabatic beds with two beds capable of removing the water vapor and CO_2 produced by 10 men. The third bed constitutes a redundant module.

Figure 4-9 shows the 3-bed system equivalent weight as a function of cycle time. Canister weight and gas loss data were taken from Figure 4-3. Although a 4-min half-cycle time is optimum on the basis of weight, a 6-min half-cycle time was selected as optimum in terms of selector valve life. The 4-min half-cycle would correspond to 2520 cycles for a 7-day mission. This is well within the capability of equipment such as the gas selector valve developed for the Airlock RCRS. However, considering the 100 Space Shuttle missions, the valve would require frequent replacement during the 10-year operational life of the Space Shuttle. This approach is acceptable, although not desirable. Here a compromise solution appears preferable. In the present state of technology, 100,000 cycles could be attained with minimum development on a gas selector valve of the size of the RCRS valve. A 100,000-cycle valve would require changing twice in the 10-year life of the Space Shuttle with a half-cycle time of 6 min. From a maintenance standpoint this is completely acceptable; only a very small weight penalty is incurred by increasing the cycle time from 4 to 6 min.

The characteristics of the 4- and 3-bed system arrangements with 4- and 10-man crews are shown in Tables 4-3 and 4-4. Data is presented for normal operation and also for situations corresponding to single and dual failures. Note that the design point for the 4-bed arrangement is the 4-man crew while the 3-bed arrangement design crew size is 10 men.

The size of the CO_2 removal portion of the bed was increased slightly for the 4-bed design. This was done to increase the effectiveness of the system so that a pCO_2 of 5.0 mm Hg could be achieved with a 10-man load.

The total weights for both approaches are listed below for the 4- and 10-man missions. The weight listed includes fixed equipment weight and gas loss penalty.

	4-Man, 7-Day Mission	10-Man, 7-Day Mission
4-Bed Design	261	354
3-Bed Design	390	426

The 3-bed design is substantially heavier than the 4-bed approach; however, it provides design performance after one failure, and performance is degraded only after a second failure with a 10-man crew. In this case the 3- and 4-bed systems have comparable performance.
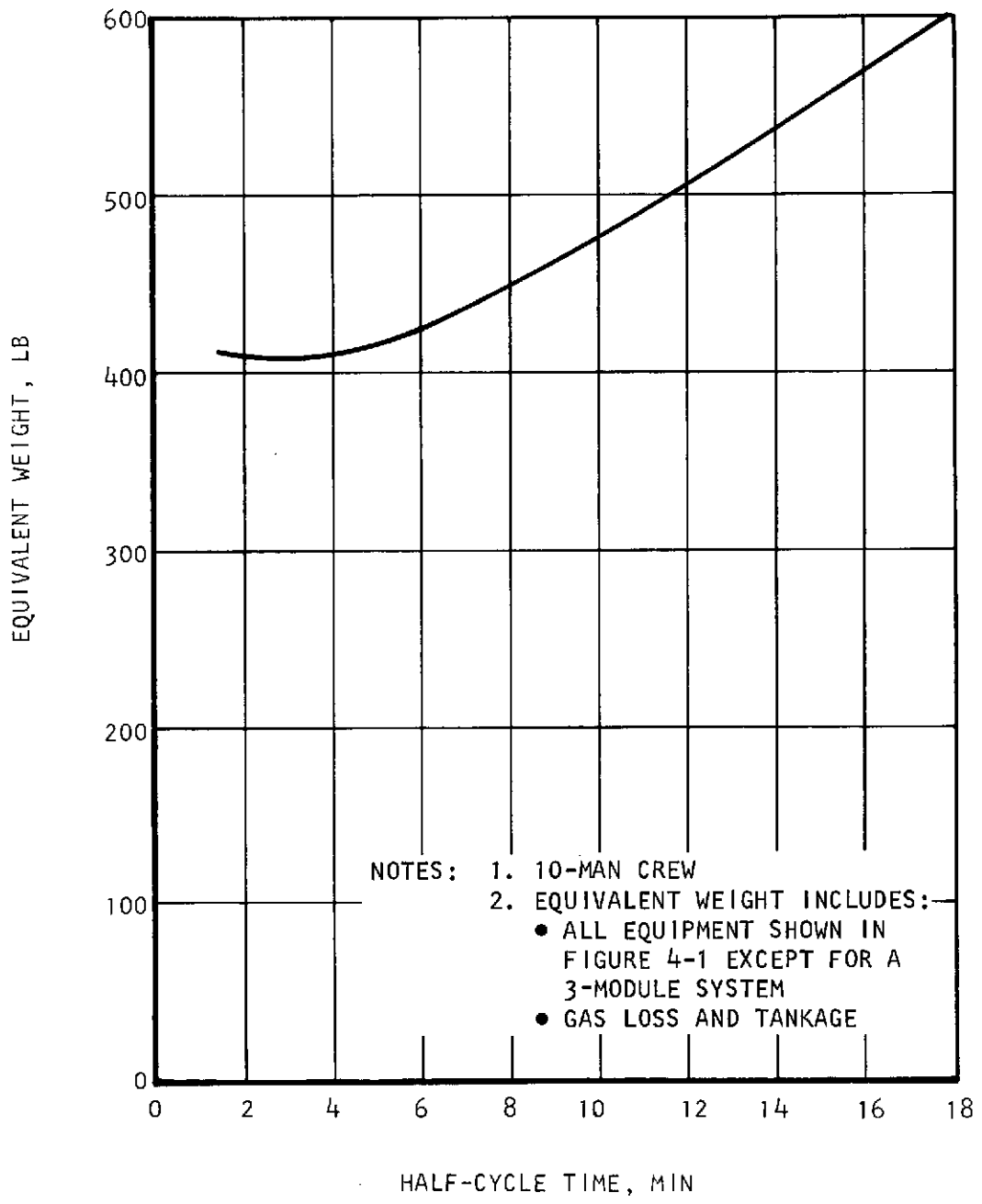
Figure 4-9. 10-Man Design Optimization

S-81005

TABLE 4-3

4-BED ADIABATIC SYSTEM CHARACTERISTICS

	4-Man Operation (Design Point)	10-Man Operation
CO_2 removal rate, lb/hr	0.417	0.95
H_2O removal rate, lb/hr	0.891	1.8
Beds on stream	2	4
Beds on standby	2	0
Cabin dewpoint, $^{\circ}F$	53.0	53.2
Cabin pCO_2, mm Hg	4.4	5.0
Airflow rate, lb/hr	106.0	212.0
Half-cycle time, min	6.0	6.0
7-day gas loss including tankage, lb	93.0	186.0
Fixed equipment weight, lb	168.0	168.0
After First Failure		
Cabin pCO_2, mm Hg	4.4	6.66
Cabin dewpoint, $^{\circ}F$	53.0	60.3
After Second Failure		
Cabin pCO_2, mm Hg	4.4	8.9
Cabin dewpoint, $^{\circ}F$	53.0	71.5

TABLE 4-4

3-BED ADIABATIC SYSTEM CHARACTERISTICS

	10-Man Operation (Design Point)	4-Man Operation
CO_2 removal rate, lb/hr.	0.95	0.417
H_2O removal rate, lb/hr	1.8	0.891
Beds on stream	2	2
Beds on standby	1	1
Cabin dewpoint, °F	53.0	53.0
Cabin pCO_2, mm Hg	5.0	4.3
Airflow rate, lb/hr	217.0	106.0
Half-cycle time, min	6.0	12.3
7-day gas loss including tankage, lb	193.0	157.0
Fixed equipment weight, lb	233.0	233.0
After First Failure		
Cabin pCO_2, mm Hg	5.0	4.3
Cabin dewpoint, °F	53.0	53.0
After Second Failure		
Cabin pCO_2, mm Hg	9.1	4.6*
Cabin dewpoint, °F	71.0	51.5*

*Half-cycle time and flow rate adjusted to 6 min. and 217 lb/hr (normal)

GARRETT AIRESEARCH MANUFACTURING COMPANY
Los Angeles, California

48<

Examination of the 10-man crew data of Table 4-3 shows that after the first failure pCO_2 and dewpoint will increase to 6.6 mm Hg and $60.3^{\circ}F$, respectively. Although this represents a performance degradation, the levels are within the maximum specified for normal operation and are acceptable. After a second failure, the contaminant levels are comparable to those achieved with the heavier 3-bed design.

For these reasons the 4-bed system is recommended for Space Shuttle application.

4-Bed System Control

Referring to Figure 4-1, it is apparent that the system flow rate must be reduced to maintain cabin dewpoint above the minimum value specified when the four men are sleeping. This can be done by incorporation of a manual valve in the process air line to the regenerable system. Figure 4-10 shows the recommended location of the regenerable system relative to other components of the cabin air circuit. At this location the entire fan ΔP is available for the design of the bed and thus provides flexibility in the detail design of the entire package.

The 4-bed adiabatic system was selected for Space Shuttle humidity and CO_2 control. The data presented previously were used in the planning and in the conduct of the development program described in Section 5 of this report.
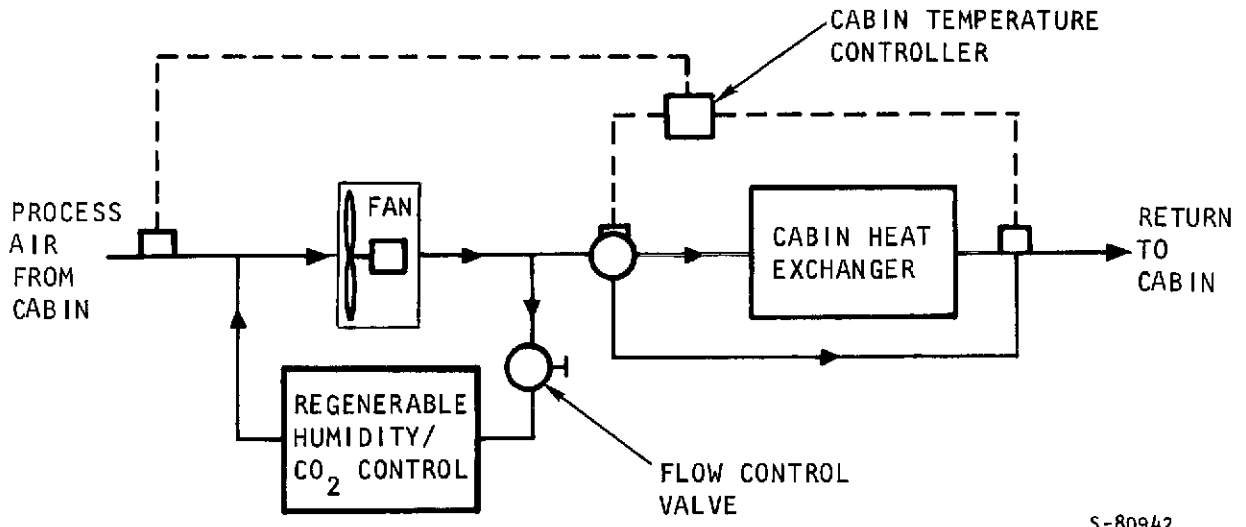
Figure 4-10. Recommended Location of the Regenerable Desiccant System

50<

SECTION 5

DEVELOPMENT TESTS

GENERAL

This section describes the test program conducted to verify the design of the 4-bed system optimized through computer analyses using the basic sorbent equilibrium and dynamic data presented in Section 2.

Reference is made to AiResearch Report 72-8851, Desiccant Humidity Control System Test Plan, which describes in detail the setup, instrumentation, and procedure for the full-scale bed testing. A sketch of the full-scale bed from the referenced report is shown in Figure 5-1. Sorbent weights and mesh sizes loaded in the test canisters were as follows: primary drier, (8.06 lb silica gel, 6 to 12 mesh); secondary drier, (3.0 lb silica gel, 6 to 12 mesh); and CO_2 sorbent, (5.25 lb 4A binderless molecular sieve, 8 to 10 mesh).

For instrumentation point reference and analysis purposes, the bed length was divided arbitrarily into 18 nodes or zones, as is shown in Figure 3-1. The process gas flow inlet was identified as node 18 and outlet as node 1. The desiccant bed consisted of a primary and a secondary section separated by the desorption plenum. This center desorption configuration was established to provide optimum desorption pressure for the secondary desiccant and for the CO_2 sorbent.

As a prelude to the long term development test, a series of three short tests was conducted over a continuous three-day period (72 hours) to shake down the test rig and instrumentation, check out system performance, and to establish a good correlation between test performance and computer predictions.

PRELIMINARY TESTING

Table 5-1 presents the operating conditions that were established for the system checkout testing.

THE SECOND CAN
IS A MIRROR IMAGE OF
THE FIRST

1-1/8 IN. O.D.
INLET AND OUTLET

STAINLESS STEEL
STANDARD FLANGE
AND COVER

1 IN. SOLENOID VALVES
ARE WELDED TO CANISTER
INLET AND OUTLET

INLET

8-3/8 IN. ID
STAINLESS PIPE

BAND HEATER (110 VAC) FOR THE
SILICA GEL SECTION OF CANISTER
NO. 2 ONLY (1-1/2 IN. WIDE,
8-1/2 IN. ID)

3/4 IN. HOLES
AROUND CANISTER
CIRCUMFERENCE

2-1/8 IN. DESPORTION PORT
FOR GAS SELECTOR VALVE

15-1/4
IN.

DESORPTION PLENUM
(2-1/2 IN. WIDE)

MOLE SIEVE BAND HEATERS
(110 VAC) LOCATED ON
BOTH CANISTERS (1-1/2 IN.
WIDE, 8-1/2 IN. ID)

1/4 IN. THICK
STAINLESS PLATE

S-81011

Figure 5-1. System Test Canister Design

TABLE 5-1

OPERATING CONDITIONS FOR SYSTEM CHECKOUT

Parameter	Day 1	Day 2	Day 3
Chamber CO_2 injection rate, lb/hr	0.46	0.24	0.46
Chamber pressure, psia	14.7 to 14.8	14.75 to 14.84	14.75
Chamber temperature, $^\circ F$	70 to 75	64 to 68	65
Bed inlet flow rate, lb/hr	97	51	96
Bed inlet dewpoint temp., $^\circ F$	52	58 to 60	58 to 60
Bed inlet temperature, $^\circ F$	62 to 65	60 to 62	60 to 82
Chamber PO_2, mm Hg	164	164	164
Chamber diluent gas	N_2	N_2	N_2

Test day 1 covered a period of 24 hours, during which the two-bed adiabatic system was operated for a total of 222 half cycles. During this period the desiccant bed performed as expected, removing practically all simulated metabolic humidity load from the process gas stream; but, for reasons not immediately apparent at the time, the CO_2 sorbent did not function as predicted, yielding a carbon dioxide partial pressure of 7.6 mm Hg at the canister inlet. In the meantime, it was decided to run the system at a lower mass flow rate to provide additional data for computer correlation.

During test day 2, a review of the test data revealed that desorption pressures were not as low as anticipated, and corrective action was taken to improve the vacuum pumping facility while the test was underway. These efforts resulted in achieving the desired desorption pressures, and the second day test run was terminated after 177 half cycles.

On test day 3 the system was operated at the original high flow conditions for a total of 21 half cycles. In contrast to the test chamber carbon dioxide partial pressure of 7.6 mm Hg obtained on the first day, during the third day test run it decreased to an average value of 6.8 mm Hg, which can be attributed to the improvements made in the vacuum pumping system. However, lower carbon dioxide partial pressures were not obtained apparently because a portion of the CO_2 sorbent had become poisoned with water during the first day due to the faulty vacuum system.

The results of the preliminary testing, together with computer correlation data, are presented in Figures 5-2 through 5-7.

Figure 5-2 presents representative test data for CO_2 partial pressures at the bed inlet and outlet plotted from test day 1 results. The bed inlet pCO_2 at the end of the 6-min half-cycle was approximately 7.6 mm Hg, instead of 5.0 mm Hg as expected, because of the relatively high desorption pressures encountered during test day 1 as shown in Figure 5-3.

Carbon dioxide partial-pressure data obtained during test day 2, after improvements were made in the vacuum pumping system, is shown in Figure 5-4. Here, with a reduced CO_2 input and flow rate, the system operated to maintain the inlet pCO_2 at 5.0 mm Hg. If the CO_2 adsorbent had not been poisoned during test day 1, the pCO_2 values would probably have been lower, approaching the computer predicted performance. The desorption pressure data plot shown in Figure 5-5 reflects the improved vacuum system operation in contrast to the data shown in Figure 5-3.

Figure 5-6 presents the pCO_2 data obtained on test day 3. Here, only the bed outlet partial-pressure data is shown, which agree closely with the computer prediction. The system was operated for only 21 cycles during test day 3, since the correlation between system performance and computer prediction appeared to be reasonably close. The CO_2 analyzer was not reinstrumented from the previous day's setup to record the inlet partial pressure. It is assumed that the inlet pCO_2 was close to an average value of 6.8 mm Hg as predicted by the computer. Desorption pressure data for test day 3 are shown in Figure 5-7. Desorption pressures at Nodes 18 and 1 (bed inlet and outlet, respectively) are lower than those obtained on test day 1 shown in Figure 5-3, attesting to the improved vacuum system operation.

The concave upward characteristic of the pCO_2 curves in Figures 5-2, 5-4, and 5-6 result from the 80-cu-ft chamber used to simulate the Shuttle cabin. In the actual Shuttle with its 2000-cu-ft cabin, the bed inlet pCO_2 will remain nearly constant.

INLET FLOW CONDITIONS (BED NO. 2)

$\dot{M}$ = 97 LB/HR
DEWPOINT = 52°F
CO_2 FLOW = 0.46 LB/HR
PO_2 = 21 PERCENT
PRESSURE = 15.3 PSIA

CYCLE NO. 120

COMPUTER PREDICTED DATA

TEST DATA
BED NO. 2
INLET NODE 18

TEST DATA
BED NO. 2
OUTLET NODE 1

CYCLE NO. 176

COMPUTER PREDICTED DATA

PCO_2, MM HG

TIME, MIN

S-81077
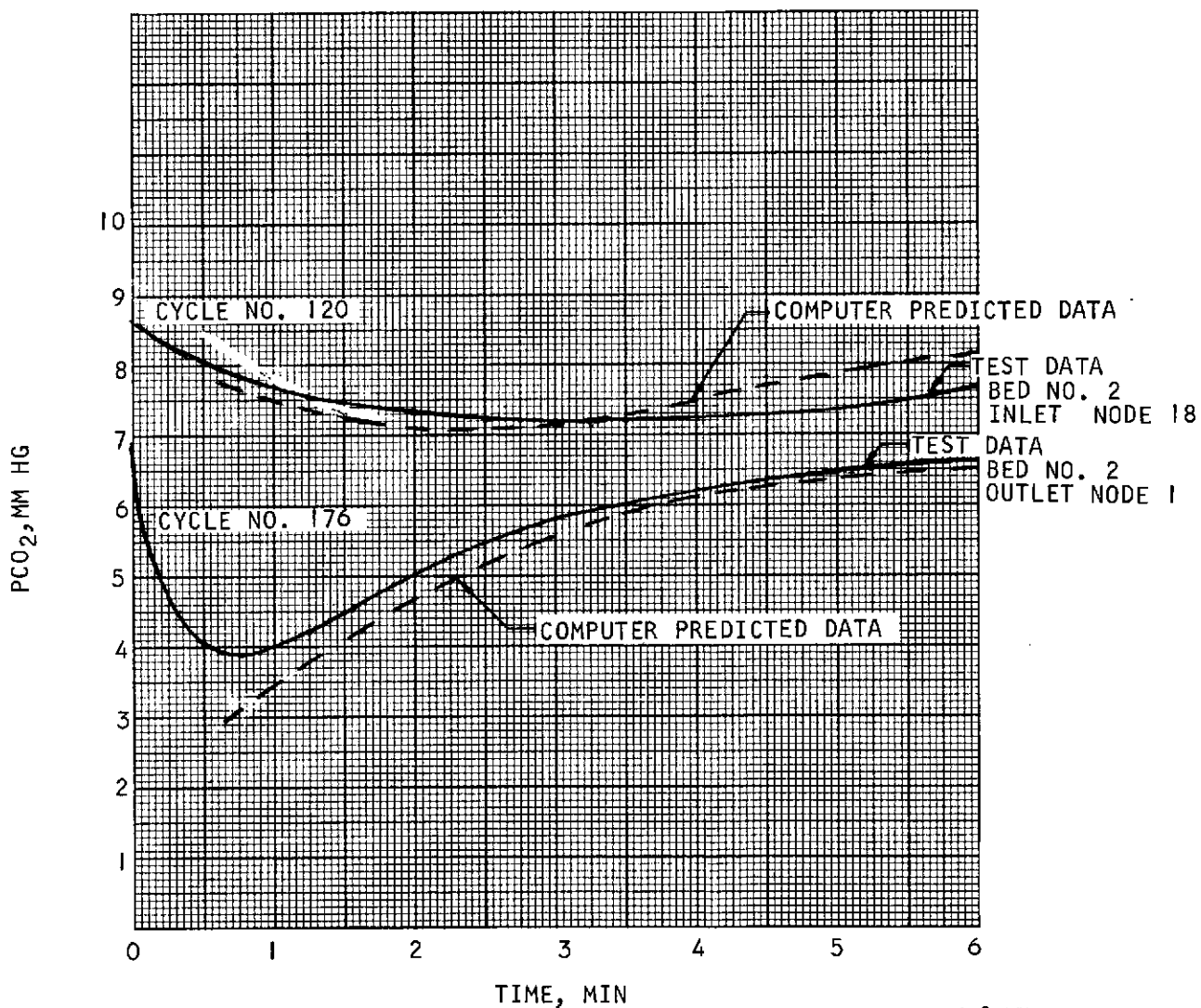
Figure 5-2. CO_2 Adsorption Data, Test Day No. 1

INLET FLOW CONDITIONS (BED NO. 2)

M = 97 LB/HR
DEWPOINT = 52°F
CO_2 FLOW = 0.46 LB/HR
PO_2 = 21 PERCENT

CYCLE NOS. 170 TO 180
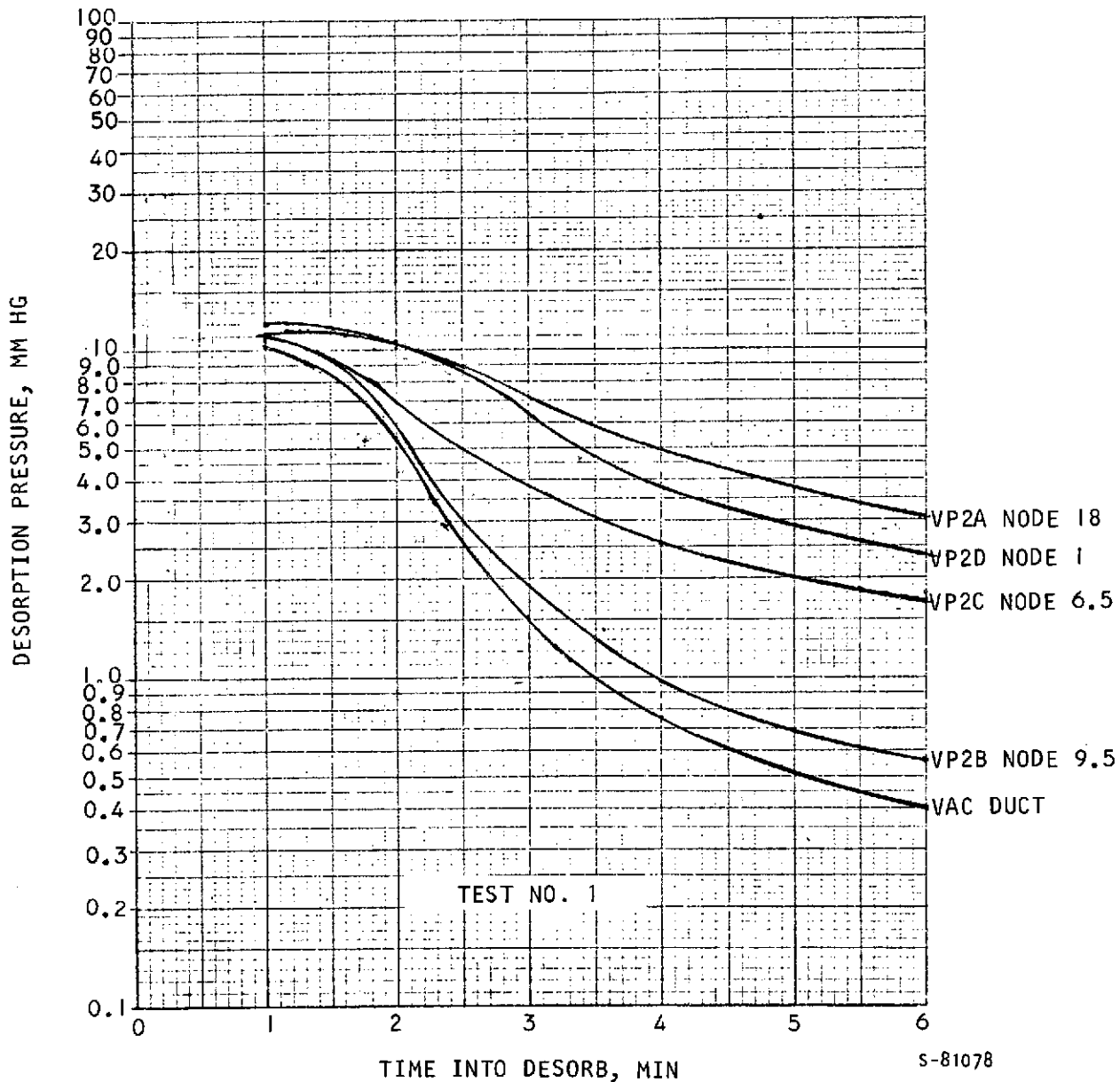
Figure 5-3. Desorption Pressure Data,
Test Day No. 1

INLET FLOW CONDITIONS (BED NO. 2)

$\dot{M}$ = 51 LB/HR
DEWPOINT = 58°F
CO_2 FLOW = 0.24 LB/HR
PO_2 = 21 PERCENT
PRESSURE = 14.85 PSIA
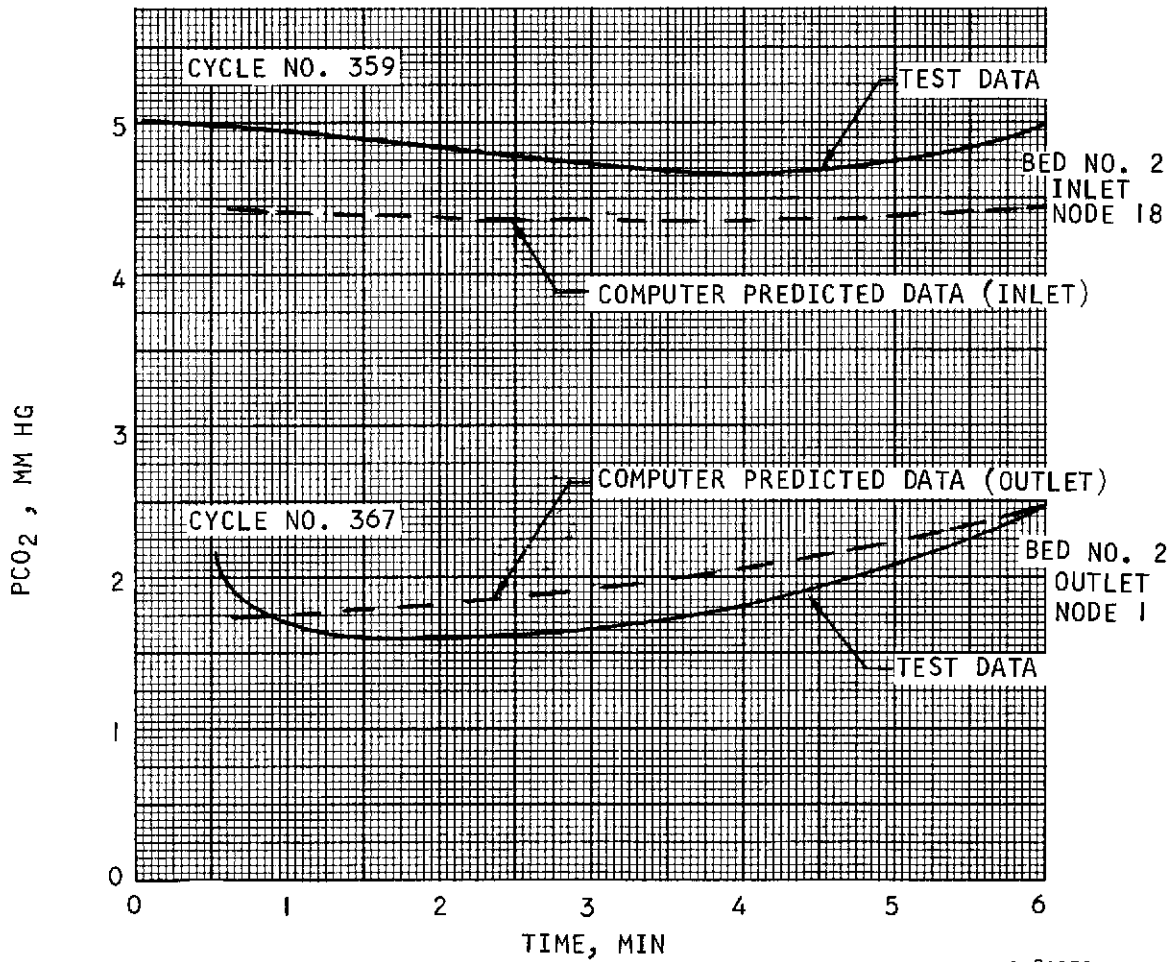
Figure 5-4. CO_2 Adsorption Data, Test Day No. 2

INLET FLOW CONDITIONS (BED NO. 2)

$\dot{M} = 51$ LB/HR
DEWPOINT = 58°F
CO_2 FLOW = 0.24 LB/HR
$PO_2 = 21$ PERCENT

CYCLE NOS. 373 to 379
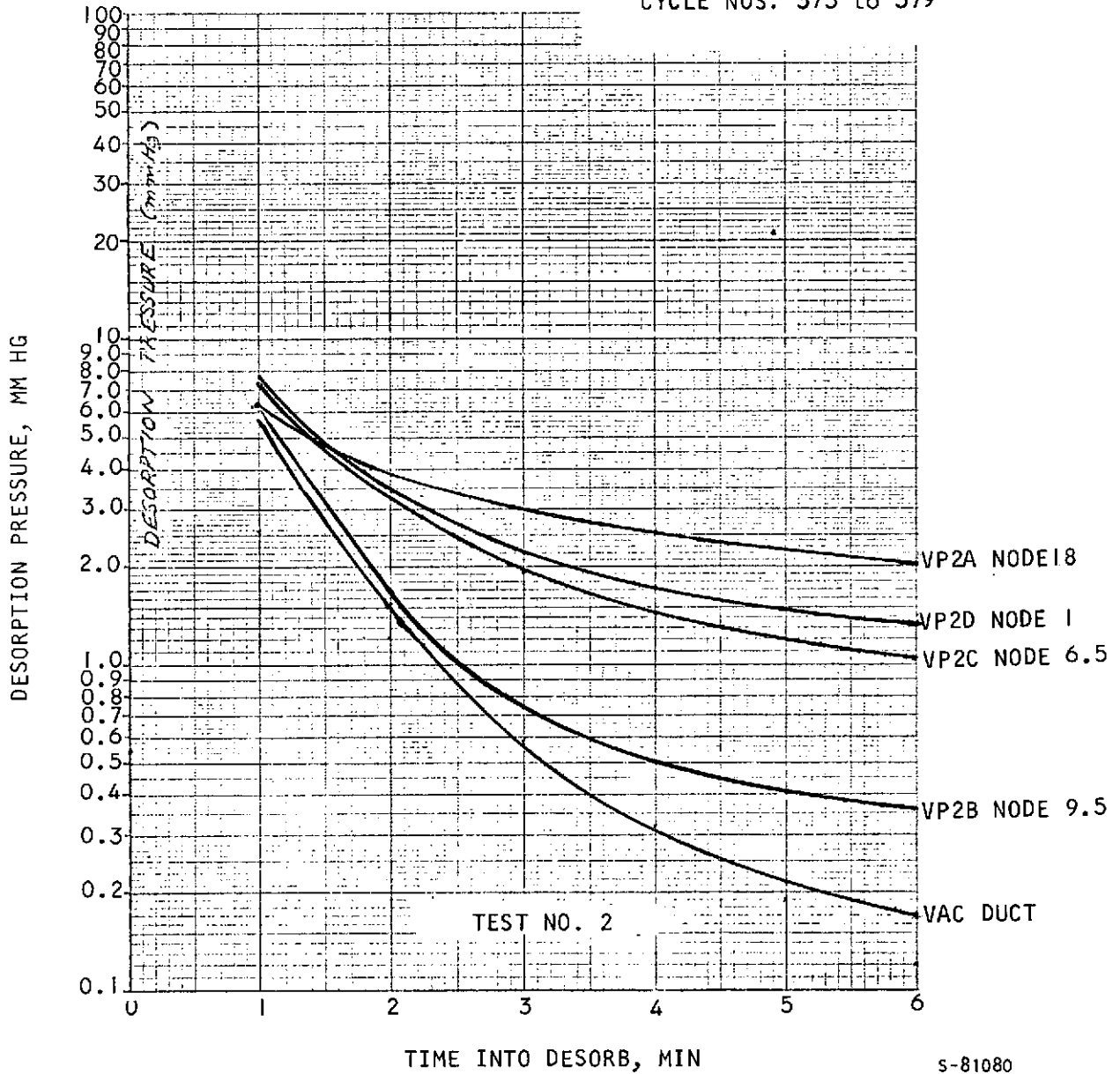
Figure 5-5. Desorption Pressure Data,
Test Day No. 2

INLET FLOW CONDITIONS (BED NO. 2)

$\dot{M}$ = 96 LB/HR
DEWPOINT = 60°F
CO_2 FLOW = 0.46 LB/HR
PO_2 = 21 PERCENT
PRESSURE = 15.5 PSIA
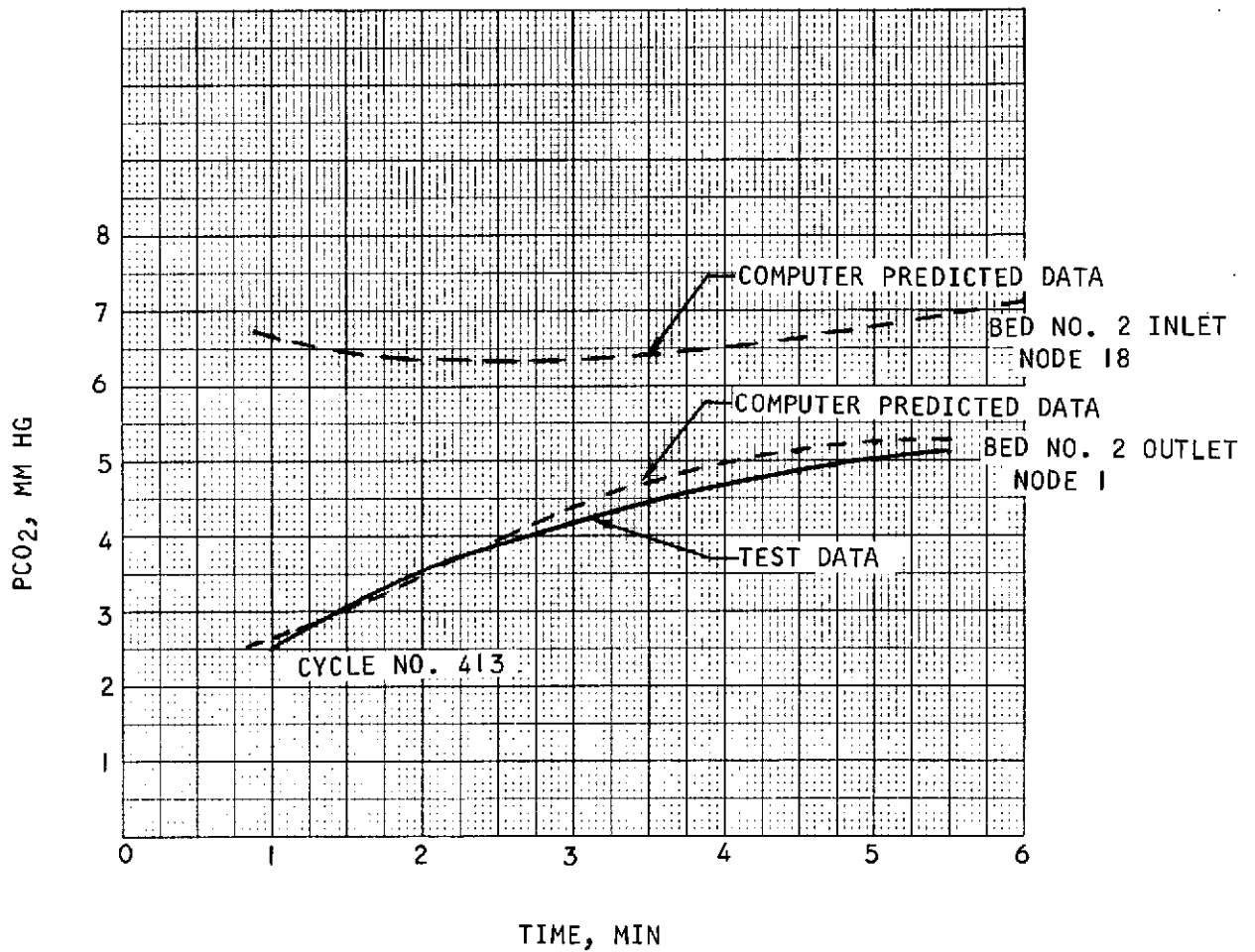
Figure 5-6. CO_2 Adsorption Data, Test Day No. 3

S-81081

INLET FLOW CONDITIONS

$\dot{M}$ = 96 LB/HR
DEWPOINT = 60°F
CO_2 FLOW = 0.46 LB/HR
PO_2 = 21 PERCENT
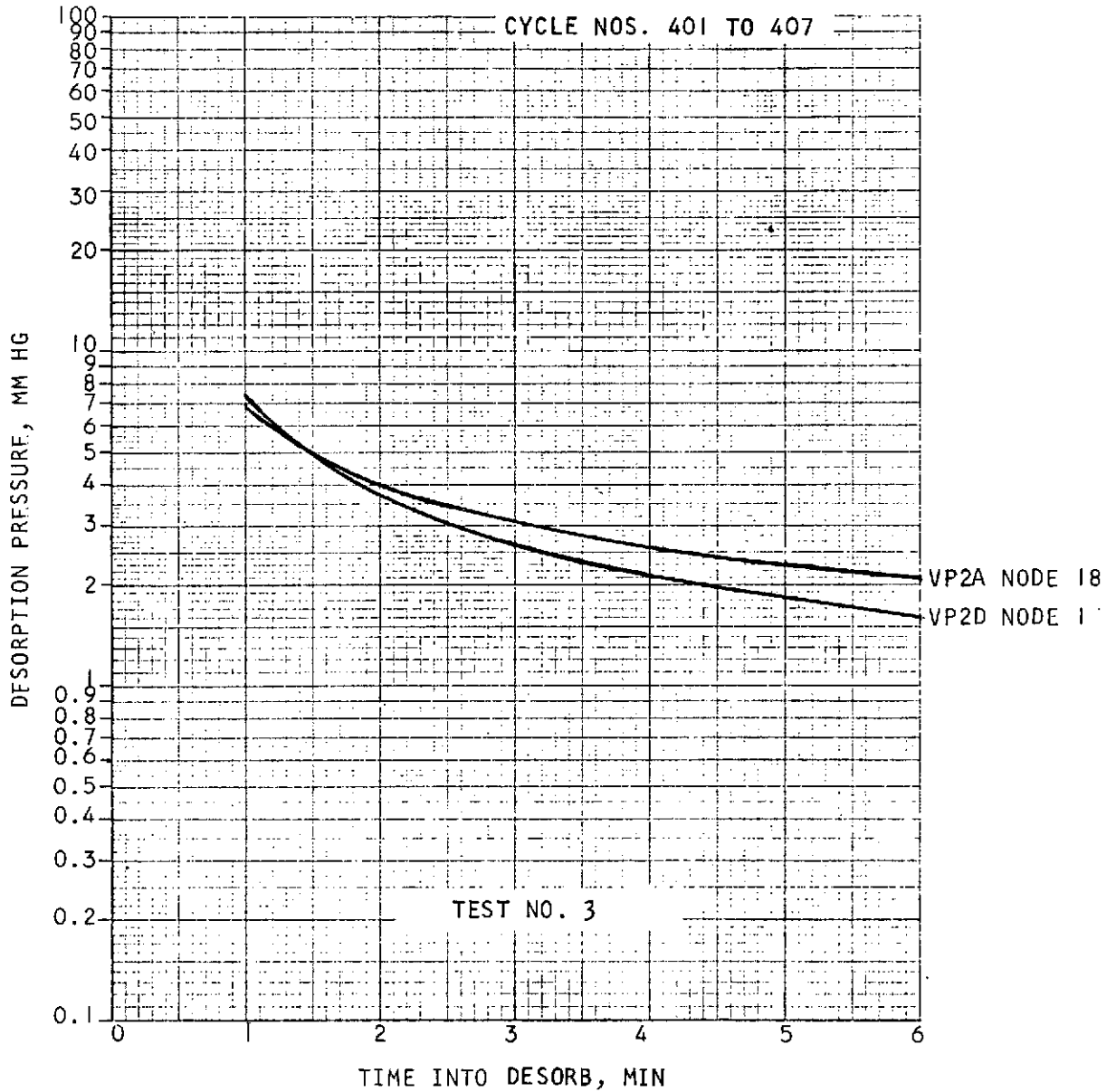
Figure 5-7. Desorption Pressure Data,
Test Day No. 3

S-81082

Because of the wide scatter in the preliminary run test data, the dewpoint temperatures have not been plotted. However, the data obtained showed dewpoint values ranging from $-40^\circ F$ to $-80^\circ F$ at the inlet face (node 6.5) of the molecular-sieve bed, leading to the conclusion that practically all the humidity load was removed.

DEVELOPMENT TESTING

Following the 3-day preliminary test described above, the beds were subjected to a prolonged bakeout, reinstalled in the test setup, and tested over an uninterrupted period of eight additional days.

Test conditions imposed on the system for test days 4 through 11 were as follows:

Parameter	Days 4 through 7	Days 8 through 10	Day 11
Chamber CO_2 injection rate, lb/hr	0.35	0.40	0.19
Chamber pressure, psia	14.8	14.8	14.8
Chamber temperature, $^\circ F$	66	68	66
Bed inlet flow rate, lb/hr	82	80 to 83	83
Bed inlet dewpoint temperature, $^\circ F$	53 to 54	52 to 56	48 to 52
Bed inlet temperature, $^\circ F$	62	62	65
Chamber PO_2, mm Hg	164	164	164
Chamber diluent gas	N_2	N_2	N_2
Number of half cycles	860	440	240

Typical test data obtained from the eight consecutive days of testing have been plotted and are shown in Figures 5-8 through 5-13.

The curves in Figures 5-8, 5-9, and 5-10 show representative adsorber inlet and output pCO_2 as a function of half-cycle time for Test Days 4, 10 and 11, respectively. The mass-transfer and diffusivity coefficients were adjusted by trial and error to obtain the close correlation between the computer performance prediction and the test data, as shown in Figure 5-8. In correlating computer
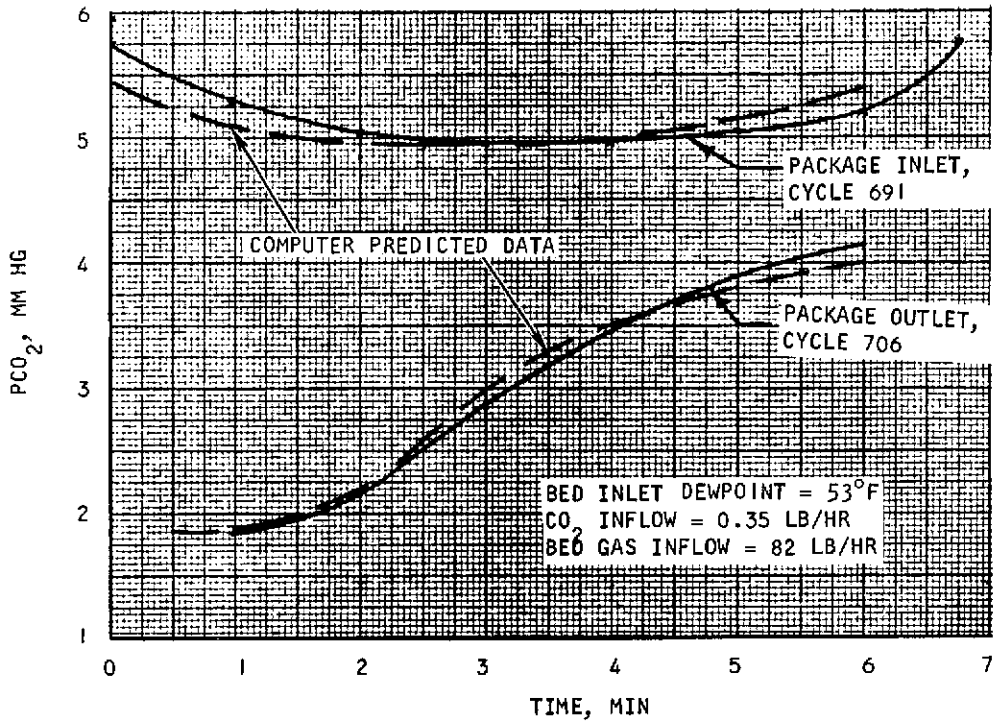
Figure 5-8. CO_2 Adsorption, Test Day 4
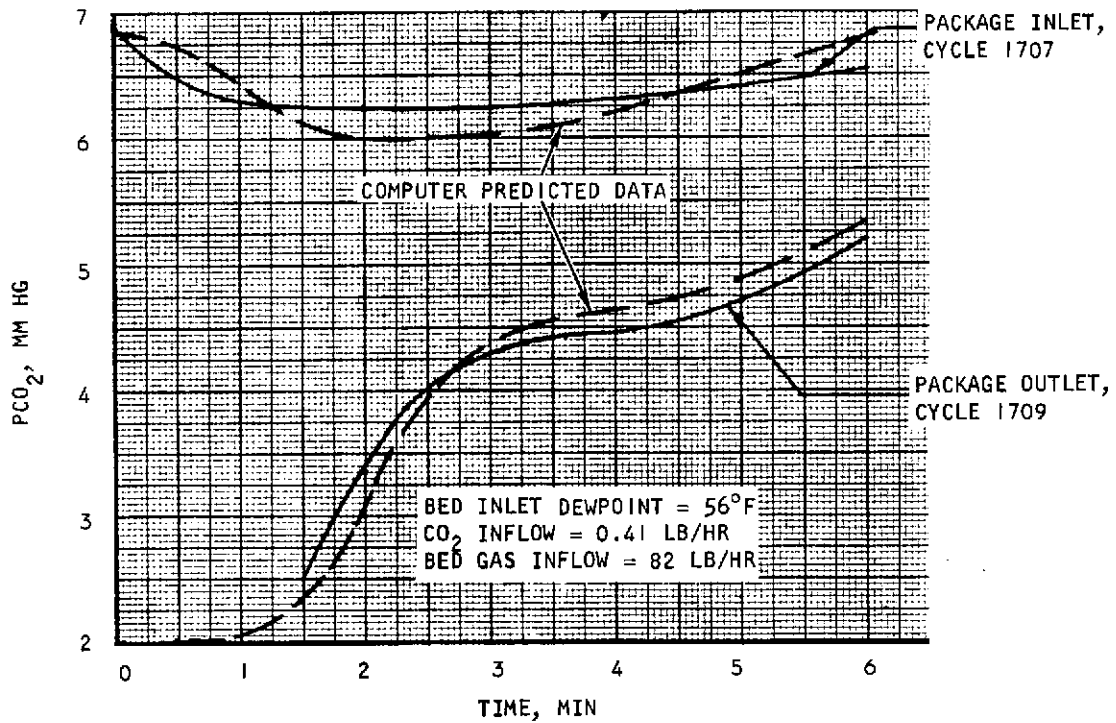
Figure 5-9. CO_2 Adsorption, Test Day 10

BED INLET DEWPOINT = 46°F
CO$_2$ INFLOW = 0.19 LB/HR
BED GAS INFLOW = 83 LB/HR

PACKAGE INLET, CYCLE 1952

COMPUTER PREDICTED DATA

PACKAGE OUTLET, CYCLE 1955

PCO$_2$, MM HG

TIME, MIN
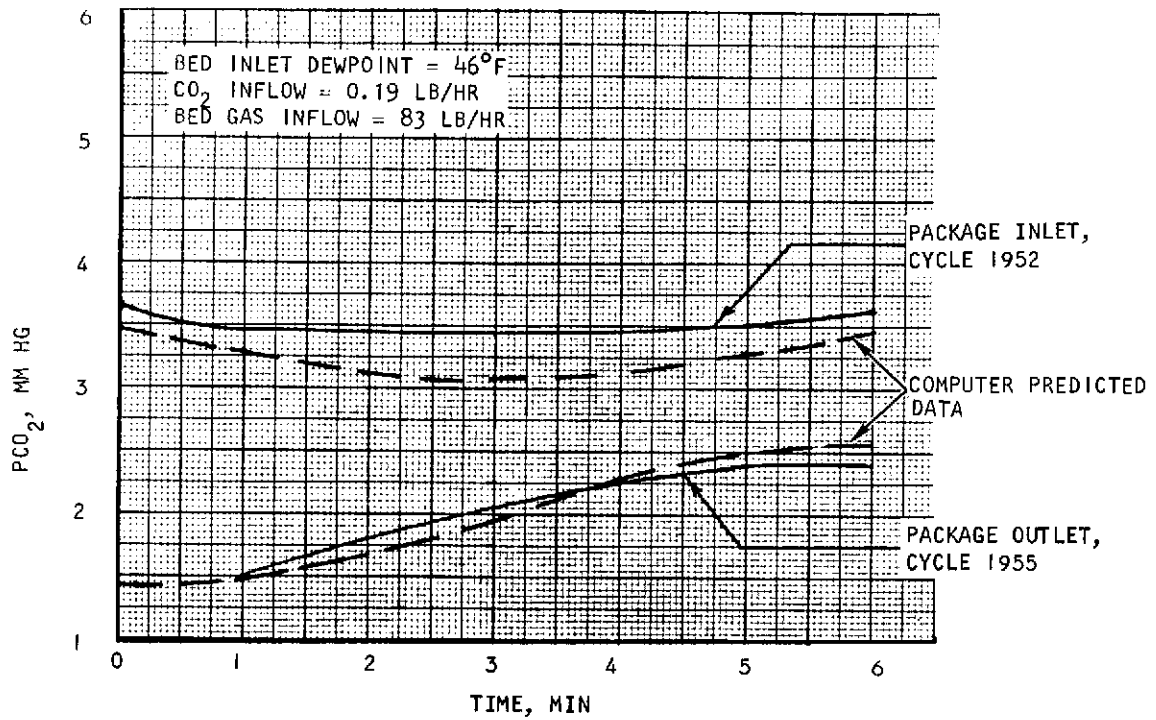
Figure 5-10. CO$_2$ Adsorption, Test Day 11

COMPUTER PREDICTED DATA (NODE 9.5)

NODE 6.5, CYCLE 689

COMPUTER PREDICTED DATA (NODE 6.5)

NODE 9.5, CYCLE 693

BED INLET DEW POINT = 54°F
CO$_2$ INFLOW = 0.38 LB/HR
BED GAS INFLOW = 82 LB/HR

DEWPOINT TEMPERATURE, °F

TIME, MIN

S-81009
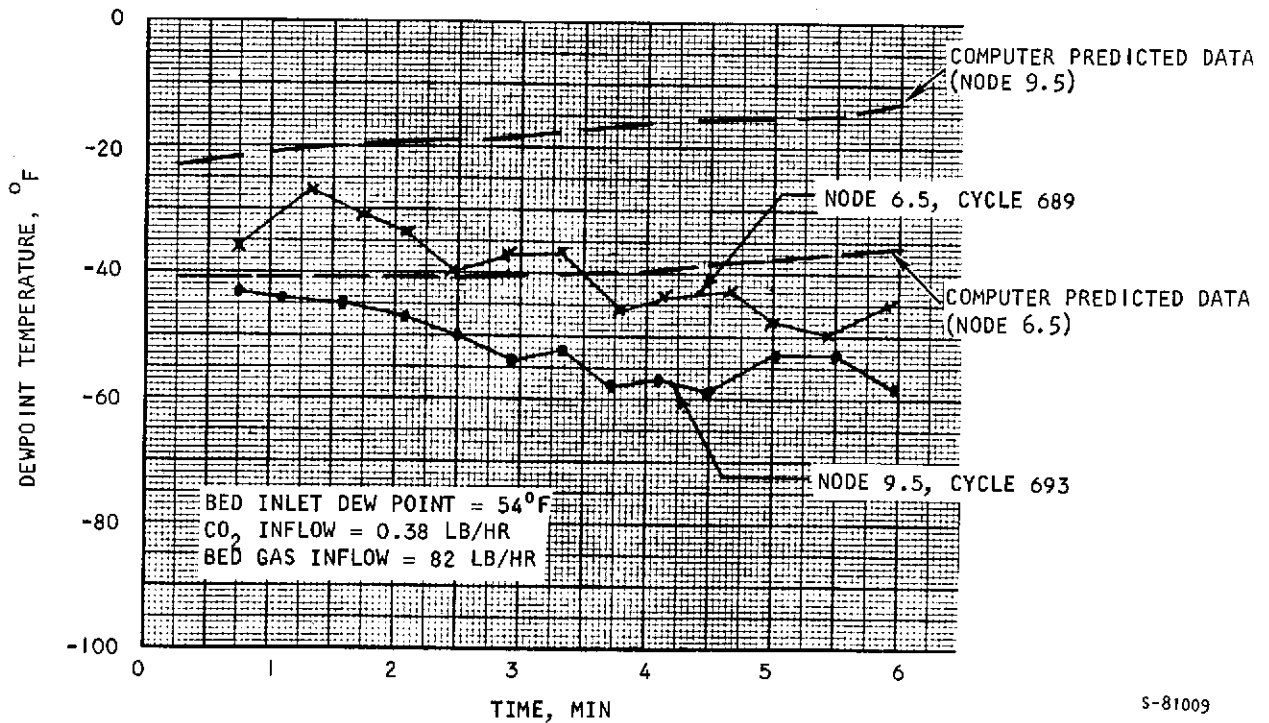
Figure 5-11. Dewpoint Temperature, Test Day 4

GARRETT AIRESEARCH MANUFACTURING COMPANY
Los Angeles, California

73-9313
Page 5-13
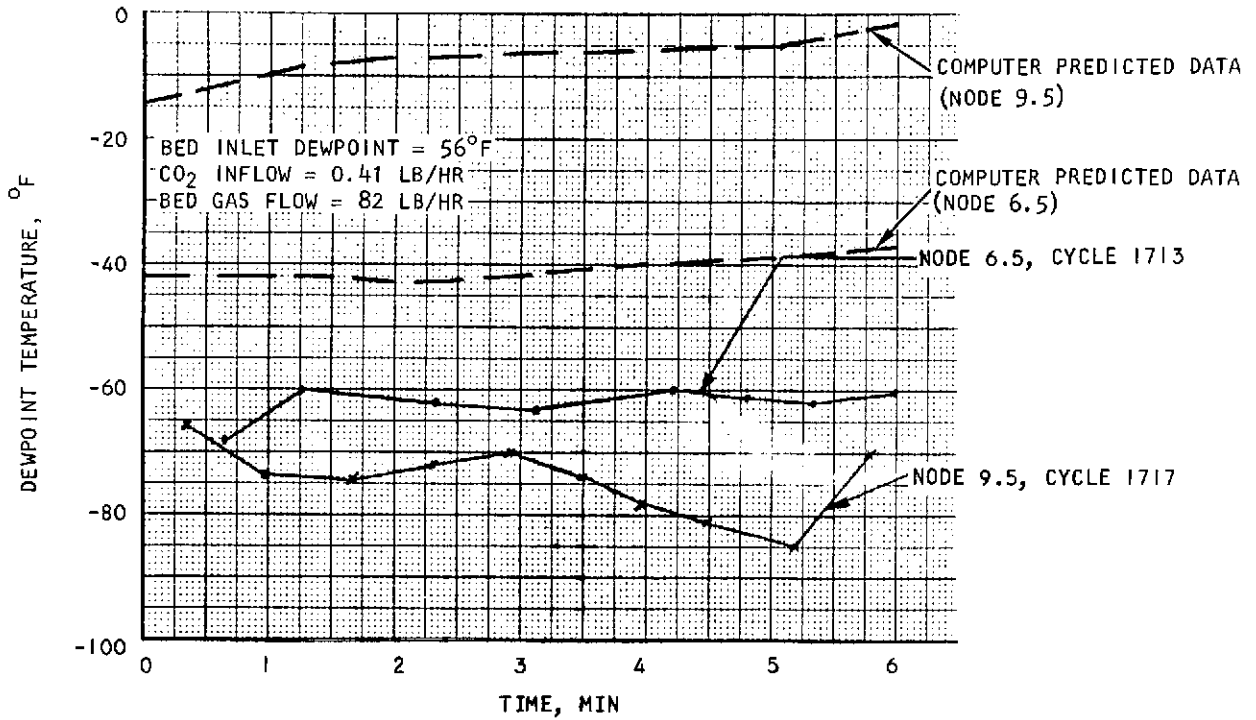
Figure 5-12. Dewpoint Temperature, Test Day 10
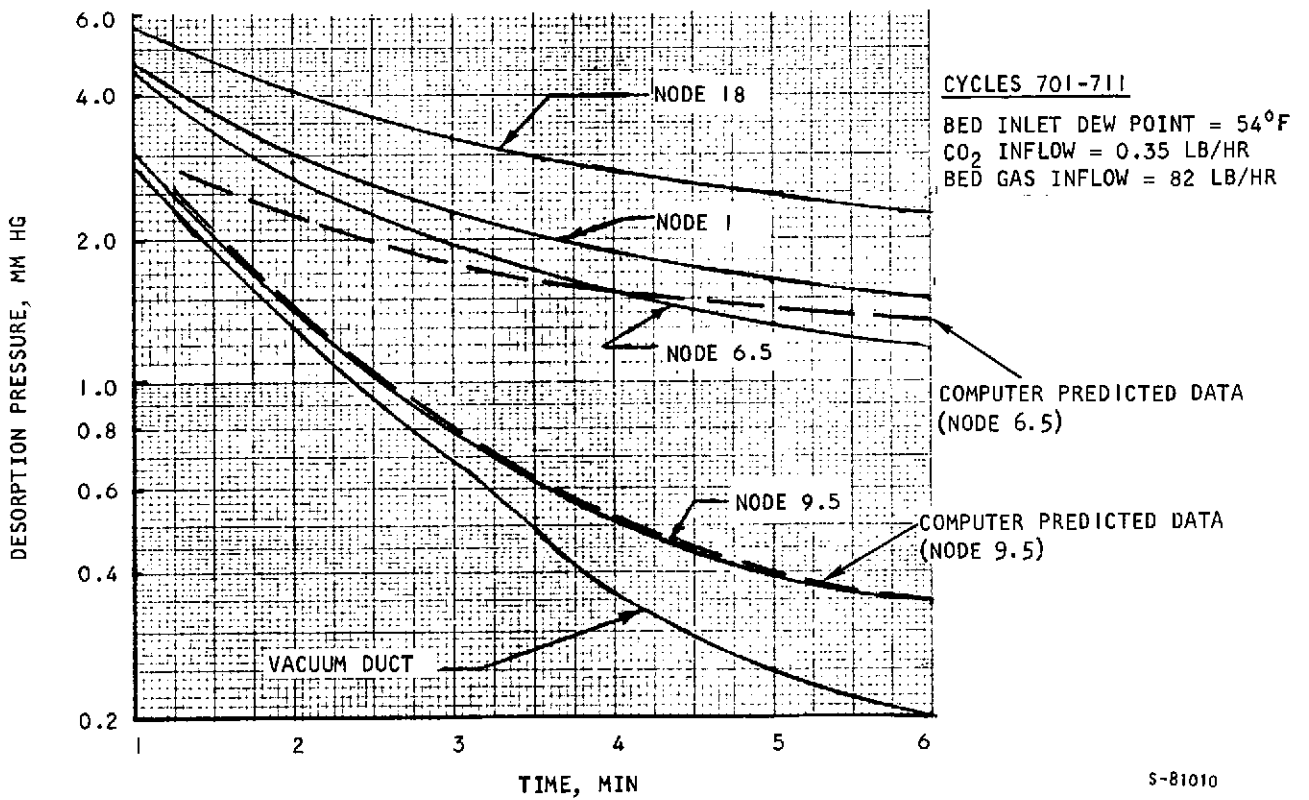
Figure 5-13. Desorption Pressure, Test Day 4

and test data for test days 10 and 11 (see Figures 5-9 and 5-10) it was found that the secondary drier was slightly undersized. As a result, node 6 of the CO_2 sorbent bed had been poisoned by water thus, accounting for the slight degradation in CO_2 removal performance of the system. The extent of water poisoning of node 6 was found to be such as to reduce the CO_2 capacity of the molecular sieve 4A in that node by about 25 percent.

Typical test dewpoint temperature data together with the computer predicted data at nodes 6.5 and 9.5 for test days 4 and 10 are shown in Figures 5-11 and 5-12, respectively. Here, a serious discrepancy is observed in the test data as the dewpoint at node 9.5 appears lower than at node 6.5, which is further downstream. Because extremely low water vapor pressures were measured at these points in the bed, there is ample basis for suspecting the accuracy of the dewpoint data, especially, in view of the pCO_2 data which appear plausible and as expected.

Figure 5-13 presents a typical plot of desorption pressures recorded at nodes 1, 6.5, 9.5, 18, and in the vacuum duct. The curves for test day 4 through test day 11 were practically identical; note the close correlation between the computer prediction and test data.

COMPUTER PROGRAM UPDATING

The development test data on the full-scale bed indicated higher chamber pCO_2 than anticipated from computer predictions based on the equilibrium and dynamic data presented in Section 2. To model the test bed performance, the dynamic mass-transfer coefficients were reduced until good correlation with the CO_2 removal performance of the full-scale bed could be reproduced accurately by the computer (see Figures 5-8, 5-9, and 5-10).

The decision to use lower values for the dynamic characteristics of the sorbent was prompted by three factors. First, the 4A binderless equilibrium curve of Figure A-4 was checked three times after careful calibration of the equilibrium test rig between each run. Second, the modeling of the full-scale test bed performance through adjustment of the sorbent diffusivity yielded excellent correlation. Finally, low dynamic properties were apparent during the CO_2 equilibrium runs. The interval of time necessary for the sorbent weight to equilibrate appeared significantly longer than with other types of molecular sieves.

The modified computer program was used to conduct final trade studies involving cycle time optimization and final bed design. These investigations are summarized in Section 6 of this report.

SECTION 6

RECOMMENDED SYSTEM

GENERAL

As a result of the full-scale development tests, the computer program was modified to account for the lower CO_2 adsorption rate of the 4A binderless molecular sieve. This resulted in CO_2 sorbent bed sizes somewhat larger than predicted on the basis of the data given in Section 2. For this reason, a final trade study was conducted on the 4-bed system arrangement to determine optimum cycle time in terms of equivalent weight (fixed equipment weight and gas loss penalty). This study showed that the 6-min half-cycle time remains optimum.

The characteristics of the recommended system are presented for design and off-design point operation. Further, preliminary component performance specifications are given.

CYCLE TIME OPTIMIZATION

Figure 6-1 shows the result of the study conducted to optimize cycle time using the upgraded computer program. Although the 4A binderless CO_2 sorbent bed is larger than shown previously (see Section 4), the optimum half-cycle time remains at 6 min. This is to be anticipated since more than 90 percent of the gas loss penalty is a direct function of the 4A bed size.

RECOMMENDED SYSTEM DEFINITION

A schematic of the recommended system arrangement is shown in Figure 6-2. Figure 6-3 shows the system's four regenerable sorbent modules. Each module incorporates the equipment shown below:

> Sorbent Bed--Electrically heated for bed conditioning (bakeout) prior to flight or in the event of poisoning during flight. Each bed contains a total of 9.8 lb of silica gel (7.0 lb for the primary drier and 2.8 lb for the secondary drier) and 8.1 lb of 4A binderless molecular sieve for CO_2 removal.
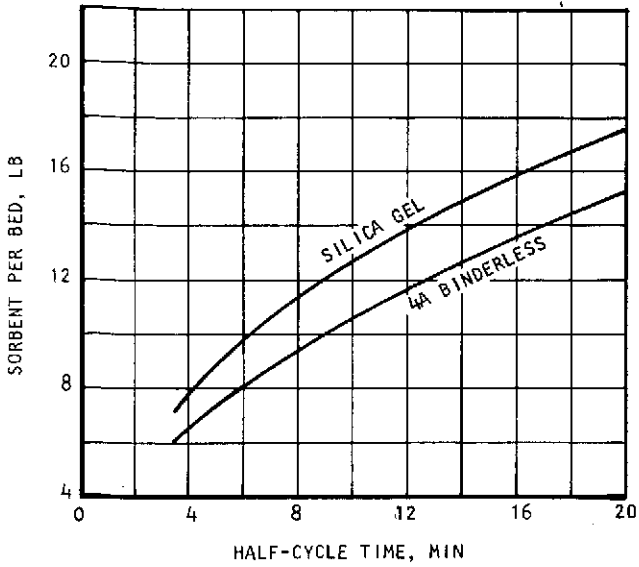
SORBENT REQUIREMENTS

7-DAY MISSION
4-BED ADIABATIC SYSTEM
4- AND 10-MAN CREWS
PCO_2 = 5 mm Hg (10-MAN LOADS)
CABIN DEWPOINT: 53°F
PROCESS AIRFLOW: 106 LB/HR/BED
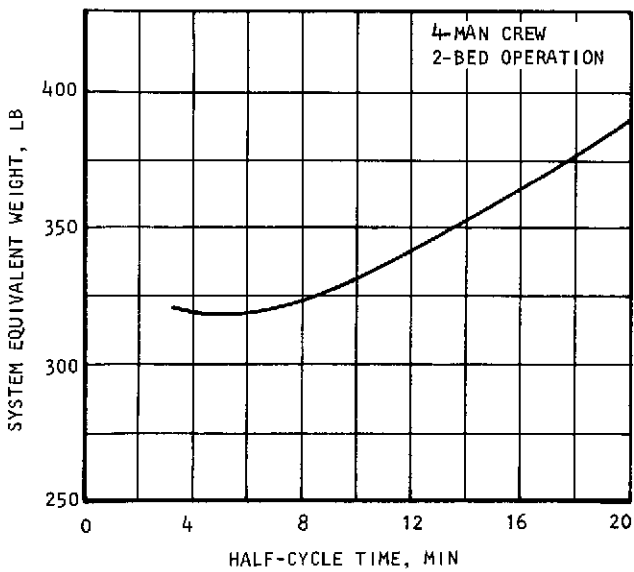
EQUIVALENT WEIGHT
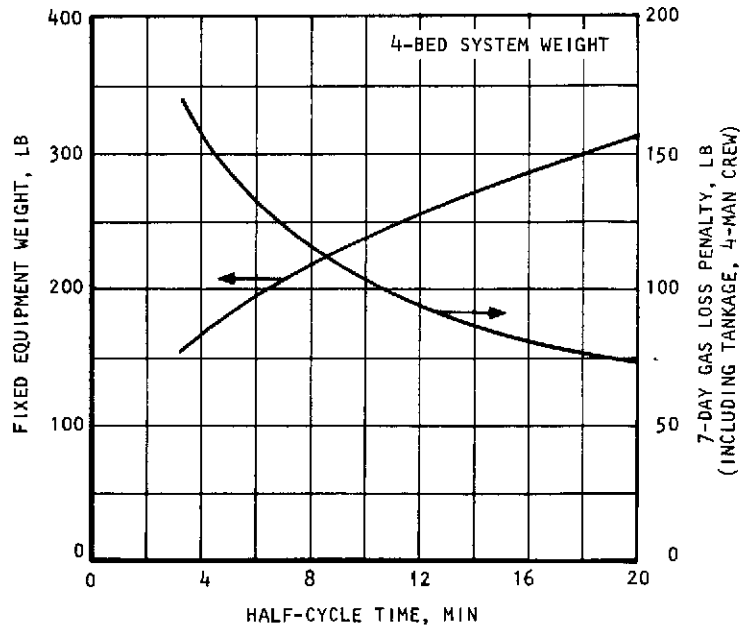
FIXED AND EXPENDABLE WEIGHTS

S-81006

Figure 6-1.   Cycle Time Optimization
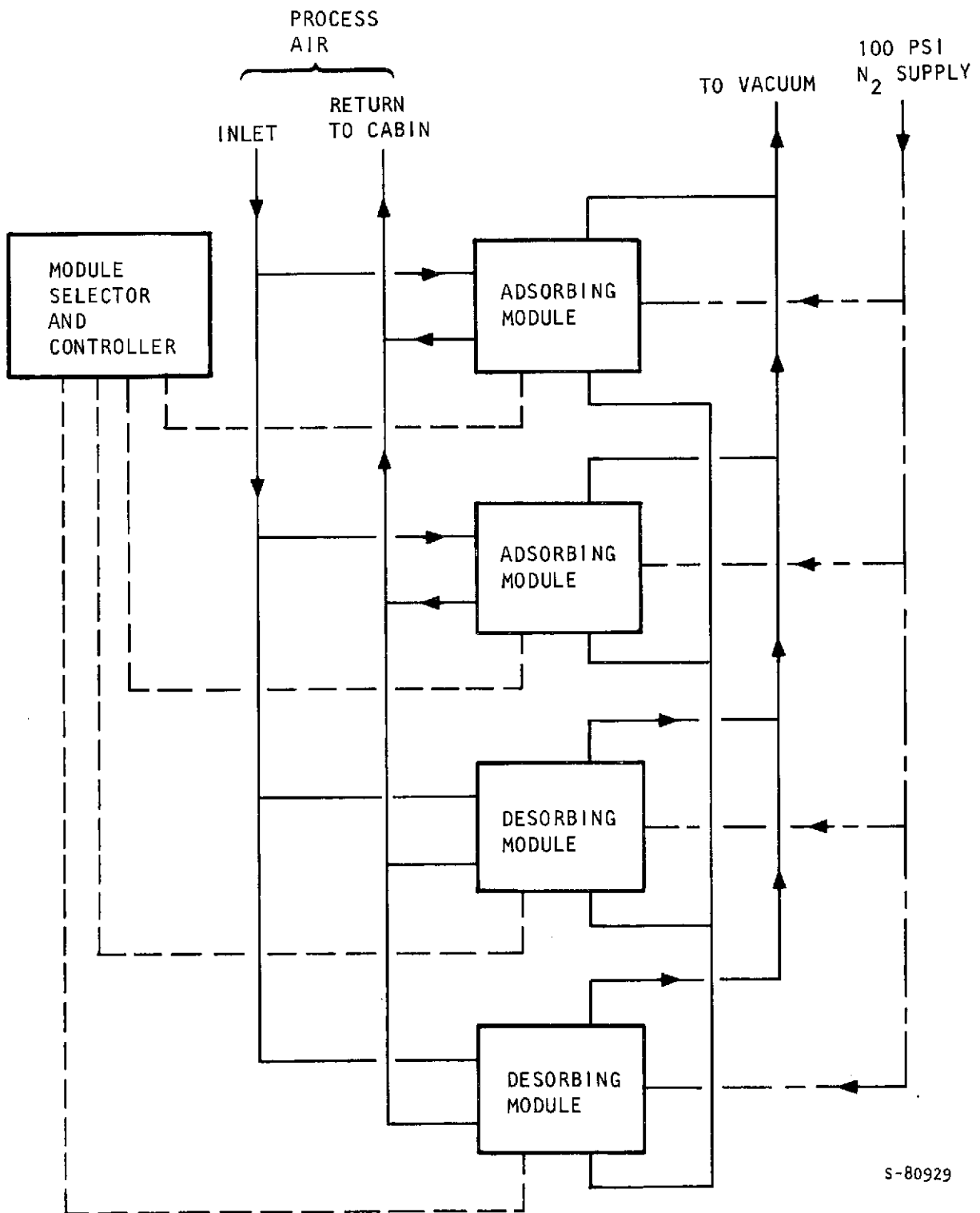
Figure 6-2. Recommended System Arrangement

VENT TO CABIN

TO VACUUM

DESORPTION
VALVE

PRESSURE
EQUALIZATION
VALVE

PROCESS
AIR
RETURN

TO CONTROLLER

TO CONTROLLER

INSULATION

TO CONTROLLER

N_2 SWITCHOVER
VALVE

HEATER
CONTROL

FROM HIGH
PRESSURE
N_2 SOURCE

VALVE
ACTUATOR

PROCESS AIR INLET

GAS SELECTOR
VALVE

PREDRIER, 7.0 LB
SILICA GEL

ELECTRICAL
HEATER

SECONDARY DRIER,
2.8 LB SILICA GEL

CO_2 SORBENT, 8.1 LB,
4A BINDERLESS MOLECULAR
SIEVE

s-80944

Figure 6-3. Sorbent System Module

Gas Selector Valve and Actuator--Directs the process air flow to and from the bed during adsorption and isolates the bed during desorption. The gas selector valve is pneumatically actuated by high-pressure N_2. Manual provisions are incorporated in the design to permit bed isolation in the event of failure.

N_2 Switchover Valve--Controls the N_2 pressure in the gas selector actuator and thus the position of the selector valve.

Pressure Equalization Valve--Exposes the bed to the pressure equalization manifold for 30 sec while the bed is isolated by means of the gas selector valve and while the vacuum desorption valve is closed.

Desorption Valve--Through this valve the bed is exposed to vacuum during the desorption period.

Heater Controller--Controls the power input to the heater so as to maintain a bed temperature of $450^{\circ}F$ to dry the sorbent prior to a mission.

Cycling of the N_2 switchover valve, desorption valve, and pressure equalization valve is controlled and timed by the system controller.

The system is designed to handle the latent and CO_2 load of four men with the beds on stream. In this mode of operation the other two modules are redundant so that design performance is maintained after two failures. With a 10-man crew all beds are active; however, after one failure performance will degrade slightly, but remain between the maximum limits specified for long-term flight. Performance data for the 4- and 10-man crew cases are shown in Table 6-1.

SYSTEM OPERATION

Prior to flight, all four beds will be regenerated by applying heat and vacuum to each bed for a sufficient period of time to reduce water loading to approximately two percent. A sorbent temperature of about $450^{\circ}F$ will be necessary for this purpose. The beds are then pressurized to sea level and allowed to cool until activation is required. Activation will consist of selecting the modules (2 or 4) to be operated and activating the controller, which controls valve cycling for the selected modules.

TABLE 6-1

CHARACTERISTICS OF THE RECOMMENDED SYSTEM

Sorbent Bed Characteristics

Silica gel bed weight.	9.8 lb (total)
4A binderless molecular sieve bed weight	8.1 lb
Bed face area	67.3 sq in.
Primary drier bed depth	5.2 in.
Secondary drier bed depth	2.1 in.
4A binderless bed depth:	5.0 in.

System Characteristics

Number of modules	4	
Total weight including structure	194 lb	
7-Day gas loss (no tankage)	O_2	N_2
4-man crew, lb	10.2	68.3
10-man crew, lb	20.4	136.6

Two modules operational with 4-man crew

Four modules operational with 10-man crew

Design performance achieved after two failures with 4-man crew

Specified performance achieved after one failure with 10-man crew

Performance Characteristics	4-Man Operation	10-Man Operation
H_2O removal rate, lb/hr	0.417	0.95
CO_2 removal rate, lb/hr	0.891	1.8
Cabin dewpoint, $^\circ F$	52.8	53.0
Cabin pCO_2, mm Hg	4.5	5.0
Process air flow rate, lb/hr	106	212
Half-cycle time, min	6	6
Performance after first failure		
Cabin pCO_2, mm Hg	4.5	6.7
Cabin dewpoint, $^\circ F$	52.8	60.3
Performance after second failure		
Cabin pCO_2, mm Hg	4.5	9.0
Cabin dewpoint, $^\circ F$	52.8	71.5

In the event of a failure in a module, the electrical circuits associated with the failed module will be deactivated and the particular module will be automatically isolated. In the case of the 4-man crew a redundant module will be activated.

COMPONENT DESCRIPTIONS

Pressure Equalizing Solenoid Valve

The pressure equalizing solenoid valve is a two-port, normally-closed shutoff valve that allows through-flow when energized. The valve is energized only during the pressure-equalizing time period. Significant requirements for the solenoid valve are listed below.

Port size, in.	1.0
Electrical power, watts (when energized)	15
Operating pressure, psia	0 to 20
Weight, lb	1.5
Actuation time, sec	30

Gas Selector Valve

The gas selector valve is a four-port, two-position, pneumatically operated, plug valve. The valve includes provisions for manual positioning in case of failure. During adsorption, process gas is directed through the bed and returned to the cabin; during desorption, the process gas is isolated from the bed. Significant requirements for the selector valve are listed below:

Port size, in.	1.5
Manual override torque, in.-lb	20 max
Positions	2 (open and close)
Operating pressure, psia	0 to 20
Weight, lb	4.5
Actuation time, sec	30
Pneumatic actuator operating pressure, psig	100

Vacuum Desorption Valve

The vacuum desorption valve is a two-port, two-position, electrically-operated spoon valve, which exposes the bed to vacuum during desorption. The valve has provisions for manual override in case of electrical power loss. Significant requirements for the desorption valve are as follows:

Port size, in.	2.75
Manual override torque, in.-lb	20 max
Operating pressure, psia	0 to 20
Electrical power, watts	30
Weight, lb	3.5
Actuation time, sec	30

Sorbent Canister

The sorbent canister, which contains the silica gel and molecular sieve, features a center point desorption port. It contains heat transfer surfaces within the housing that carry heat from heater elements external to the housing. The heater elements are sized to provide a $450^\circ F$ bakeout capability. Temperature control is provided by thermostats installed within the adsorber housing. Significant requirements for the adsorber bed are listed below:

Absorber port size (inlet-outlet), in.	1.5
Desorb port size, in.	2.75
Water sorbent, 6-10 mesh silica gel, lb	9.8
CO_2 sorbent, 1/16 in. 4A binderless, lb	8.1
Sorbent bed face area, sq in.	67.3
Primary drier bed depth, in.	5.2
Secondary drier bed depth, in.	2.1
CO_2 sorbent bed depth, in.	5.0
Weight, lb	35.9
Operating pressure, psia	0 to 20
Electrical power, watts	600

Controller

The controller is a solid-state, hermetically-sealed device that controls the desired bed cycle rate and pressure equalization time. It contains controls to select the module to be activated. The start sequence is at a given point in the timing program. Significant requirements for the controller are listed below:

Half-cycle time, min	6
Pressure equalization time, sec	30
Operating pressure, psia	0 to 20
Timing circuit power, watts	4.0
Weight, lb	5.0

N_2 Switchover Valve

The solenoid switchover valve controls the N_2 pressure in the gas selector valve actuator. The valve is a four-way, two-position solenoid valve featuring an inlet port, a vent port and two actuator ports. In cyclic operation each actuator port is connected alternately to the inlet and vent ports.

Operating pressure psig:	250 max
Flow requirements at 100 psig and 70°F, lb/min	0.2
Pressure drop at rated flow, psid	5.0
Electrical power, watts	12
Cycle time, min	6
Weight, lb	0.8

APPENDIX A

RESULTS OF EQUILIBRIUM AND DYNAMIC
MASS-TRANSFER TESTS

APPENDIX A

RESULTS OF EQUILIBRIUM AND DYNAMIC MASS-TRANSFER TESTS

EQUILIBRIUM TEST RESULTS

The equilibrium adsorption isotherms have been plotted from the test data and are shown in Figure A-1 through A-5.

DYNAMIC MASS-TRANSFER TEST RESULTS

Figures A-6 through A-13 show the results of the dynamic adsorption tests.
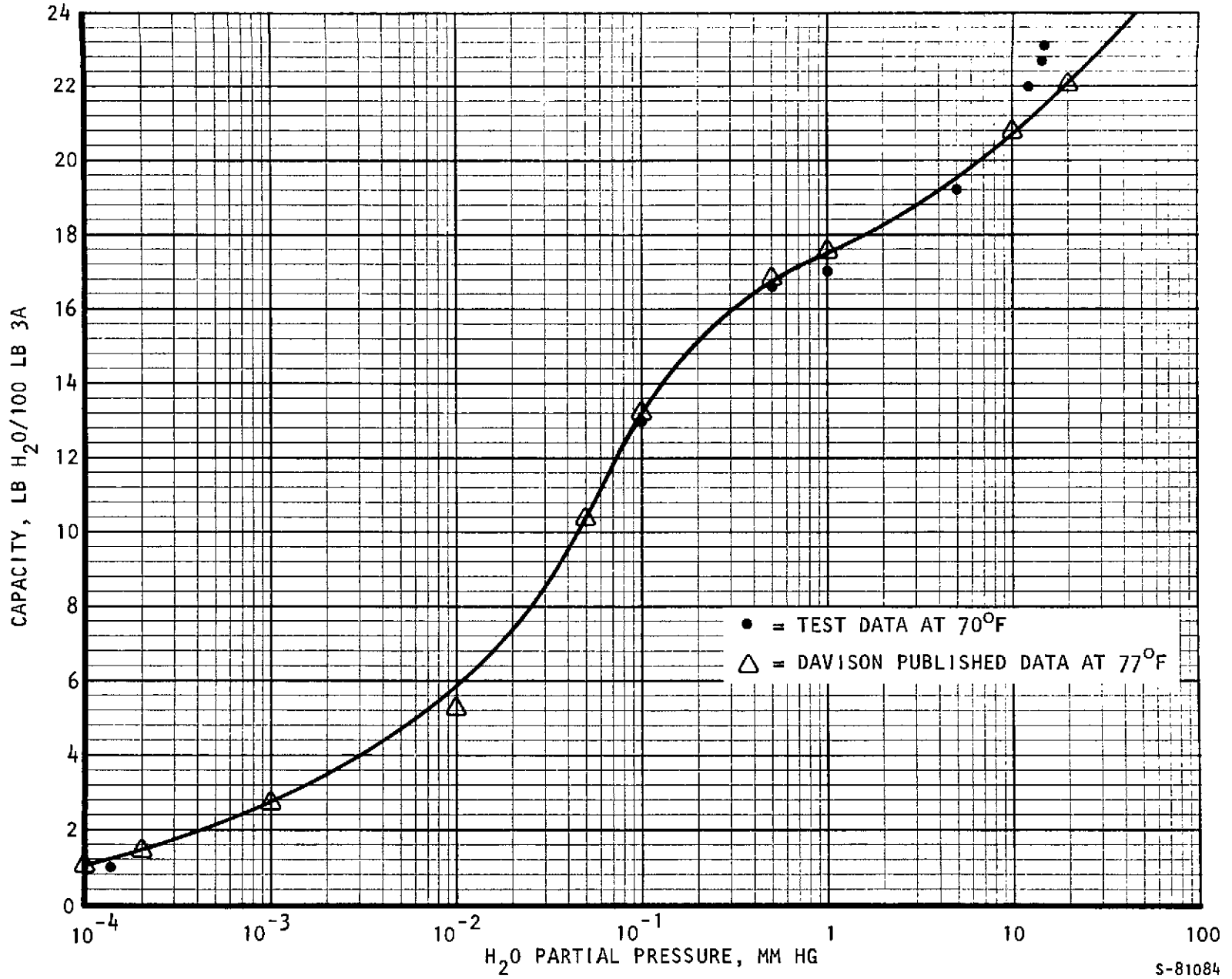
Figure A-1. Water Equilibrium Data--Linde 3A Regular, 1/16-in. Pellets (7/24/72)
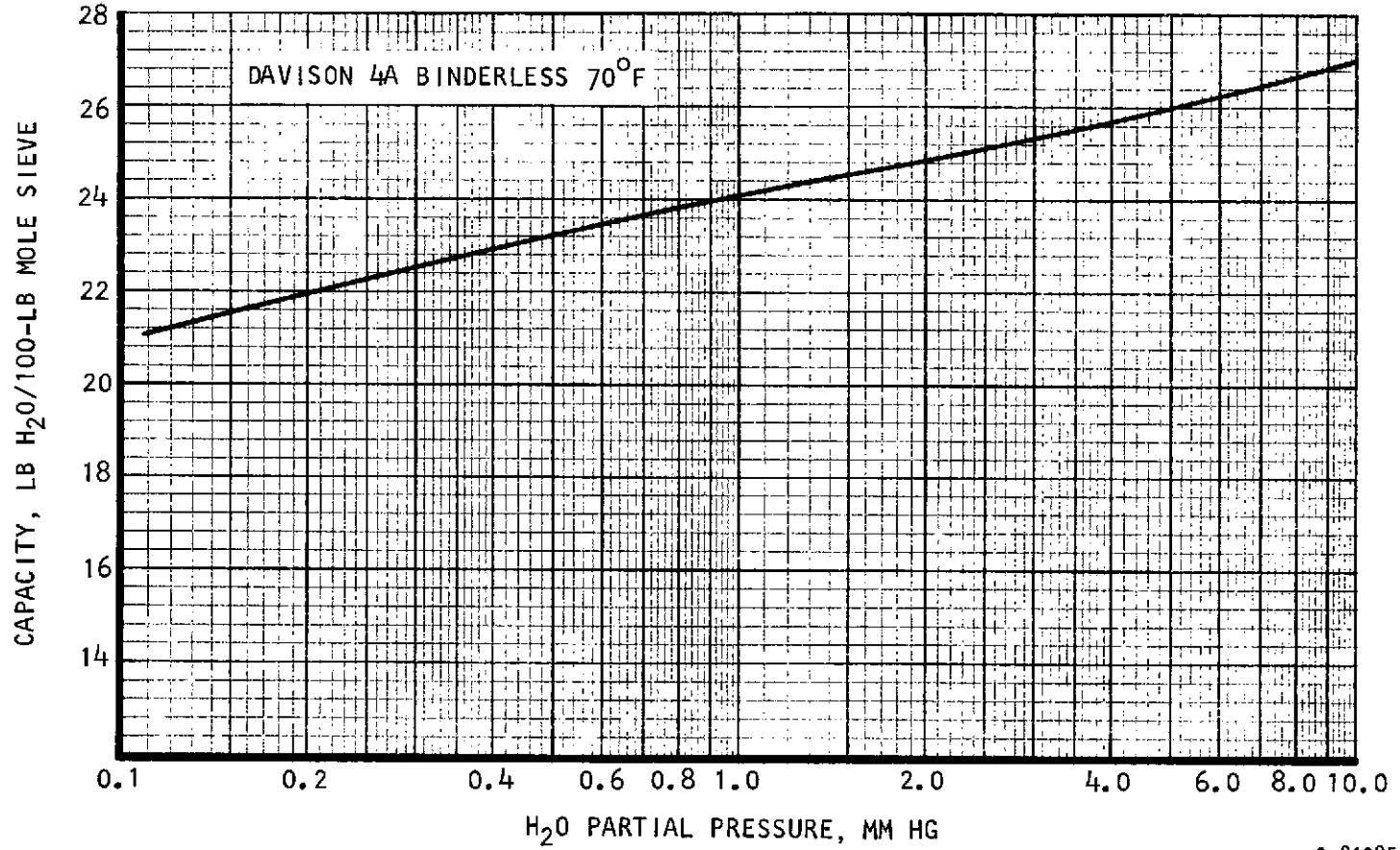
S-81084

Figure A-2. Water Equilibrium Data--Davison 4A Binderless, 70°F Isotherm
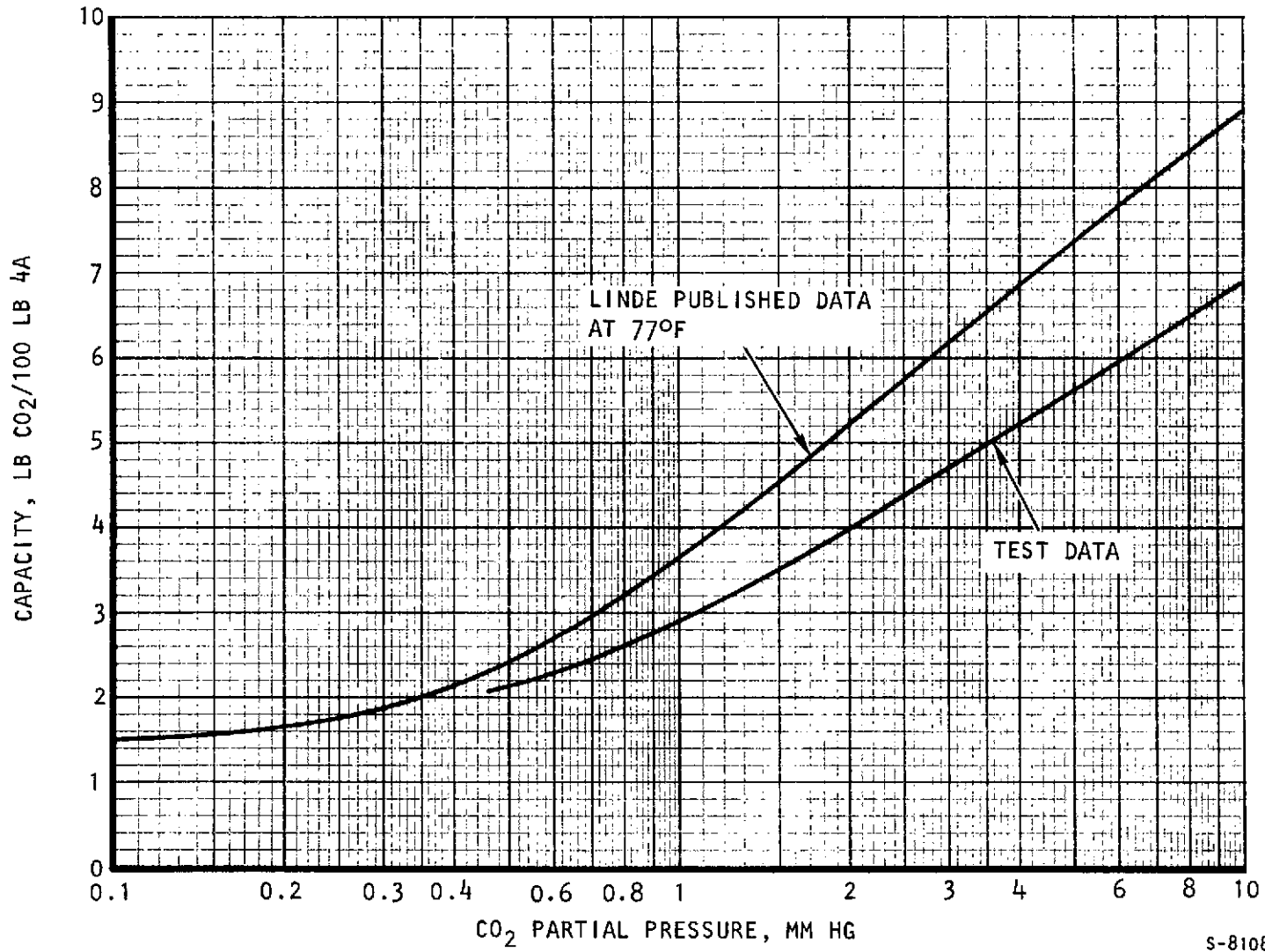
S-81085

Figure A-3. Carbon Dioxide Equilibrium Data--Linde 4A Regular,
1/16-in. Pellets, 70°F Isotherm (8/3/72)
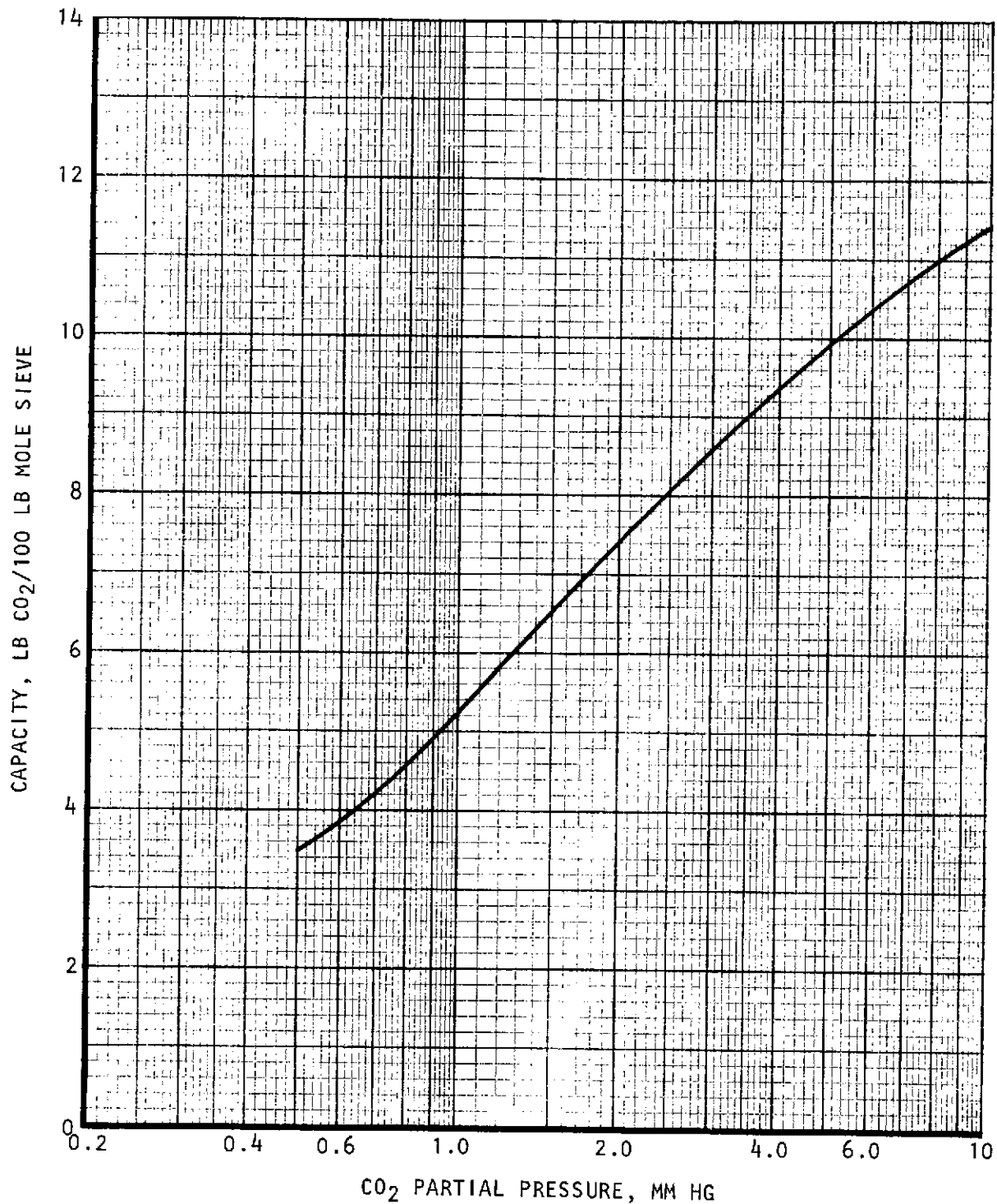
Figure A-4. Carbon Dioxide Equilibrium Data--Davison 4-A Binderless, 70°F Isotherm
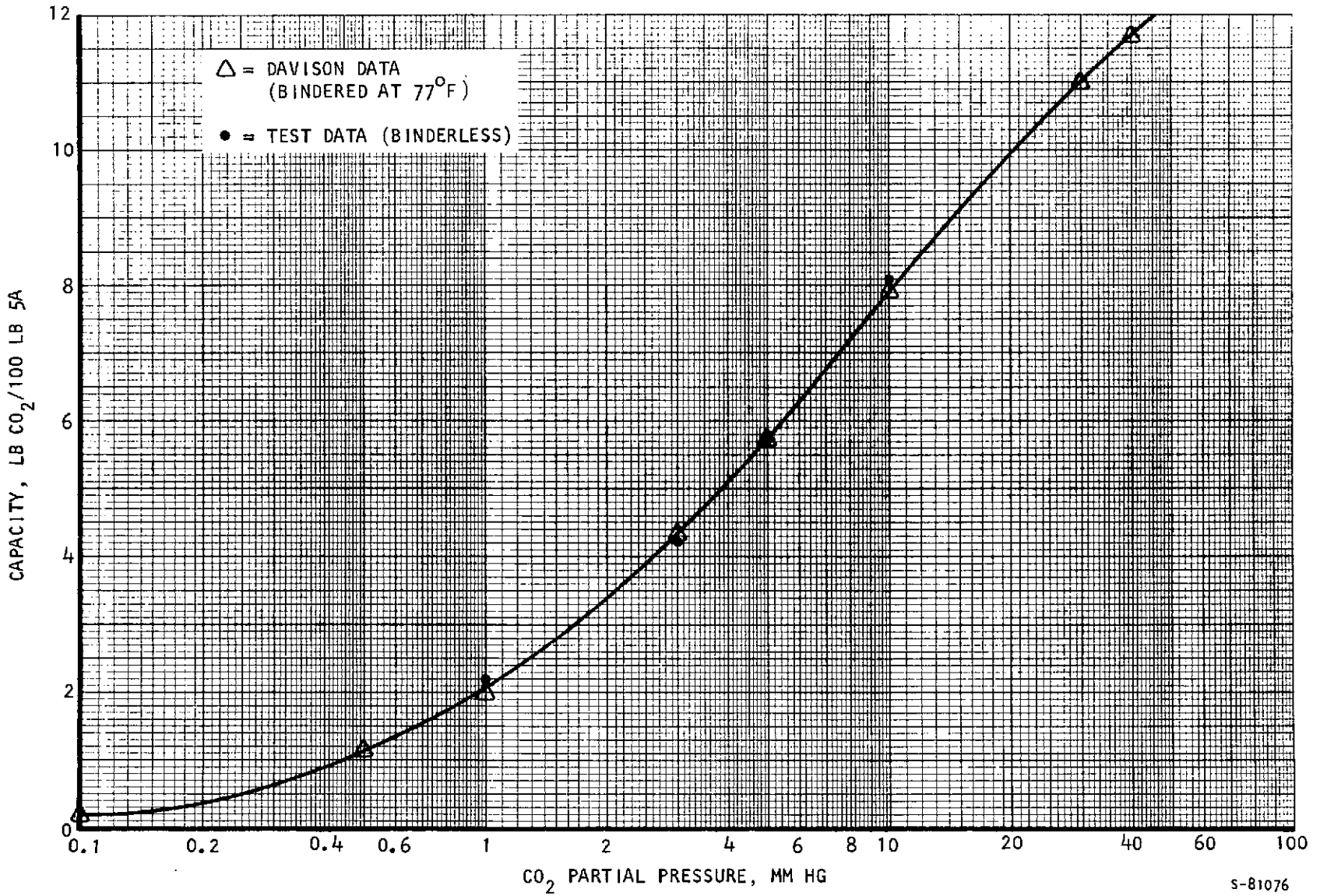
Figure A-5. Carbon Dioxide Equilibrium Data--Davison 5A Binderless, Grade 625, 1/8-in. Pellets, 70°F Isotherm (8/1/72)

H$_2$O PARTIAL PRESSURE AT BED OUTLET, MM HG

BED SIZE = 0.83 IN. DIA x 1 IN. LONG, 6 GRAMS 3A,1/8 IN. PELLETS
BED INLET PRESS = 22.1 PSIA, BED INFLOW = 9800 SCCM N$_2$
BED INLET DEW POINT = 66°F, 16.6 MM HG
BED INITIAL WATER LOAD = 0.3 PERCENT

TIME, MIN
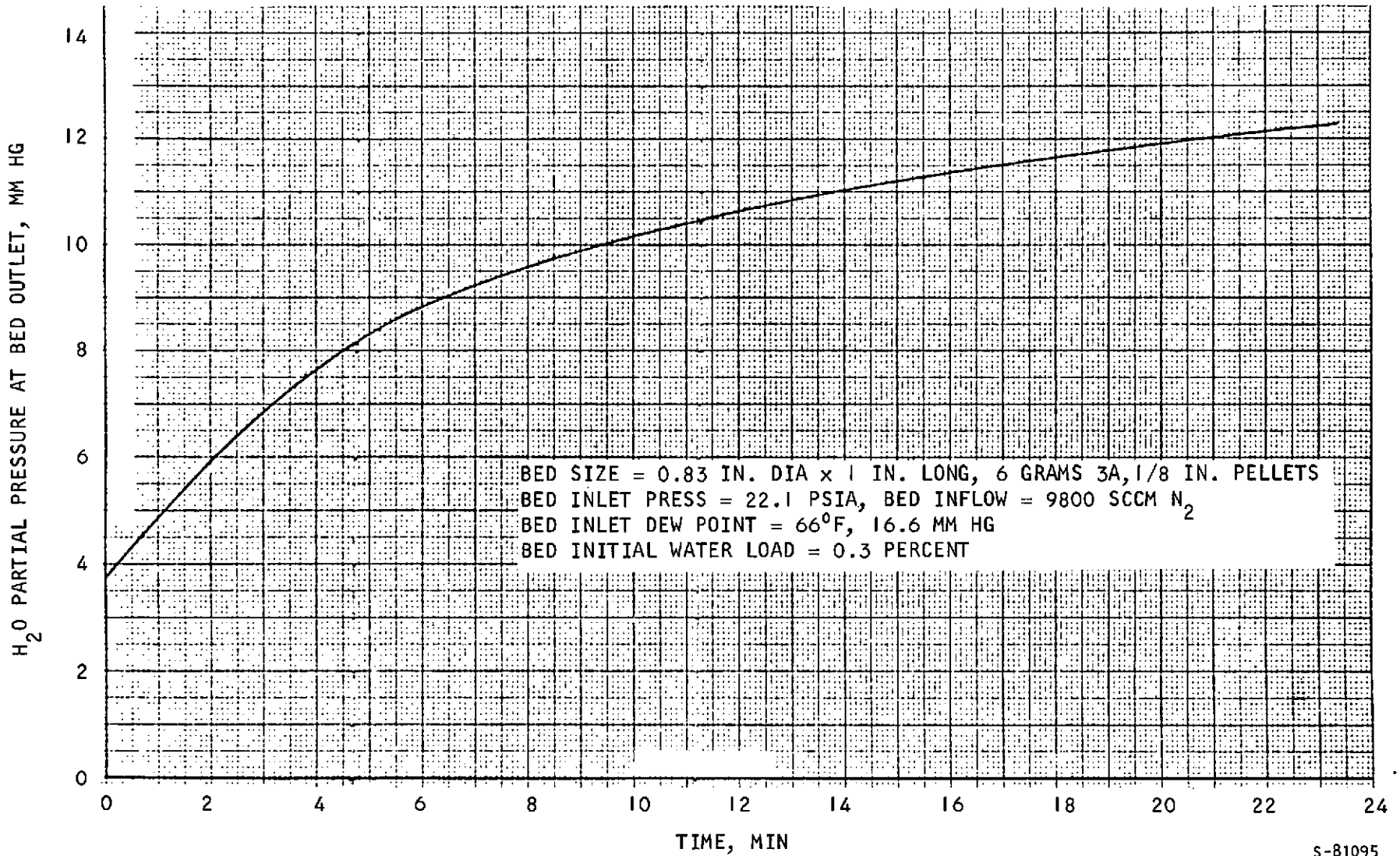
S-81095

Figure A-6.   Water Adsorption, Linde 3A Regular, 70°F
Dewpoint 66°F

H$_2$O PARTIAL PRESSURE AT BED OUTLET, MM HG

BED SIZE = 0.83 IN. DIA X 1 IN. LONG, 6 GRAMS 3A, 1/8 IN. PELLETS
BED INLET PRESS = 20.6 PSIA, BED INFLOW = 10,240 SCCM N$_2$
BED INLET DEW POINT = 63°F, 14.9 MM HG
BED INITIAL WATER LOAD = 0.3 PERCENT

TIME, MIN
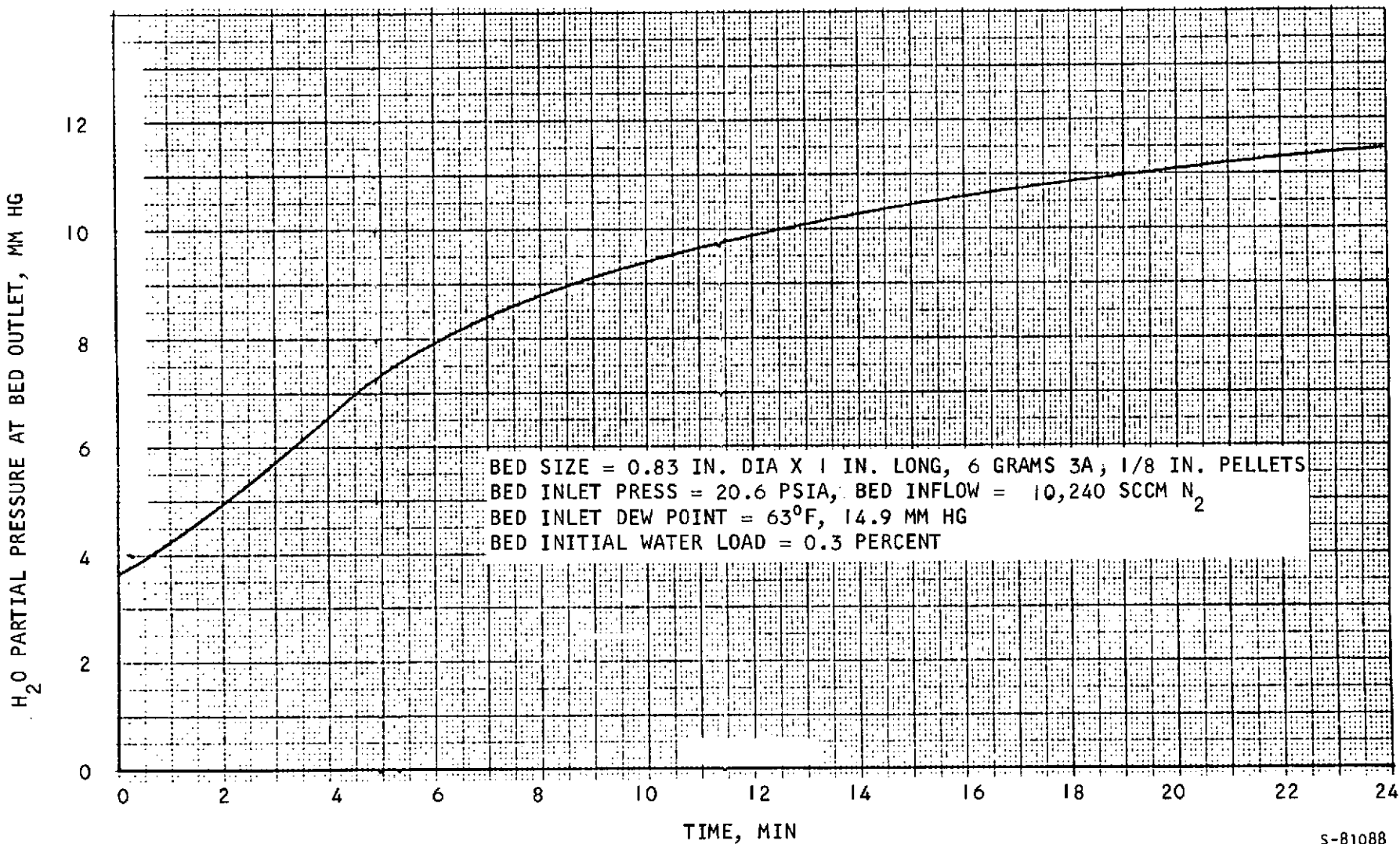
S-81088

Figure A-7. Dynamic Test, Water Adsorption, Linde 3A Regular, 14.9 mm Hg
Partial Pressure, 1/2 in. Pellets, 120°F
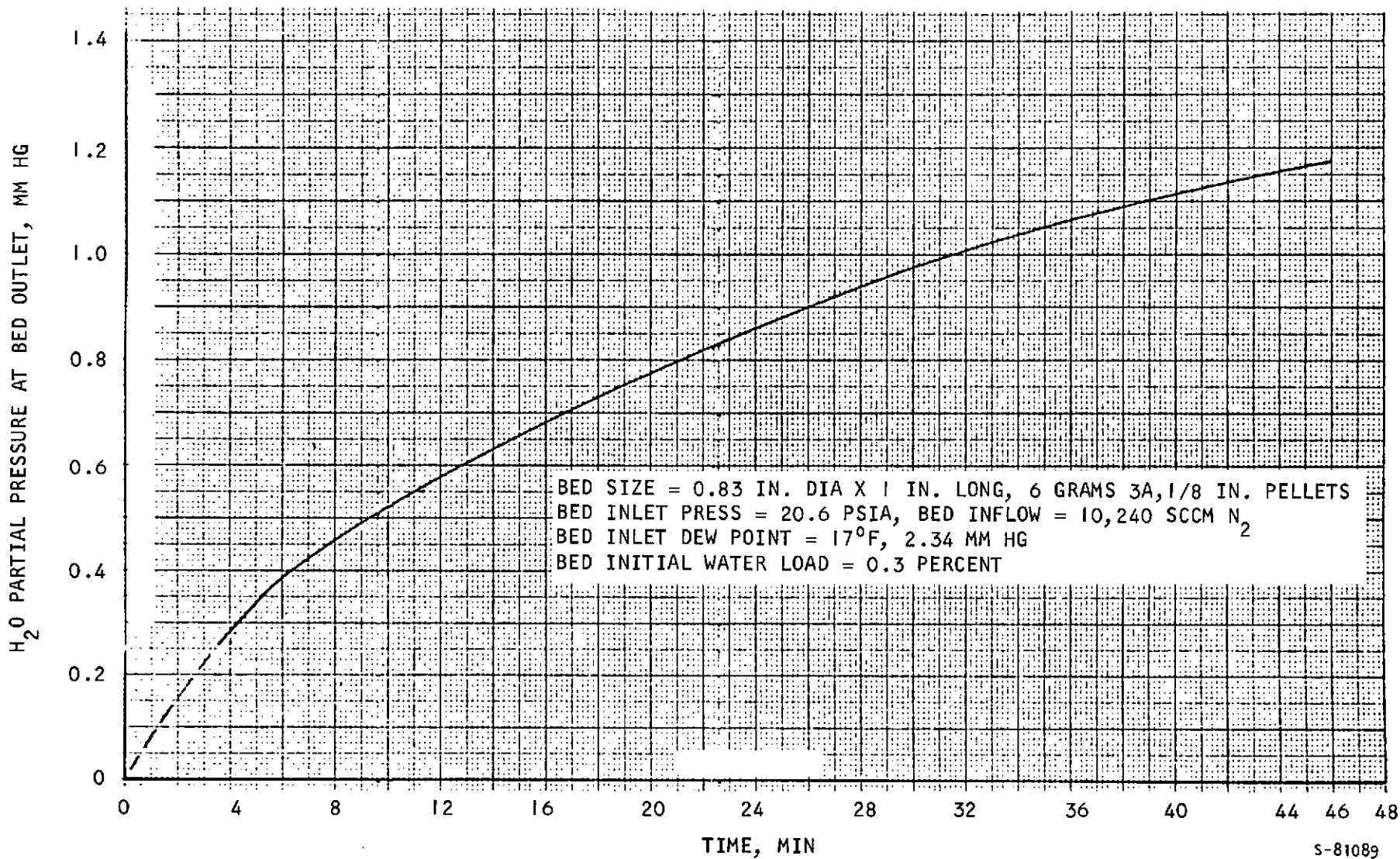
Figure A-8. Dynamic Test, Water Adsorption, Linde 3A Regular, 2.34 mm Hg
Partial Pressure, 1/8 in. Pellets, 120°F
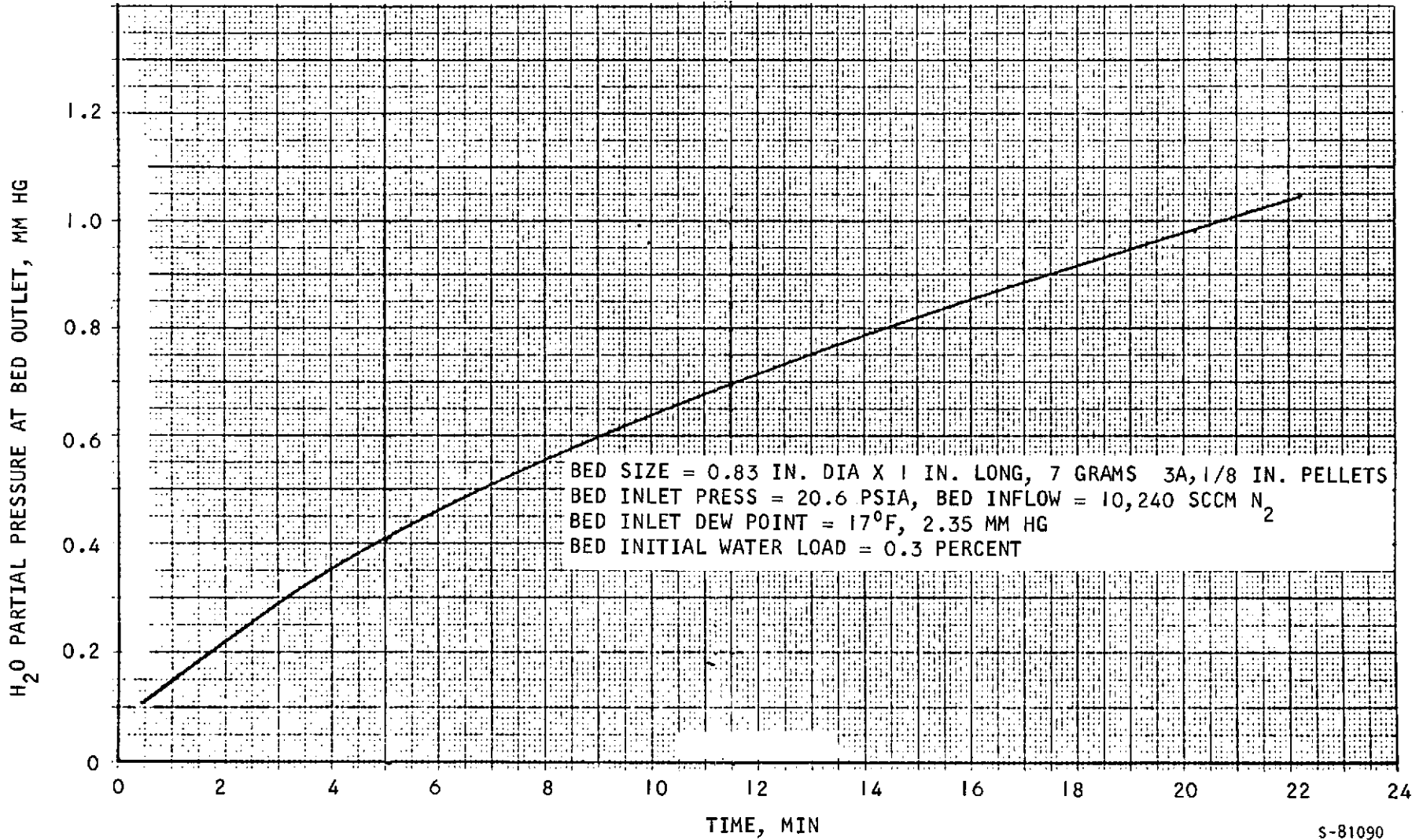
Figure A-9. Dynamic Test, Water Adsorption, Linde 3A Regular, 2.35 mm Hg Partial Pressure, 1/8-in. Pellets, 120°F

S-81090

BED SIZE = 0.83 IN. DIA. X 1 IN. LONG, 6 GRAMS 4A, 1/8 IN. DIA. SPHERES
BED INLET PRESS = 22.1 PSIA, BED INFLOW = 9750 SCCM N_2
BED INLET PCO_2 = 7.44 MM HG
BED INITIAL WATER LOAD = 0.55 PERCENT
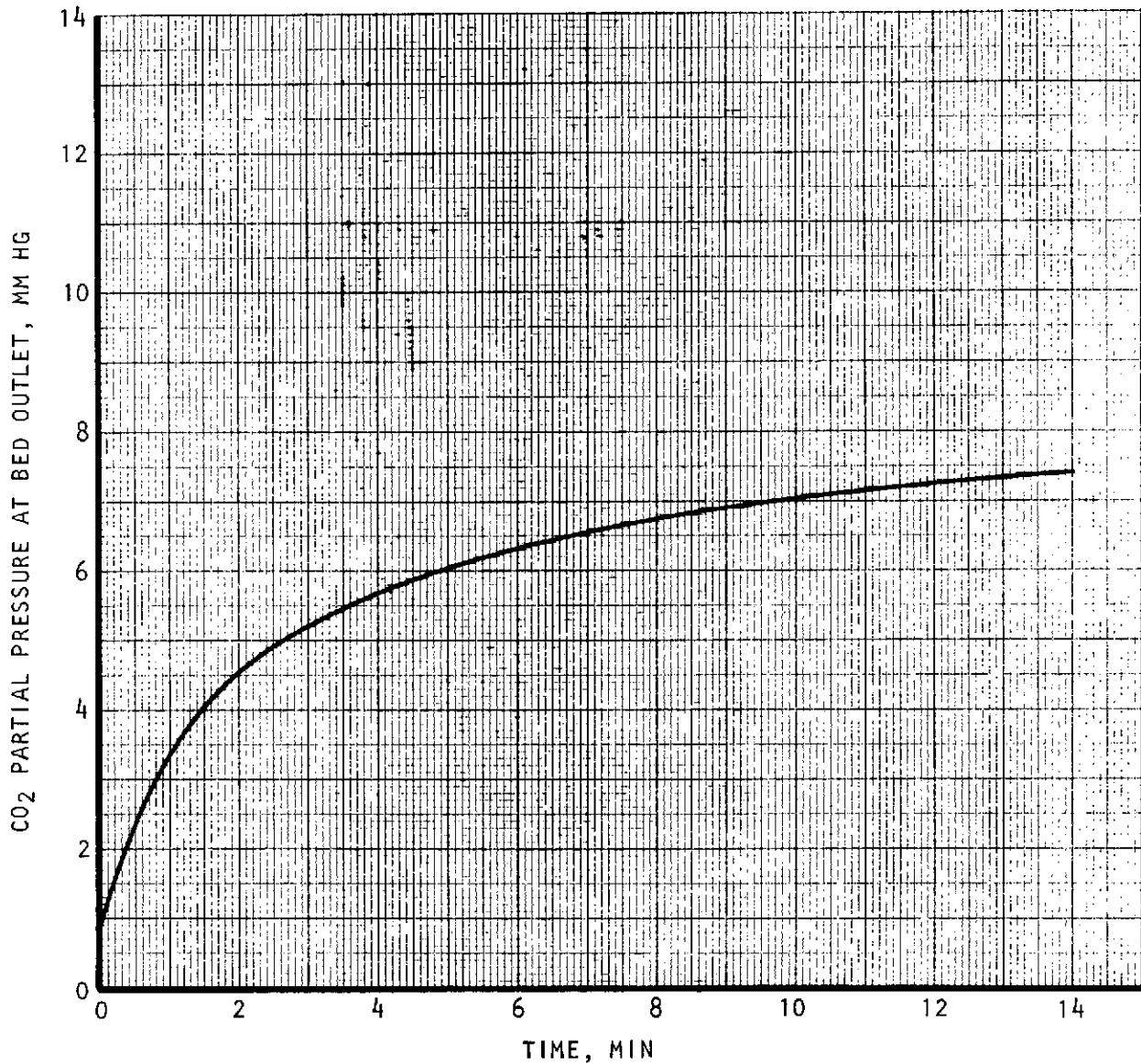
S-81091

Figure A-10.   Dynamic Test, CO_2 Adsorption, Davison 4A Binderless,
7.44 mm Hg Partial Pressure, 1/8-in. dia Spheres 70°F

BED SIZE = 0.83 IN. DIA X 1 IN. LONG, 7 GRAMS 4A, 1/8 IN. DIA. SPHERES
BED INLET PRESS = 22.1 PSIA, BED INFLOW = 9750 SCCM N_2
BED INLET PCO_2 = 8.27 MM HG
BED INITIAL WATER LOAD = 0.55 PERCENT
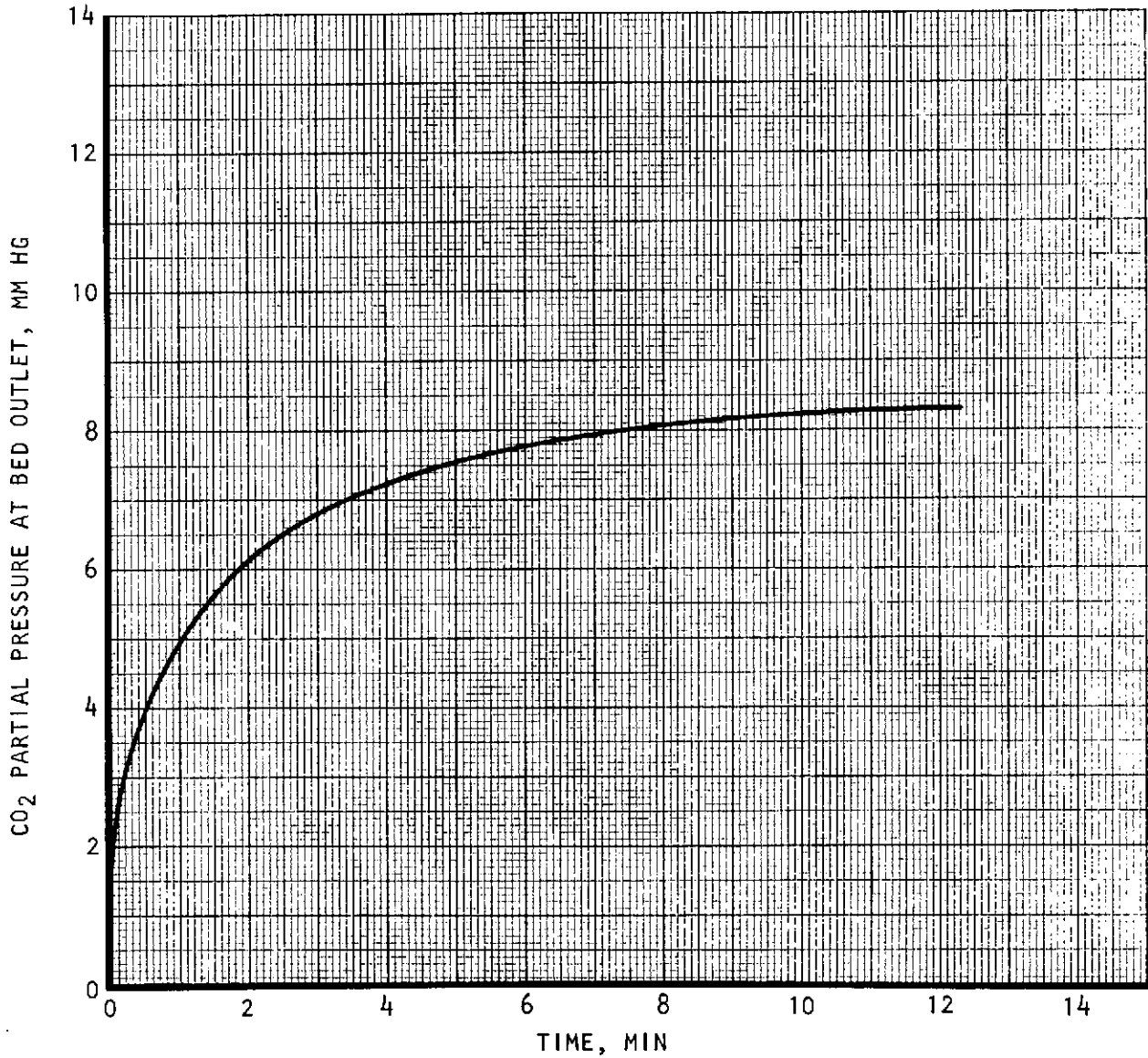
S-81092

Figure A-11.   Dynamic Test, CO_2 Adsorption, Davison 4A Binderless,
8.27 mm Hg Pressure, 1/8-in. dia Spheres 120°F

>88<

BED SIZE = 0.83 IN. DIA X 1 IN. LONG, 6 GRAMS 5A, 1/8 IN. PELLETS
BED INLET PRESS = 21.8 PSIA, BED INFLOW = 9580 SCCM N_2
BED INLET P CO_2 = 7.27 MM HG
BED INITIAL WATER LOAD = 0.5 PERCENT

CO_2 PARTIAL PRESSURE AT BED OUTLET, MM HG

TIME, MIN

S-81093
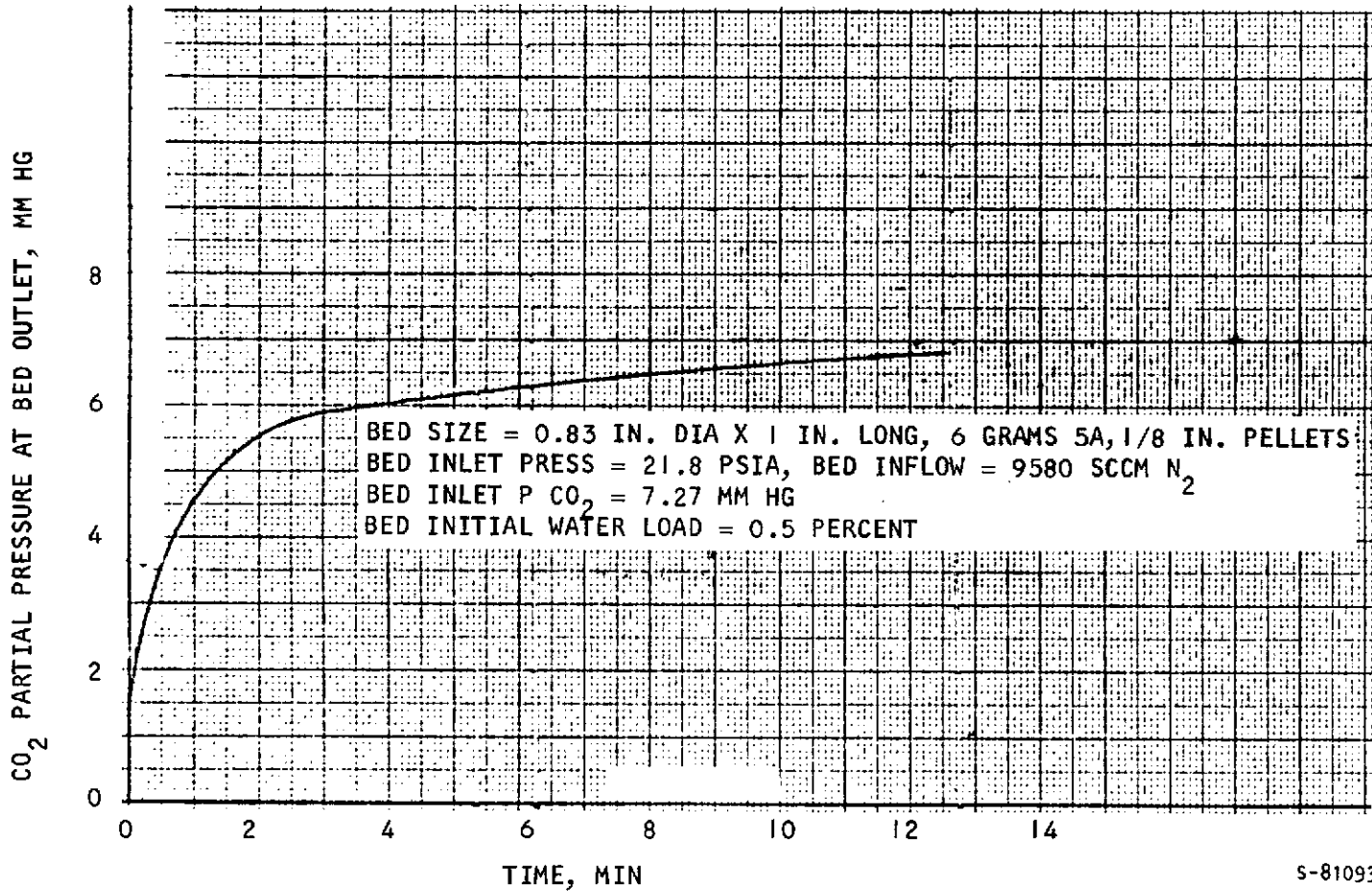
Figure A-12.   Dynamic Test, CO_2 Adsorption, Davison 5A Binderless, 7.27 mm Hg
Partial Pressure, 1/8-in. Pellets, 70°F

CO$_2$ PARTIAL PRESSURE AT BED OUTLET, MM HG

BED SIZE = 0.83 IN. DIA X I IN. LONG, 7 GRAMS. 5A, 1/8 IN. PELLETS
BED INLET PRESS = 21.8 PSIA, BED INFLOW = 9580 SCCM N$_2$
BED INLET P CO$_2$ = 7.64 MM HG
BED INITIAL WATER LOAD = 0.5 PERCENT

TIME, MIN

S-81094
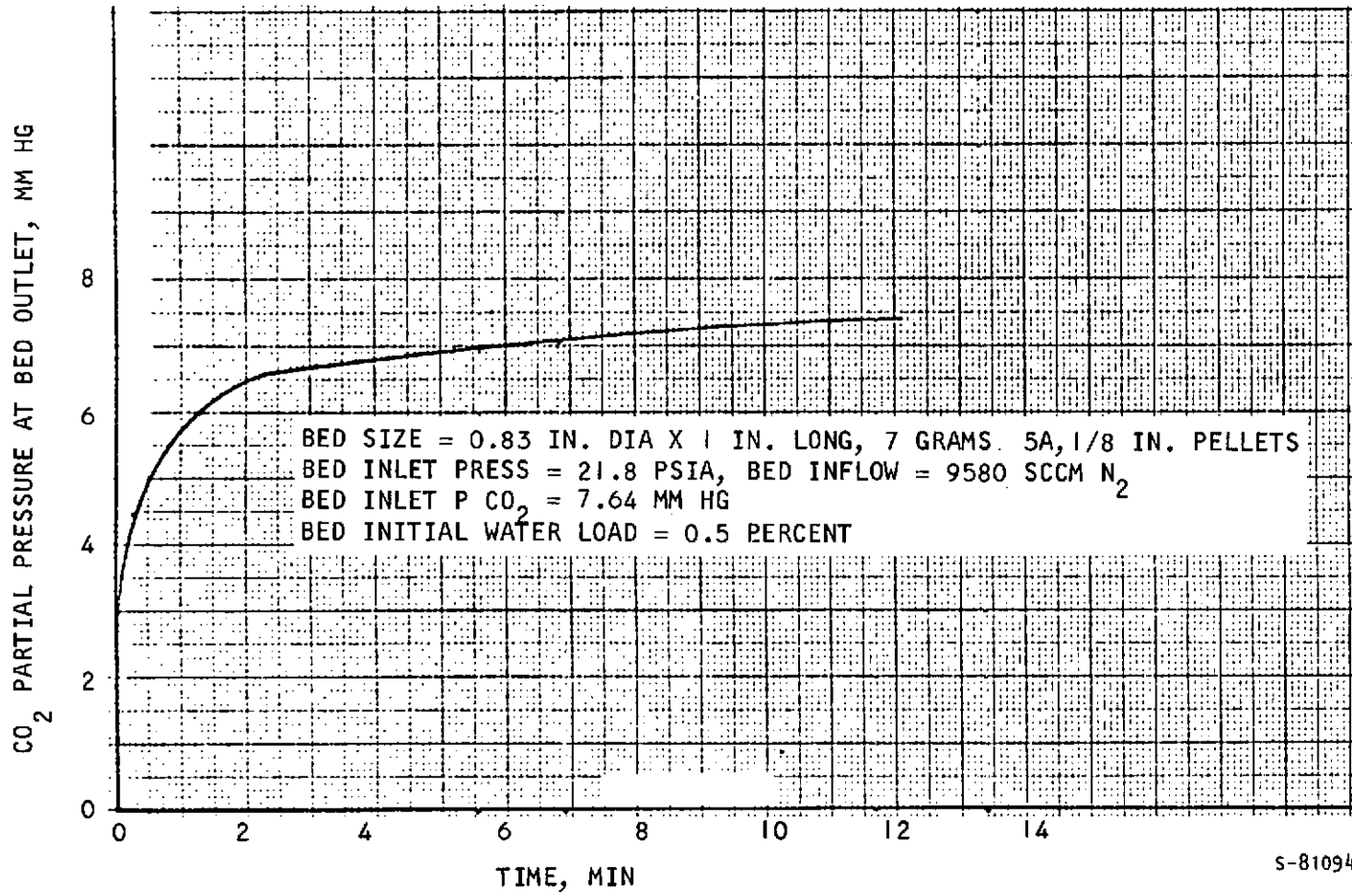
Figure A-13.   Dynamic Test, CO$_2$ Adsorption, Davison 5A Binderless, 7.64 mm Hg
Partial Pressure, 1/8-in. Pellets, 120°F

APPENDIX B

AIRESEARCH REPORT 72-8851, TEST PLAN,
DESICCANT HUMIDITY CONTROL SYSTEM

AIRESEARCH MANUFACTURING COMPANY
Los Angeles, California

TEST PLAN
DESICCANT HUMIDITY CONTROL SYSTEM

NATIONAL AERONAUTICS AND SPACE ADMINISTRATION
MANNED SPACFFLIGHT CENTER (NASA MSC)
CONTRACT NO. NAS 9-12956

72-8851   November 20, 1972

Number of pages ___17___   Prepared by ___Staff___

Approved by _____
                  M. Gee

Approved by _____
                  T. C. Coull

CONTENTS

73-9313
Page B-2

72-8851
Page 11

AIRESEARCH MANUFACTURING COMPANY
Los Angeles, California

93<

INTRODUCTION

This document presents the plan devised to accomplish the development testing of the Desiccant Humidity Control System, as required by Contract NAS 9-12956.

Included in this section are the test bed configuration and detailed schematics and charts depicting the test facility and instrumentation required for facility control and to fully define the test bed performance. The controlled bed inputs and bed instrumentation points are identical to the required computer program inputs.

The data collected from these development tests will be utilized to update the computer program for final system optimization.

DEVELOPMENT TESTING

The test program will consist of testing to provide verification of the test bed performance for a 10-man, 4-bed system nominal and 1-bed failure modes; 4-man, 2-bed system nominal mode; and bed capacity (maximum bed adsorb time) for a 10-man, 4-bed system.

The test beds will be installed into a 80-cubic-foot altitude-type chamber with special test equipment and instrumentation installed. Special test equipment and instrumentation will be essentially the same as that utilized for the Airlock RCRS program. Figures 1 through 9 schematically depict test equipment and instrumentation points. Tables 1 through 4 list the test parameters to be monitored.

TEST PROCEDURE

Initially, both test beds will be baked out (one at a time) at 400°F and exposed to vacuum until water loading in the 4A binderless is equal to or less than 2 percent by weight. After each bakeout, the bed will be cooled in the desorb position until internal temperatures are less than 100°F.

The chamber will then be closed with the automatic PO_2 control set to 21 percent at a total pressure of 14.7 psia. The inflow compressor will be started and set to 98 lb/hr and the bed cyclic operation begun. Water and carbon dioxide

AIRESEARCH MANUFACTURING COMPANY
Los Angeles, California

94<

73-9313
Page B-3

72-8851
Page 1

flow will be started to simulate a 10-man, 4-bed system. Initial system performance data will be placed into the computer program to determine if system inputs, process flow rate, and or cycle time should be adjusted to obtain optimum bed performance. The test conditions will then be maintained for approximately the next five days, at which time the test conditions will be modified to simulate a single bed failure for a 10-man, 4-bed system.

Upon completion of the above, both beds will be regenerated at 400°F while exposed to vacuum. After the appropriate cooldown, one bed will be subjected to a continuous adsorb cycle with inputs of a 10-man, 4-bed system to determine actual bed capacity. Prior to CO_2 sorbent poisoning, both beds will be placed into cyclic operation with the system inputs adjusted to simulate a 4-man, 2-bed system.

Data from the above tests will be utilized to refine the AiResearch computer program that will be utilized to optimize the final desiccant humidity control system bed.

Expected test conditions (i.e., CO_2 flow, H_2O flow, process flow rates, and temperatures) are as follows:

(a) Chamber conditions, general

Chamber temperature	70°F
Chamber pressure, total	14.7 psia
Chamber oxygen pressure	3.1 psia

(b) 10-man, 4-bed system, nominal

Chamber conditions noted above, plus:

Bed inlet PCO_2	5.0 mm Hg
Bed inlet dewpoint	53°F
Bed process flow	98 lb/hr
Bed half-cycle time	6 min

(c) 10-man, 4-bed system, 1-bed failure

Chamber conditions noted above, plus:

Bed inlet PCO_2	6.7 mm Hg
Bed inlet dewpoint	53°F
Bed inlet process flow	98 lb/hr
Bed half-cycle time	6 min

AIRESEARCH MANUFACTURING COMPANY
Los Angeles, California

95<

73-9313
Page B-4

72-8851
Page 2

(d) 4-man, 2-bed system, nominal

Chamber conditions noted above, plus:

Bed inlet PCO_2	4.2 mm Hg
Bed inlet dewpoint	53°F
Bed inlet process flow	98 lb/hr
Bed half-cycle time	6 min

It should be noted that the above test conditions may vary slightly, depending on the initial bed performance data.

TEST SCHEDULE

Test Days	Description
1 - 7	Regeneration and simulation of normal operation (10-man, 4-bed configuration)
7 - 10	Simulation of 1-bed failure (10-man, 3-bed configuration)
10 - 11	Regeneration and bed capacity
11 - 12	Simulation of normal system operation (4-man, 2-bed configuration)

TEST RESULTS

The test results will be submitted as part of the final report, required by Task 6 of the contract Work Breakdown Structure.

AIRESEARCH MANUFACTURING COMPANY
Los Angeles, California

96<

73-9313
Page B-5

72-8851
Page 3

TABLE 1
SYSTEM INPUT PARAMETERS

Designator	Description
OFI	O_2-N_2 inflow to chamber
WFI	H_2O injection flow rate - Fisher-Porter
WF2	H_2O condensed at heat exchanger - graduated cylinder
COFI	CO_2 injection flow rate - Fisher-Porter
CLFI	Heat exchanger coolant flow - Fisher-Porter
--	Vaporizer heat input - Simpson wattmeter

TABLE 2
GAS ANALYSIS MEASUREMENTS

Designator	Description	Range	Type Record
DTI	Package outlet dewpoint	-100 to +100°F	Strip chart
DT2	Package inlet dewpoint	↑	↑
DT3	Bed 2 pre-dry inlet dewpoint		
DT4	Chamber dewpoint	↓	↓
DT5	Bed 2 pre-dry outlet dewpoint	-100 to +100°F	Strip chart
PCO_2-1	Package outlet dewpoint CO_2	0 to 15 mm Hg	Beckman IR-15A strip chart
PCO_2-2	Package inlet CO_2	↑	↑
PCO_2-3	Bed 2 pre-dry inlet CO_2		
PCO_2-4	Chamber CO_2	↓	↓
PCO_2-5	Bed 2 pre-dry outlet CO_2	0 to 15 mm Hg	Beckman IR-15A strip chart
PO_2-1	Package outlet O_2	0 to 800 mm Hg	Beckman F-3 strip chart
PO_2-2	Package inlet O_2	↑	↑
PO_2-3	Bed 2 pre-dry inlet O_2		
PO_2-4	Chamber O_2	↓	↓
PO_2-5	Bed 2 pre-dry outlet O_2	0 to 800 mm Hg	Beckman F-3 strip chart

GARRETT AIRESEARCH MANUFACTURING COMPANY
Los Angeles, California

97<

73-9313
Page B-6

72-8851
Page 4

TABLE 3
PRESSURE MEASUREMENTS

Designator	Description	Range	Type Record
PG1	Beds 1 and 2 in/out ΔP gage	0 to 20 in. H_2O	Visual
PG2	Beds 1 and 2 inlet pressure	0 to 25 psia	↑
PG3	Package flowmeter ΔP	0 to 20 in. H_2O	
PG4	Package flowmeter outlet pressure	0 to 20 psia	
PG5	Cabin pressure	0 to 25 psia	↓
PG6	Actuator pressure	2 to 200 psia	Visual
VP13	Vacuum duct pressure	0 to 30 mm	Visual
VP1A	Bed 1 inlet, desorption pressure	↑	↑
VP1B	Bed 1 plenum, desorption pressure		
VP1C	Bed 1 mole sieve, desorption pressure		
VP1D	Bed 1 outlet, desorption pressure		
VP2A	Bed 2 inlet, desorption pressure		
VP2B	Bed 2 plenum, desorption pressure		
VP2C	Bed 2 mole sieve, desorption pressure		
VP2D	Bed 2 outlet, desorption pressure	0 to 30 mm ↓	Visual ↓

AIRESEARCH MANUFACTURING COMPANY
Los Angeles, California

95<

73-9313
Page B-7

72-8851
Page 5

TABLE 4
THERMOCOUPLE DESIGNATION

	I.D.	Temp Rec Chan No	Conn No	Pin No	Line No	Remarks
COMPRESSOR OUT	T1	1-A	TC1	1,2	1	2-in. probe
VAPORIZER OUT	T2	2-A	TC1	3,4	2	2-in. probe
HX COOLANT IN	T3	3-A	TC1	5,6	3	1-1/2-in probe
HX COOLANT OUT	T4	4-A	TC1	7,8	4	1-1/2-in. probe
PACKAGE INLET	T5	5-A	TC1	9,10	5	1-1/2-in. probe
PACKAGE OUTLET	T6	6-A	TC1	11,12	6	1-1/2-in. probe
CHAMBER	T15	15-A	TC1	29,30	15	Weld wire
CHAMBER	T16	16-A	TC1	31,32	16	Weld wire
CHAMBER (RESERVE)	T17	17-A	TC1	33,34	17	Weld wire
CHAMBER (RESERVE)	T18	18-A	TC1	35,36	18	Weld wire
BED NO 2 (see schem)	T7	7-B	TC2	13,14	7	5-in. probe
BED NO 2 (see schem)	T8	8-B	TC2	15,16	8	↑
BED NO 2 (see schem)	T9	9-B	TC2	17,18	9	
BED NO 2 (see schem)	T10	10-B	TC2	19,20	10	
BED NO 2 (see schem)	T11	11-B	TC2	21,22	11	
BED NO 2 (see schem)	T12	12-B	TC2	23,24	12	
BED NO 1 (see schem)	T13	13-B	TC2	25,26	13	
BED NO 1 (see schem)	T14	14-B	TC2	27,28	14	
BED NO 1 (see schem)	T19	19-B	TC2	1,2	1	
BED NO 1 (see schem)	T20	20-B	TC2	3,4	2	
BED NO 1 (see schem)	T21	21-B	TC2	5,6	3	
BED NO 1 (see schem)	T22	22-B	TC2	7,8	4	↓
BED NO 1 (see schem)	T23	23-B	TC2	9,10	5	5-in. probe
BED NO 1 SKIN TEMP	ST1	1-B	TC3	1,2	1	A2 welded T/C to unit
BED NO 1 SKIN TEMP	ST2	2-B	TC3	3,4	2	↑
BED NO 1 SKIN TEMP	ST3	3-B	TC3	5,6	3	
BED NO 1 SKIN TEMP	ST4	4-B	TC3	7,8	4	
BED NO 1 SKIN TEMP	ST5	5-B	TC3	9,10	5	
BED NO 2 SKIN TEMP	ST6	6-B	TC3	11,12	6	
BED NO 2 SKIN TEMP	ST7	15-B	TC3	29,30	15	
BED NO 2 SKIN TEMP	ST8	16-B	TC3	31,32	16	
BED NO 2 SKIN TEMP	ST9	17-B	TC3	33,34	17	↓
BED NO 2 SKIN TEMP	ST10	18-B	TC3	35,36	18	A2 welded T/C to unit

NOTES: (1) Record "A" range = 0° to $200^\circ F$
       (2) Record "B" range = 0° to $500^\circ F$
       (3) Conn TC3 pins 25-26 (Line 13) to vaporizer o'temp

AIRESEARCH MANUFACTURING COMPANY
Los Angeles, California

99<

73-9313
Page B-8

72-8851
Page 6

SOLENOID VALVE	VOLTAGE	RELAY #
SV₁	115 VAC	K₁
SV₂	115 VAC	K₂
SV₃	115 VAC	K₃
SV₄	115 VAC	K₄
SV₅	115 VAC	K₅
SV₆	115 VAC	K₆
SV₇	28 VDC	K₇
SV₈	28 VDC	K₈
SV₉	28 VDC	K₉
SV₁₀	28 VDC	K₁₀
SV₁₂	115 VAC	K₄
SV₁₃	115 VAC	K₄

TIME, MIN.

☐ = ENERGIZED

Figure I. Solenoid Valve Program

THE
SECOND CANISTER
IS A MIRROR IMAGE
OF THE FIRST

1⅛" O.D.
INLET & OUTLET

STAINLESS STEEL
STANDARD FLANGE
AND "COVER"

1" SOLENOID VALVES
ARE WELDED TO
CAN. INLET & OUTLET

INLET

8 ⅜" I.D.
STAINLESS PIPE

¾" HOLES AROUND CAN.
CIRCUMFERENCE

15 ¼"

DESORPTION
PLENUM
(2½" WIDE)

¼" THICK
STAINLESS PLATE

BAND HEATER (110 V.A.C.) FOR THE
SILICA GEL SECTION OF CAN.
NO. 2 ONLY. (1½" WIDE, 8½" I.D.)

2⅛" DESORPTION PORT
FOR THE "RCRS" GAS
VALVE

MOLE SIEVE BAND HEATERS
(110 V.A.C.) LOCATED ON
BOTH CANISTERS
(1½" WIDE, 8½" I.D.)

Figure 2.   System Test Canister Design

SYSTEM TEST WIRING DIAGRAM
DESICCANT HUMIDITY CONTROL SYSTEM

G.V. 1

G.V. 2
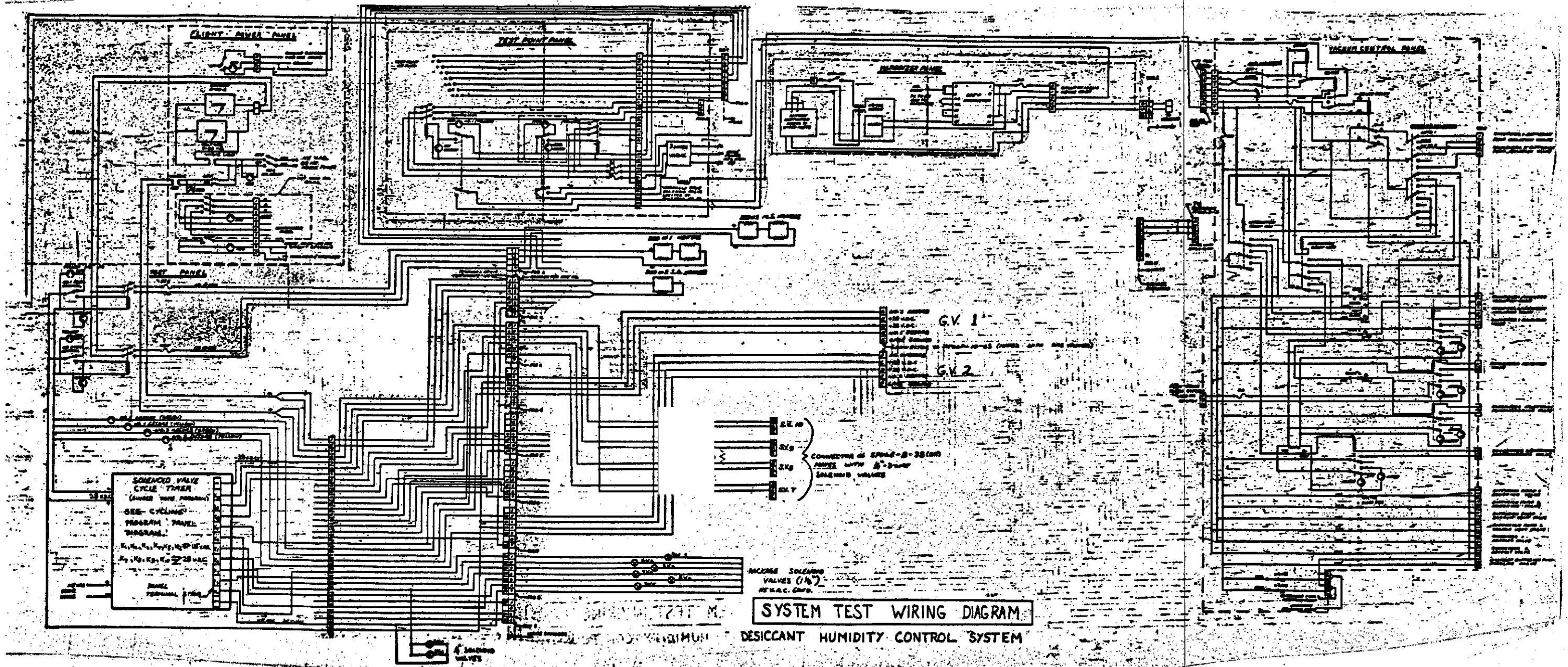
Figure 3. System Test Wiring Diagram

SEE INSTRUMENTATION
SCHEMATIC FOR
DETAILED VACUUM
PRESSURE TAPS & LINES
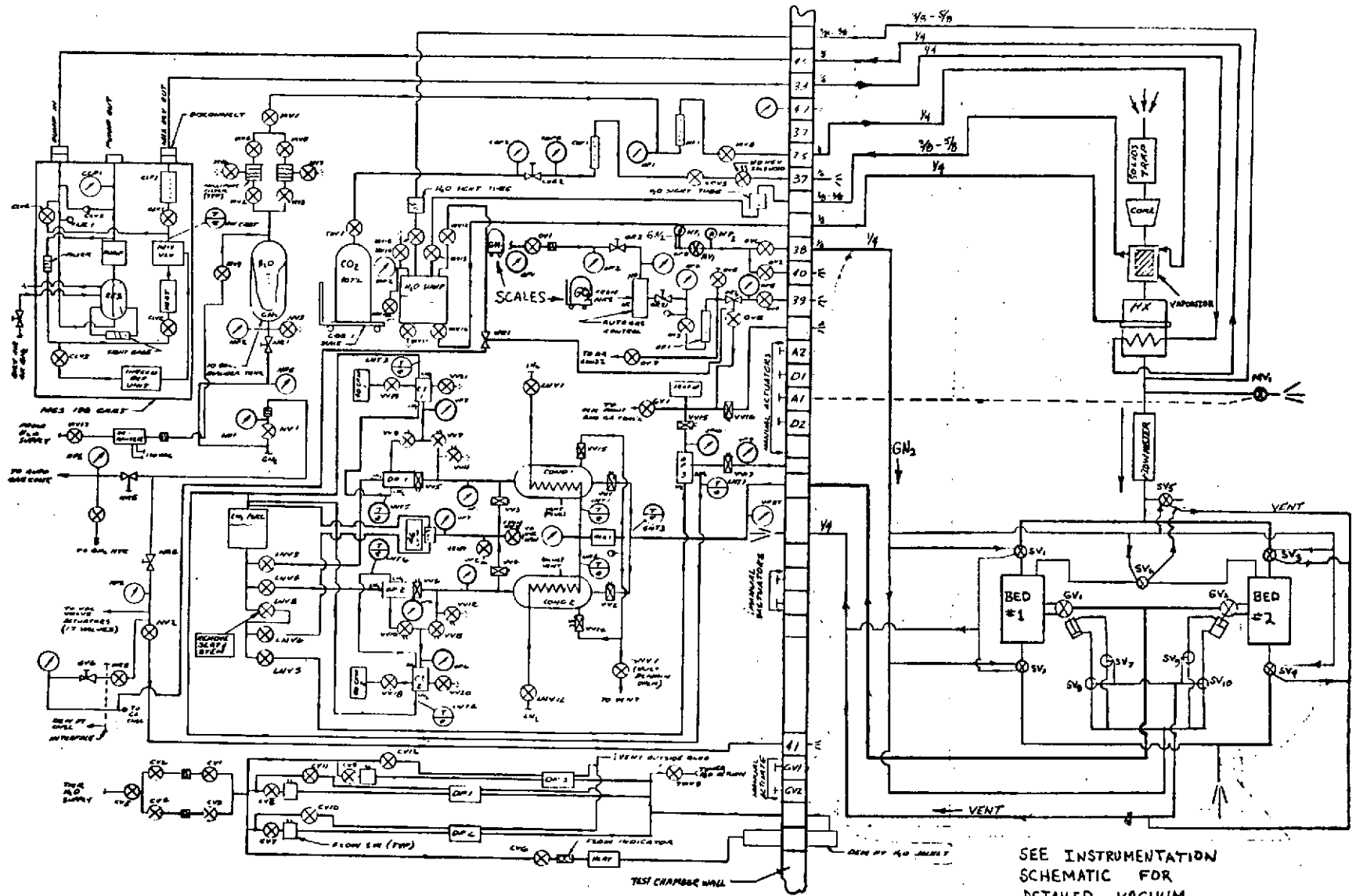
Figure 4.   System Test Plumbing
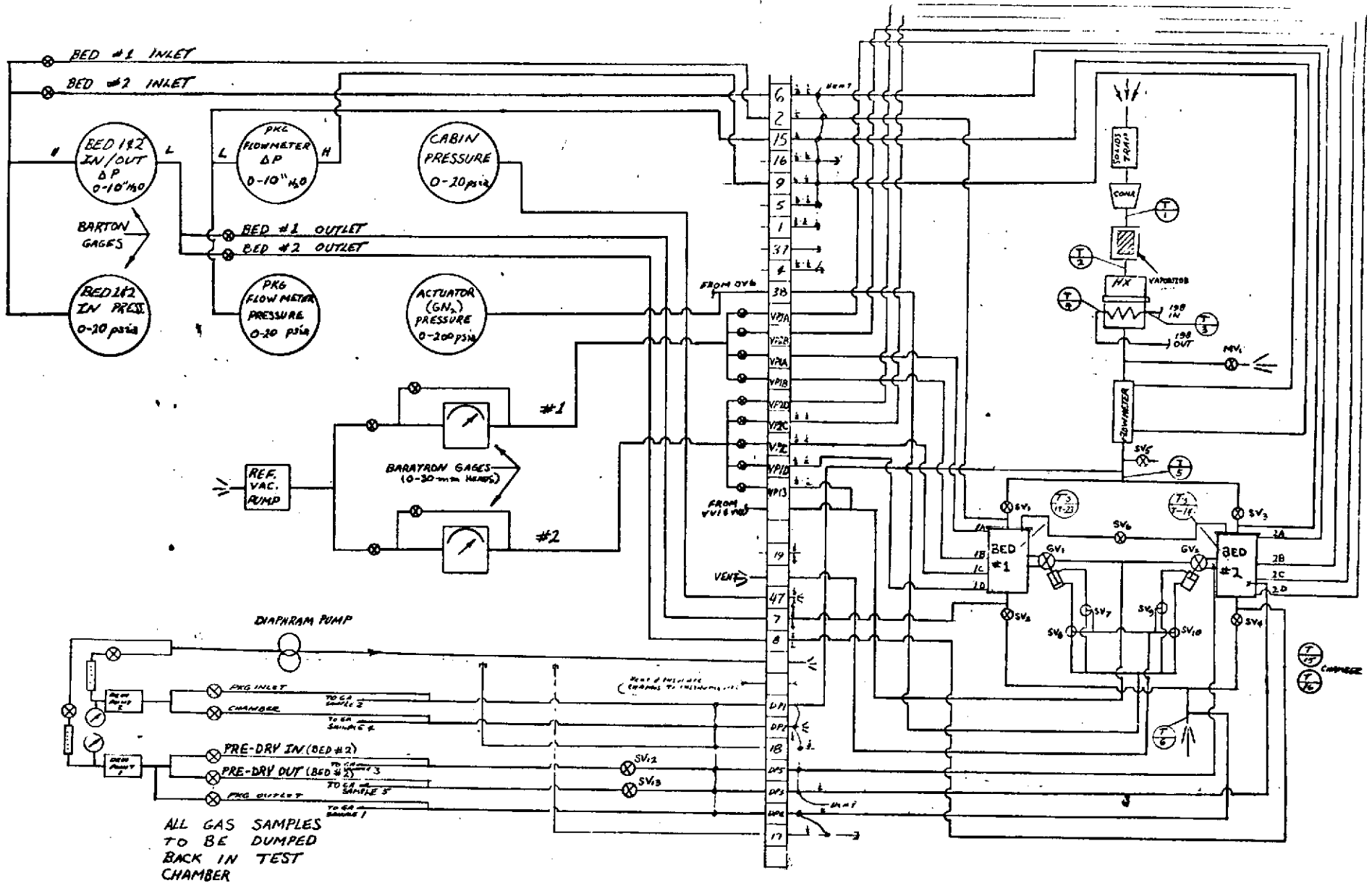
Figure 5. System Test Instrumentation
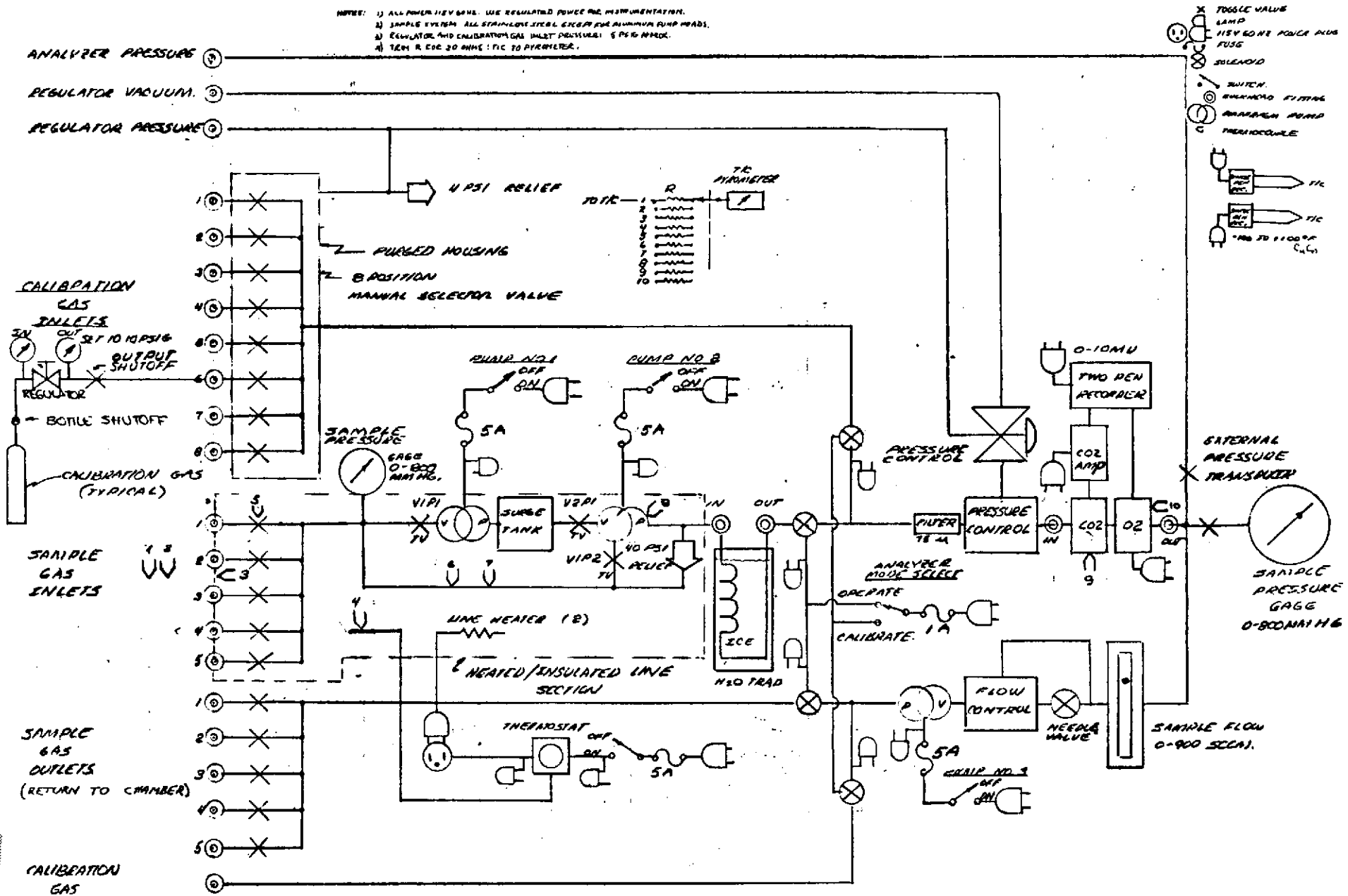
Figure 6. Gas Analysis Console
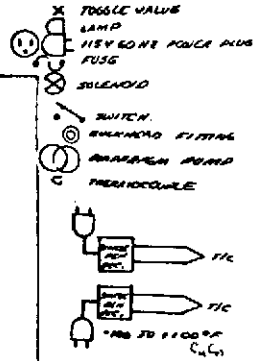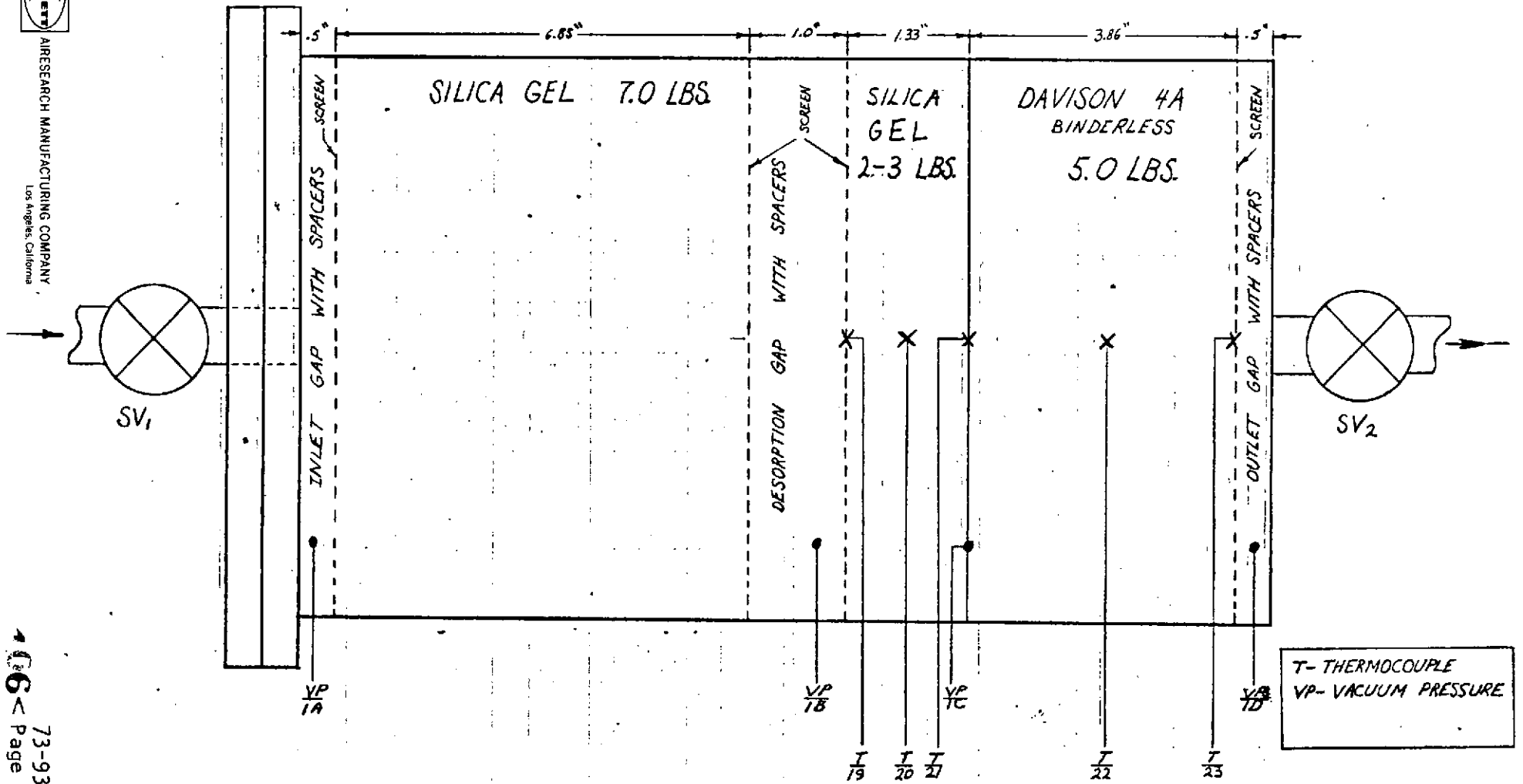
Figure 7. Bed No. I Instrumentation
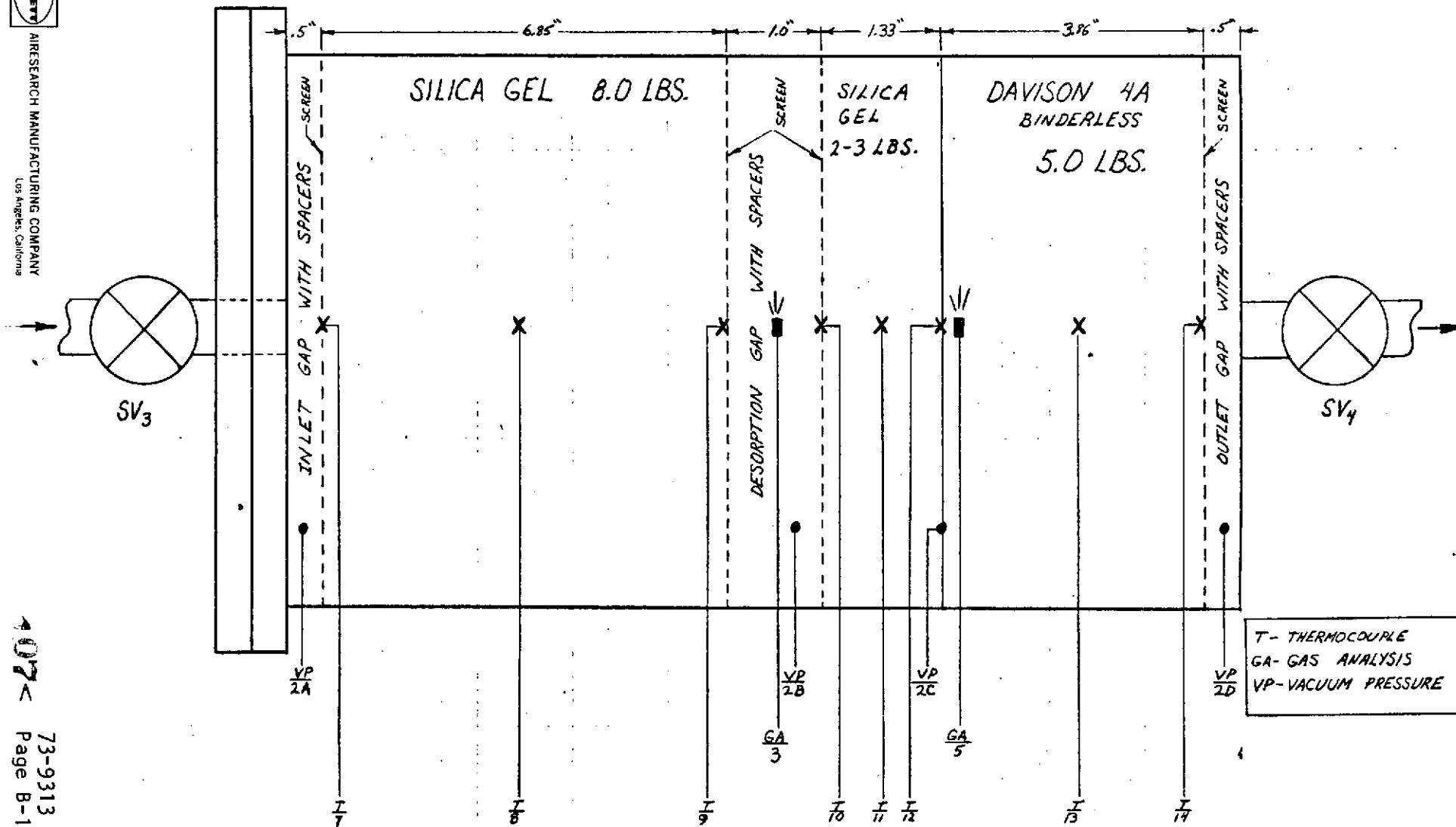
Figure 8.   Bed No. 2 Instrumentation

| TIME (MIN:SEC)	SOLENOID VALVE #	TYPE VALVE (VOLTS, N.O. or N.C)	VALVE OPERATION	ENERGIZED OR DE-ENERGIZED	DESCRIPTION OF OPERATION
0:00	SV1	115 V.A.C. N.C.	CLOSES	DE-ENERGIZE	BED #1 INLET OFF
0:00	SV2	115 V.A.C. N.C.	CLOSES	DE-ENERGIZE	BED #2 OUTLET OFF
0:00	SV5	115 V.A.C. N.C.	OPENS	ENERGIZE	FLOW BYPASS ON
0:00	SV10	28 V.D.C. N.C.	OPENS	ENERGIZE	BED #2 DESORB OFF
0:15	SV10	28 V.D.C. N.C.	CLOSES	DE-ENERGIZE	
0:15	SV6	115 V.A.C. N.C.	OPENS	ENERGIZE	PRESSURE EQUALIZE ON
0:45	SV6	115 V.A.C. N.C.	CLOSES	DE-ENERGIZE	PRESSURE EQUALIZE OFF
0:45	SV7	28 V.D.C. N.C.	OPENS	ENERGIZE	BED #1 DESORB ON
1:00	SV7	28 V.D.C. N.C.	CLOSES	DE-ENERGIZE	
0:45	SV3	115 V.A.C. N.C.	OPENS	ENERGIZE	BED #2 INLET ON
1:00	SV5	115 V.A.C. N.C.	CLOSES	DE-ENERGIZE	FLOW BYPASS OFF
1:00	SV4	115 V.A.C. N.C.	OPENS	ENERGIZE	BED #2 OUTLET ON
1:00	SV12	115 V.A.C. N.C.	OPENS	ENERGIZE	GAS SAMPLE #3 ON
1:00	SV13	115 V.A.C. N.C.	OPENS	ENERGIZE	GAS SAMPLE #5 ON
7:00	SV12	115 V.A.C. N.C.	CLOSES	DE-ENERGIZE	GAS SAMPLE #3 OFF
7:00	SV13	115 V.A.C. N.C.	CLOSES	DE-ENERGIZE	GAS SAMPLE #5 OFF
7:00	SV3	115 V.A.C. N.C.	CLOSES	DE-ENERGIZE	BED #2 INLET OFF
7:00	SV4	115 V.A.C. N.C.	CLOSES	DE-ENERGIZE	BED #2 OUTLET OFF
7:00	SV5	115 V.A.C. N.C.	OPENS	ENERGIZE	FLOW BYPASS ON
7:00	SV8	28 V.D.C. N.C.	OPENS	ENERGIZE	BED #1 DESORB OFF
7:15	SV8	28 V.D.C. N.C.	CLOSES	DE-ENERGIZE	
7:15	SV6	115 V.A.C. N.C.	OPENS	ENERGIZE	PRESSURE EQUALIZE ON
7:45	SV6	115 V.A.C. N.C.	CLOSES	DE-ENERGIZE	PRESSURE EQUALIZE OFF
7:45	SV9	28 V.D.C. N.C.	OPENS	ENERGIZE	BED #2 DESORB ON
8:00	SV9	28 V.D.C. N.C	CLOSES	DE-ENERGIZE	
7:45	SV1	115 V.A.C. N.C.	OPENS	ENERGIZE	BED #1 INLET ON
8:00	SV5	115 V.A.C. N.C.	CLOSES	DE-ENERGIZE	FLOW BYPASS OFF
8:00	SV2	115 V.A.C. N.C.	OPENS	ENERGIZE	BED #1 OUTLET ON
14:00 →0:00					

Figure 9. Solenoid Valve Operating Sequence